STOCHASTIC LIFE-CYCLE ANALYSIS OF DETERIORATING INFRASTRUCTURE SYSTEMS AND AN APPLICATION TO REINFORCED CONCRETE BRIDGES

A Dissertation

by

RAMESH KUMAR

Submitted to the Office of Graduate Studies of
Texas A&M University
in partial fulfillment of the requirements for the degree of

DOCTOR OF PHILOSOPHY

Approved by:

Co-Chairs of Committee,	Paolo Gardoni
	Joseph M. Bracci
Committee Members,	Daren B. H. Cline
	Luciana Barroso
Head of Department,	John M. Niedzwecki

December 2012

Major Subject: Civil Engineering

ABSTRACT

Infrastructure systems are critical to a country's prosperity. It is extremely important to manage the infrastructure systems efficiently in order to avoid wastage and to maximize benefits. Deterioration of infrastructure systems is one of the primary issues in civil engineering today. This problem has been widely acknowledged by engineering community in numerous studies. We need to evolve efficient strategies to tackle the problem of infrastructure deterioration and to efficiently operate infrastructure.

In this research, we propose stochastic models to predict the process of deterioration in engineering systems and to perform life-cycle analysis (LCA) of deteriorating engineering systems. LCA has been recognized, over the years, as a highly informative tool for helping the decision making process in infrastructure management. In this research, we propose a stochastic model, SSA, to accurately predict the effect of deterioration processes in engineering systems. The SSA model addresses some of the important and ignored areas in the existing models such as the effect of deterioration on both capacity and demands of systems and accounting for different types of failures in assessing the life-span of a deteriorating system. Furthermore, this research proposes RTLCA, a renewal theory based LCA model, to predict the life-cycle performance of deteriorating systems taking into account not only the life-time reliability but also the costs associated with operating a system. In addition, this research investigates the effect of seismic degradation on the reliability of reinforced concrete (RC) bridges. For this purpose, we model the seismic degradation process in the RC bridge columns which are the primary lateral load resisting system in a bridge. Thereafter, the RTLCA model

along with SSA model is used to study the life-cycle of an example RC bridge located in seismic regions accounting for seismic degradation. It is expected that the models proposed in this research will be helpful in better managing our infrastructure systems.

DEDICATION

I dedicate this dissertation to my dear parents, wife and brother

ACKNOWLEDGEMENTS

I am grateful to Dr. Paolo Gardoni, Associate Professor, Department Civil and Environmental Engineering in University of Illinois, Urbana-Champaign, for providing me with the opportunity to pursue PhD under his able guidance and for providing the funding for my research.

I express my gratitude to Dr. Daren Cline, Professor, Department of Statistics in Texas A&M University, College Station, for providing his crucial guidance that helped me understand and apply the method of stochastic processes in my research.

I sincerely thank Dr. Colleen Murphy for providing me the opportunity to work on her research project that provided the financial support for a part of my doctoral studies.

I thank Dr. Joseph Bracci and Dr. Luciana Barroso for accepting to serve in my PhD committee and for their invaluable guidance and time.

I thank my former PhD committee member Dr. Jose Roesset for serving in my committee and for providing his invaluable suggestions.

I thank Zachry Department of Civil Engineering, Texas A&M University, National Science Foundation (NSF) and Texas Transportation Institute (TTI) for providing the funding for my doctoral studies in the form of GAT and GAR.

Finally, I thank my parents, my grandparents, my brother and family members for their constant encouragement and inspiration. I give my very special thanks to my wife for her patience and invaluable support. Also, here I thank my friends, specifically; Luis, Sashikanth and Armin, for sharing their knowledge with me.

TABLE OF CONTENTS

LIST OF FIGURES

Page

LIST OF TABLES

Page

1. INTRODUCTION

1.1 Background

Governments invest immensely in building infrastructure systems because they are critical to the socio-economic prosperity in any country. While building new infrastructure is essential, it is equally important to efficiently operate the built infrastructure to maximize the benefits. Lack of planning and shortsighted objectives in handling infrastructure systems may lead to massive wastage of resources and can often lead to mass inconvenience and social distress.

Deterioration of infrastructure systems is a pressing issue in civil engineering today. In a recent study, the American Society of Civil Engineers (ASCE) gave an overall poor rating (grade D) to the state of infrastructure in USA (ASCE 2011) and estimated that the average age of bridges in USA is 43 years and 12.1% of the nation's bridges are structurally deficient. The collapse of Minneapolis Bridge on August 1st, 2007, that killed 13 and injured 145 others, served a reminder of the risk that deteriorating infrastructure poses to the society. One of the factors contributing to this collapse was indeed found to be the corrosion of the gusset plates in the bridge truss (NTSB 2008). While the existing infrastructure has to be upgraded, it must be precisely planned keeping in mind the overall long-term safety and economy.

Deterioration in infrastructure systems, similar to any engineering system, is caused by the service loads imposed on the system during the routine use, the unexpected events of extreme loads and the unfavorable chemicals present in the environment or in the construction materials. The corrosion of steel reinforcement in reinforced

concrete (RC) structures caused by the chlorides present in the atmosphere is a common example of deterioration caused by the environment (Ahmad 2003). In seismically active regions, structures are subject to multiple earthquakes in their life-span which causes accumulation of seismic damage in the structures that may eventually lead to failure (Park and Ang 1985).

Research has progressed in various directions to find the solution for the problem of infrastructure deterioration or general structural deterioration. Some of the prominent research areas are: retrofit of structures (Saadatmanesh et al. 1997), development of damage detection and health monitoring of systems (Pines and Aktan 2002), improvement of the durability of construction materials (Mehta 1994), development of new design philosophies with emphasis on durability and long-term performance objectives (Flint and Billington 2011) and analysis of life-cycle cost and life-cycle reliability of systems (Kong and Frangopol 2003).

In recent years, life-cycle analysis (LCA) has been recognized as a valuable tool for efficient infrastructure management. In this dissertation, by LCA, we mean the method or methods for analyzing the life-time performance of systems. In general, a LCA study involves the prediction of the time-dependent reliability of systems, considering deterioration if necessary, and is often extended to estimate the life-cycle cost considering the cost of construction and occasional repairs. Usually, the LCA of an engineering system operating under an unregulated and uncertain environment, as typically is the case with infrastructure systems, is a highly complex problem. A LCA study

requires extensive modeling of uncertainty associated with the loads, harsh environmental conditions and deterioration processes.

1.2 Research objectives

The overall objective of this research is to develop a novel LCA model for deteriorating engineering systems that can address some of the existing short comings in the models available in existing literature. Furthermore, this research aims to perform LCA of reinforced concrete (RC) bridges subject to deterioration caused by earthquakes occurring during its life span. Additionally, this research aims to develop closed-form solutions that can enable quick assessment of failure probability of infrastructure systems subject to natural hazards. The specific objectives of this research, in the order they are presented in this dissertation, are as follows:

1. To assess the effect of seismic degradation on the reliability of RC bridges.
2. To develop a general stochastic model that can be used to model the deterioration process in engineering systems.
3. To develop a general stochastic LCA model to assess the life-time reliability and costs associated to operating a deteriorating engineering system and to conduct the LCA of an example RC bridge subject to seismic degradation.
4. To develop a closed-form approach for quick and reasonably accurate estimation of the failure probability of infrastructure systems subject to natural hazards.

1.3 Methodology

The adopted methodology specific to each objective is described in the following:

1. *To assess the effect of seismic degradation on the reliability of RC bridges.* To meet this objective, we focus on; (i) the low-cycle fatigue of longitudinal reinforcement in the bridge columns and (ii) the seismic degradation of static pushover properties of the columns caused by earthquakes. Low-cycle fatigue of the longitudinal steel has been reported as one of the potential causes of failure of bridge columns during earthquakes (Mander et al. 1994; Brown and Kunnath 2004). Similarly, the static pushover properties of RC bridge columns undergo unfavorable changes due to cyclic degradation of concrete and consequently the reliability of the bridge decreases.

   In order to capture the effect of the above mentioned degradation phenomena, we develop probabilistic models to predict the deterioration processes. The proposed probabilistic models are developed through statistical regression methods. The data required to develop the proposed models is generated by conducting virtual experiments, wherein quasi-static cyclic lateral load tests and nonlinear time-history analysis (NTHA) are conducted in finite element (FE) software OpenSees (McKenna et al. 2008). The Bayesian approach (Box and Tiao 1992) is used to compute the model parameters in the probabilistic models.

2. *To develop a general stochastic model that can be used to model the deterioration process in engineering systems.* To meet this objective, we propose a novel stochastic deterioration model named SSA that provides semi-analytical solutions to predict the life-time and the level of deterioration of a general deteriorating engineering system. The SSA model addresses some of the short comings in the existing stochastic deterioration models in the literature. The proposed stochastic model ac-

counts for the effect of deterioration processes on both demand and capacity of the system and considers deterioration process as a combination of shock deterioration, generally caused by extreme events, and gradual deterioration, generally caused by chemicals present in the environment and construction materials.

3. *To develop a LCA model for deteriorating engineering systems and conduct the LCA of a RC bridge subject to seismic degradation.* To meet this objective, we propose a novel LCA model named RTLCA applicable to a wide variety of engineering systems and operation strategies. The model is based on renewal theory (Grimmett and Stirzaker 2001). Based on the RTLCA model, we develop computationally efficient solutions to compute important quantities that describe the life-cycle of a system. The proposed model is applied to perform LCA of an example RC bridge located in a seismic region. The proposed probabilistic models are used to account for seismic degradation in the LCA of the bridge.
4. *To develop a closed-form solution to estimate the failure probability of infrastructure systems subject to natural hazards.* To meet this objective we propose a improved mathematical form for hazard curves which satisfactorily fits the data points for hazard curve values and also enables a closed form solution to compute the annual failure probabilities for systems. The proposed closed-form is not only computationally efficient but also provides valuable insight regarding the design of systems.

1.4 Organization of the dissertation

This dissertation adopts the Sections method to present the work. After this introduction, the rest of the dissertation consists of five sections (Section 2 to Section 6) that present the research work and a section (Section 7) that presents the overall summary and conclusions from the work. In addition to the introduction and conclusions, presented in Section1 and Section 7 respectively, sections 2 to 6 provide their individual introductions and conclusions.

Section 2 proposes the probabilistic model to predict the effect of low-cycle fatigue damage in longitudinal reinforcing steel on the reliability of bridges. Section 3 proposes the probabilistic models for seismic degradation of static pushover properties of RC columns. Section 4 presents the stochastic formulation to model a general deterioration process. Section 5 presents the RTLCA formulation for conducting LCA of deteriorating engineering systems and presents the LCA of RC bridges accounting for seismic degradation. Section 6 presents the closed-form approach to compute the probability of failure of systems subject to natural hazards. Section 7 summarizes the dissertation and presents the conclusions from this research.

2. SEISMIC DEGRADATION OF RC BRIDGE COLUMNS DUE TO LOW-CYCLE FATIGUE*

2.1 Introduction

Bridges are one of the most critical and vulnerable systems in a transportation network. Their failures typically result in fatalities, inconveniences to the users, and expensive and time consuming repairs. Therefore, they have to be designed with utmost care to provide sufficient safety and preferably uninterrupted service to the users. In particular, in seismic regions, earthquakes are a major concern for the safety of bridges and they have attracted major attention and resources from the departments of transportations and transportation research agencies.

Several studies have focused on the seismic vulnerability of reinforced concrete (RC) bridges in as-built condition (e.g., Basöz and Kiremidjian 1996; Basöz and Mander 1999; Shinozuka et al. 2000; Gardoni et al. 2002, 2003; Choe et al. 2007; Zhong et al. 2008, 2009; Huang et al. 2010). Also, there exists substantial research on the performance of RC bridges with post-earthquake repairs (Saadatmanesh et al. 1997; Xiao and Ma 1997; Li and Sung 2003 and Schoettler et al. 2005). However, we often need to assess the seismic vulnerability of the structures that are in a degraded state due to past events. Val and Stewart (2005), Choe et al. (2008, 2009), Zhong et al. (2009), Ghosh and Padgett (2010), and Gardoni and Rosowsky (2011) evaluate the seismic vulnerability of RC bridges subject to corrosion of the longitudinal reinforcement.

* Reprinted with permission from "Modeling structural degradation of RC bridge columns subjected to earthquakes and their fragility estimates" by Kumar and Gardoni, 2012. *Journal of Structural Engineering*, 137, 42-51, Copyright [2012] by American Society of Civil Engineers.

While evaluating the vulnerability of structurally degraded bridges, researchers have typically ignored the effect of seismic damage accumulated in the past earthquakes. Cumulative seismic damage is an important phenomenon to consider because in seismically active regions typically multiple damaging earthquakes are experienced by a structure in its service life. The importance of assessing the vulnerability of structures with seismic damage can be realized from the recent seismic events witnessed in New Zealand (2011) and in Northern Italy (2012), where multiple damaging earthquakes occurred within a span of six months allowing limited time for repairs. Particularly in New Zealand earthquakes, buildings performed well in the first earthquake but collapsed immediately after the second earthquake.

There can be various forms of seismic damage and depending on the structural system or component a particular type of seismic damage may be important. Park and Ang (1985) proposed a general model based on the combination of energy dissipation and ductility to compute the cumulative seismic damage for any structure. By appropriate calibration, this model can be used with some accuracy for a variety of structural components. Mander and Cheng (1995) and El-Bahy et al. (1999a, 1999b) found that low-cycle fatigue is a potential cause of failures of RC bridge columns during earthquakes. This type of damage is caused due to several strain cycles in longitudinal steel caused during the earthquakes. Excessive low-cycle fatigue damage typically causes a sudden rupture of longitudinal steel resulting in the flexural failure of the RC column. The research on seismic damage of RC bridge columns is so far limited to the

quantification of the seismic damage and has not been extended to evaluate the vulnerability of the damaged structures.

The objective of this section is to illustrate the vulnerability of RC bridge columns that have accumulated low-cycle fatigue damage in longitudinal steel during past earthquakes. For this purpose, first we estimate the probability of observing multiple damaging earthquakes in a bridge's service life so as to emphasize on the need of evaluating the vulnerability of RC bridges with cumulative seismic damage. Then, this section develops a probabilistic model to estimate the degraded deformation capacity of an RC bridge column that has accumulated low-cycle fatigue damage. For this purpose, first we use an existing low-cycle fatigue model for reinforcing steel to develop a probabilistic model for computing degradation in curvature capacity of RC sections. This model is then incorporated in the model developed by Choe et al. (2007) that computes the deformation capacity of RC bridge columns based on the curvature capacity of the plastic hinge region. The proposed probabilistic model is developed using the data from *virtual experiments* wherein quasi-static cyclic load tests of RC columns are conducted using the finite element (FE) method. Finally, the proposed model is used to assess the fragilities of three example RC columns for given values of deformation demands and low-cycle fatigue damage.

This section is organized into seven major sub-sections. The second subsection computes the probabilities of multiple damaging earthquakes in a bridge's service life. The third subsection discusses the phenomenon of low-cycle fatigue damage in reinforcing steel and its effect on the curvature capacity of RC column sections.

Thereafter the fourth subsection discusses the procedure followed to conduct the virtual experiments for generating the required data. The fifth subsection proposes the probabilistic model for degradation in curvature capacity. The sixth subsection computes the degradation in deformation capacity based on the proposed model for deterioration in curvature capacity and presents the fragility estimates for three example RC columns. Finally, the seventh subsection presents the conclusions from this section.

2.2 Probability of occurrence of damaging earthquakes

This subsection computes the probabilities of observing multiple damaging earthquakes in San Francisco, CA considering two cases. Case 1 considers that no prior information is available about the occurrence of past earthquakes in the service life of the bridge. Case 2 considers that one damaging earthquake has already occurred in the past service life of the bridge. Case 1 is relevant to the bridges that are newly built or will be built in the future. Case 2 is relevant to the bridges that have withstood a damaging earthquake in the past (e.g., bridges that have already experienced the 1994 Northridge Earthquake and still face the probability of experiencing another earthquake in the remaining service life). The probabilities for both Case 1 and Case 2 are computed in two ways: (a) considering main shocks only, and (b) considering both main shocks and aftershocks.

2.2.1 Damaging earthquakes

This study considers a damaging earthquake as the earthquake that can cause a moderate or greater level of damage to RC bridges. These earthquakes can be both main shocks and aftershocks. Since damage cannot be determined deterministically from the intensity of an earthquake, we define a damaging main shock as the one with peak

ground acceleration (PGA) corresponding to 0.5 probability of exceeding the moderate level of the damage. For identifying damaging earthquakes, we use the empirical seismic fragility curves developed for RC bridges by Basöz and Kiremidjian (1996). These fragility curves were developed based on the damage to bridges observed in 1994 Northridge Earthquake. We define a damaging aftershock as the one that has Richter magnitude M_a greater than or equal to $M_m - 1$, where M_m is the magnitude of the main shock. Richter magnitude instead of PGA is chosen to identify damaging aftershocks because currently in the literature the probability of aftershocks is computed based on Omori's law (Utsu 1961) that uses Richter magnitude. However, it must be noted that seismic damage to structures may not always demonstrate a strong correlation with the Richter magnitude. The idea behind choosing $M_m - 1$ as the threshold for identifying damaging aftershocks is that following a main shock of magnitude M_m aftershocks of magnitude $M_m - 1$ might also be damaging even though of smaller magnitude.

2.2.2 Case 1(a): No prior information, main shocks only

We compute the probability, $P_m(i, T_S)$, of observing i main shocks in a time span T_S using a time-independent Poisson process (Ang and Tang 2007), where the rate of arrival of main shocks λ_m corresponding to a PGA is obtained from the probabilities provided by USGS (2002). The value of $P_m(i, T_S)$ is given as follows:

$$P_m\left(i, T_S\right) = \frac{\left(\lambda_m T_S\right)^i e^{-\lambda_m T_S}}{i!} \tag{2-1}$$

We can compute

$$P_m\left(i=1,T_S\right)=\left(\lambda_m T_S\right)e^{-\lambda_m T_S} \tag{2-2}$$

$$P_m\left(i\geq 2,T_S\right)=1-e^{-\lambda_m T_S}-\left(\lambda_m T_S\right)e^{-\lambda_m T_S} \tag{2-3}$$

2.2.3 Case1(b): No prior information, main shocks and aftershocks

The rate of arrival of aftershocks of a magnitude M_a greater than or equal to M, following a main shock of magnitude M_m is given by Reasenberg and Jones (1989) as follows:

$$\lambda_a\left(t,M\right)=10^{B_1+B_2\left(M_m-M\right)}\left(t+c\right)^{-p} \tag{2-4}$$

where $\lambda_a(t,M)=$ the time-dependent rate, $t=$ time elapsed since the main shock, and B_1, B_2, c and p are regional seismicity parameters. The probability, $P_a(\cdot)$, of one or more aftershocks of magnitude $M_1\leq M_a<M_2$ in the time range, $\tau_1\leq t<\tau_2$, given that the main shock of magnitude M_m occurred at $t=0$, can be written as (Reasenberg and Jones 1989)

$$P_a\left(M_1,M_2,\tau_1,\tau_2\right)=1-\exp\left[-\int_{M_1}^{M_2}\int_{\tau_1}^{\tau_2}\lambda_a\left(t,M\right)dtdM\right] \tag{2-5}$$

From Eq (2-5), the probability, $P_a'(t)$, of observing no aftershocks of magnitude $M_a\geq M_m-1$ within a time span, t, after a main shock of magnitude M_m can be written as

$$P_a'\left(t\right)=1-P_a\left(M_m-1,\infty,0,t\right)=\exp\left\{\frac{10^{B_1+B_2}}{B_2\ln 10}\left[\frac{c^{1-p}-\left(t+c\right)^{1-p}}{1-p}\right]\right\} \tag{2-6}$$

Considering both main shocks and aftershocks ($M_a \geq M_m - 1$), the probabilities; $P(k=1, t=T_S)$ of exactly one earthquake in time-span T_S and $P(k \geq 2, t=T_S)$ of two or more earthquakes in time-span T_S are given by Eqs. (2-7) through (2-9).

$$P(k=1, t=T_S) = P_m(i=1, t=T_S)\left[\int_0^{T_S} P_a'(T_S-\tau)\, h_m(\tau)\, d\tau\right] \tag{2-7}$$

where $h_m(\tau) =$ the probability density function of the time τ of observing a main shock such that one main shock was observed in the time-span T_S and $0 \leq \tau \leq T_S$. The probability distribution of the time of occurrence of a main shock is a uniform distribution, $h_m(\tau) = 1/T_S$. Substituting the value of $h_m(\tau)$ in Eq (2-7) gives

$$P(k=1, t=T_S) = P_m(i=1, t=T_S)\left[\frac{1}{T_S}\int_0^{T_S} P_a'(T_S-\tau)\, d\tau\right] \tag{2-8}$$

$$P(k \geq 2, t=T_S) = 1 - P_m(k=0, t=T_S) - P(k=1, t=T_S) \tag{2-9}$$

2.2.4 Case 2(a): One main shock has already occurred; main shocks only

The probabilities of observing exactly one main shock, $k=1$, or two or more main shocks, $k \geq 2$, in the time-span T_S given that a main shock has already occurred at $t_1 \leq T_L$ are given as follows:

$$P_m(k=1, t=T_S \,|\, t_1 \leq T_S) = P_m(k=0, T_S - t_1) = e^{-\lambda_m (T_S - t_1)} \tag{2-10}$$

$$P_m(k \geq 2, t=T_S \,|\, t_1 \leq T_S) = 1 - P_m(k=0, T_S - t_1) \tag{2-11}$$

2.2.5 Case2(b): One main shock has already occurred; main shocks and aftershocks

Now including both main shocks and aftershocks, the probabilities of observing exactly one earthquake $P(k=1, t=T_S \mid t_1 \leq T_S)$ and two or more earthquakes

$P(k \geq 2, t = T_S \mid t_1 \leq T_S)$ in the time-span T_S conditioned on the event that a main shock already occurred at $t_1 \leq T_S$ can be written as follows:

$$P\left(k = 1, t = T_S \middle| t_1 \leq T_S\right) = \left\{P_a'\left(T_S - t_1\right) P_m\left(k = 0, T_S - t_1\right)\right\} \tag{2-12}$$

$$P\left(k \geq 2, t = T_S \middle| t_1 \leq T_S\right) = 1 - P\left(k = 1, t = T_S \middle| t_1 \leq T_S\right) \tag{2-13}$$

2.2.6 Numerical example for San Francisco, CA

The values of the seismic constants as reported by Reasenberg and Jones (1989) for California are $B_1 = -1.67$, $B_2 = 0.91$, $c = 0.05$ and $p = 1.08$. The value of PGA for damaging main shock is found to be $1.0g$ ($g = 9.812\ \text{m/s}^2$) and λ_m corresponding to $1.0g$ is found to be 2.67E–04 year^{-1}. The probabilities are computed for $T_S = 75$, 150 and 200 years and an example analysis for $t_1 = 4$ years is performed.

Table 2-1 shows that the probability of observing two or more damaging earthquakes is smaller compared to that of observing only one such earthquake within the service life of a bridge if only main shocks are considered. However, if damaging aftershocks are considered then the probability of observing more than one damaging earthquake is nearly equal to that of observing only one damaging earthquake in a bridge's service life. From Table 2-2, it is seen that the bridges that experience an earthquake early in their service lives, still stand a considerable chance to experience another damaging earthquake in their remaining service life. The values of probabilities in Table 2-2 are larger than the corresponding values in Table 2-1 because one main shock has been observed already in the fourth year. In Table 2-2, the probabilities of observing just one damaging earthquake decreases with increase in T_S which indicates

that it is more likely to have multiple damaging earthquakes than one damaging as T_S increases. Moreover, it can be seen that in all the cases, the probability of observing more than one damaging earthquake becomes more important as we increase the service life of the bridge. From the observations in Table 2-1 and Table 2-2, it can be concluded that the research on structural degradation of bridges caused by multiple earthquakes is important for a far-sighted seismic design.

Table 2-1. Probability of occurrence of damaging earthquakes in San Francisco

	Main shocks only		Main and Aftershocks	
No. of earthquakes	1	≥ 2	1	≥ 2
T_S (years)	Probability			
75	19.7E−03	0.198E−03	11.7E−03	8.1E−03
100	26.1E−03	0.352E−03	15.2E−03	11.2E−03
200	50.7E−03	1.40E−03	28.5E−03	23.6E−03

Table 2-2. Probability of occurrence of damaging earthquakes in San Francisco given that one such earthquake has occurred in the fourth year of the service life

	Main shocks only		Main and Aftershocks	
No. of earthquakes	1	≥ 2	1	≥ 2
T_S (years)	Probability			
75	981.0E−03	18.8E−03	549.0E−03	451.0E−03
100	975.0E−03	25.4E−03	536.0E−03	464.0E−03
200	949.0E−03	51.1E−03	501.0E−03	499.0E−03

2.3 Low-cycle fatigue of reinforcing steel and degradation in curvature capacity of RC sections

In general, any material can withstand only a certain maximum number of load cycles at a given strain amplitude. This maximum number of cycles is defined as the fatigue life for the material. The plots depicting the relationship between strain amplitudes and the corresponding number of cycles are commonly called S-N curves. A typical relation for S-N curves is shown in Eq. (2-14).

$$\varepsilon_a = c_1 \left(2N_f\right)^{c_2} \tag{2-14}$$

where ε_a = the failure strain, $2N_f$ = the number of half-cycles to failure and, c_1 and c_2 are empirical constants. There are two different approaches for writing Eq. (2-14). In one approach, ε_a is equal to the total strain (Koh and Stephens 1991), and in another approach, ε_a is equal to the plastic strain (e.g., Coffin 1954; Manson 1953 and Mander et al. 1994). Based on the strain amplitude, the fatigue can be high-cycle or low-cycle. In high-cycle fatigue, the strain amplitudes are within the elastic limit and the number of cycles to failure is high (e.g., for steel, high-cycle fatigue may need millions of cycles for failure). In low-cycle fatigue the strains are larger than the elastic limit and the number of cycles to failure is relatively less (e.g., reinforcing steel may need less than 100 cycles at 2% strain and less than five at 6% strain). Strain amplitudes are seldom constant in real life loads and more so for seismic loads. Based on Miner's rule (Miner 1945), the following linear damage accumulation model is commonly used to predict the fatigue failure:

$$DI = \sum_{i=1}^{n} \frac{1}{2N_{fi}(\varepsilon_{ai})} \tag{2-15}$$

where $DI =$ damage index, $2N_{fi} =$ the number of half-cycles to failure at the strain amplitude ε_{ai} of the i^{th} half-cycle, and $n =$ the number of half-cycles at which DI is computed. The value of DI indicates the fatigue damage in the material and for a perfect damage model the material should fail if $DI \geq 1.0$. This formulation is applicable for both constant and variable strain amplitude.

The curvature capacity of an RC section is defined as the curvature at which either the reinforcing steel or the concrete reaches its failure strain. A typical well designed RC column in as-built condition is most likely to fail due to excessive compressive strain in the confined concrete caused by bending of the column. However, with the accumulation of low-cycle fatigue damage, the rupture of the longitudinal steel may govern the failure of the RC section. The degradation in curvature capacity of RC sections due to low-cycle fatigue of the longitudinal steel is expected to follow the curve shown in Figure 2-1. In the figure, ϕ_u and ϕ_u' are the ultimate curvature capacities of the undamaged and the damaged section, respectively and DI is the low-cycle fatigue damage in the longitudinal steel. The parameter DI_{tr} is the threshold value of DI such that for $DI \leq DI_{tr}$, the failure of the RC section is due to the compressive failure of the concrete and for $DI > DI_{tr}$, the failure of the section is due to the rupture of the longitudinal steel. The variable DI_{tr} is a characteristic of the column section and does not depend on the drift histories.

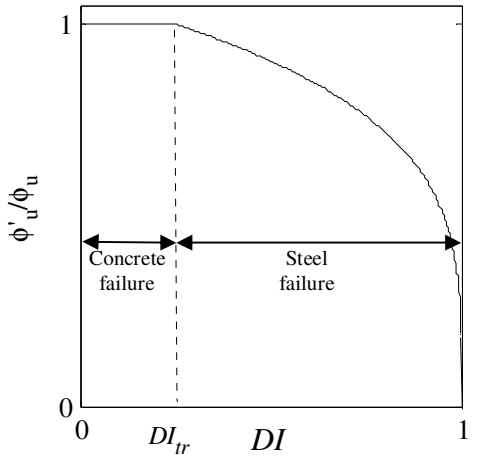

Figure 2-1. Deterioration in curvature capacity

Using Eqs (2-14) and (2-15), the failure strain for a material with $DI > 0.0$ is derived next. The idea behind the derivation is to compute ε_f as the strain amplitude that causes an incremental damage equal to the remaining damage $(1-DI)$ in one quarter of a cycle (i.e., equivalent to a single pushover). Thus, ε_f is just enough to make DI equal to 1.0 in a single pushover. For a given DI, an expression is derived for the strain amplitude ε_f that causes failure (i.e., it causes damage equal to $1-DI$) in a quarter cycle. It can be written from Eq. (2-15) that

$$\left(1-DI\right)=\frac{0.5}{2N_f} \tag{2-16}$$

where the value 0.5 is used in the fraction $0.5/2N_f$ because it is assumed that the failure is caused by the loading part of the cycle (or one quarter cycle). This assumption is made to be consistent with the definition of deformation capacity of RC columns

(Gardoni et al. 2002), where the failure is assumed to occur in a single pushover. If the failure is assumed to take place in one half-cycle (i.e., considering both loading and unloading) then the fraction in Eq. (2-16) should be equal to $1/2N_f$. Substituting the expression for $2N_f$ from Eq. (2-16) in Eq. (2-14) the following is obtained:

$$\varepsilon_f = c_1\left(\frac{0.5}{1-DI}\right)^{c_2} \tag{2-17}$$

It can be verified that by using either 1.0 or 0.5 in Eq (2-16) that the value of ε_f changes only by a factor of 1.28. This implies that the assumption of whether the failure occurs in a quarter cycle or a half cycle is not expected to have significant effects.

The values of c_1 and c_2 used in this study are 0.07 and −0.31, respectively, as found by Brown and Kunnath (2004) for bars with diameter of 28.5 mm (#9 bars). The values of c_1 and c_2 are currently available in the literature (Mander et al. 1994; Brown and Kunnath 2004) only for bars with diameter 15.9 mm - 28.5 mm (#5 - #9 bars). Since larger bar sizes are more appropriate for typical Caltrans designs (Caltrans 2006), we use the values of c_1 and c_2 for #9 bars. These values are practically the same as those for #8 bars but different from those for smaller bar sizes. Therefore, the proposed model is applicable to columns with #8 and #9 bars. Further research is needed to verify the values of c_1 and c_2 for larger bar sizes more representative of Caltrans design specifications and design practice.

2.4 Virtual experiments

A database of sample RC columns is created to represent the material and geometric properties of current seismic design specifications. Table 2-3 shows the range of the 10

basic column properties that are sufficient to characterize an RC bridge column. The ranges of the column properties are chosen based on parameters for Caltrans single-bent overpass bridges provided by Mackie and Stojadinović (2005). To maximize the information content of the database and minimize the required number of columns, combinations of values of the column properties are selected using the D-optimal experimental design method (Atkinson and Donev 1992). The goal of the D-optimal design method is to minimize the determinant of the sample covariance matrix of the design parameters (here the column properties). As a rule of thumb, the size of a sample needs to be at least 5 times the number of the design parameters. Therefore in this experimental design uses a sample size of 60 RC columns.

Table 2-3. Ranges of the column properties in the experimental design

Parameter	Symbol	Range	Units
Height	H_c	3.988-10.008	M
Diameter	D_c	0.44-2.50	M
Longitudinal reinforcement ratio	ρ_{sl}	1.0-4.2	%
Transverse reinforcement ratio	ρ_{sv}	0.278-1.170	%
Compressive strength of concrete	f_c'	20.00-55.02	MPa
Yield strength of steel	f_y	275.10-519.87	MPa
Ultimate strength of steel	f_u	482.63-689.48	MPa
Clear cover	$cover$	35.0-100.0	Mm
Axial load ratio[a]	P_r	0.03-0.15	-
Aspect ratio	H_c / D_c	4.0-9.0	-

[a] $P_r = 4P_u / (\pi f_c' D_c^2)$, where P_u is the axial load on the column.

2.4.1 Finite element model of RC bridge columns

Several cyclic load tests on a variety of RC columns have been conducted in the past research and the test data can be found in the database compiled by Taylor et al. (2003). However, the database does not report all the information (e.g., number of cycles to failure) that is needed to develop a model for the degradation of the deformation capacity of RC columns. Therefore, virtual experiments are performed using FE model of RC columns in OpenSees (McKenna et al. 2008).

Various material models are available in OpenSees to model the cyclic behavior of RC components. We use the force-based *nonlinearBeamColumn* element to model the columns. Based on a sensitivity study it is found that two elements, each of about half the total length of the column, provide a good accuracy of the model while being computationally inexpensive. The sensitivity study is conducted by comparing the laboratory hysteresis data of RC columns with the results from the FE analysis. The cross section of each column is divided into 20-40 radial slices depending on its size and the number of bars. The column is modeled as a vertical cantilever with fixed base. The material models for the reinforcing steel and the concrete are chosen to account for the relevant phenomena that contribute to the structural degradation. The unconfined cover concrete and the confined core concrete are modeled separately by incorporating a uniaxial concrete model developed by Hoshikuma et al. (1997) in the concrete model *Concrete02* available in OpenSees. The deterioration in stiffness of concrete is captured by the hysteretic behavior of *Concrete02*. A trilinear uniaxial material model called *Hysteretic* capable of simulating strength deterioration, stiffness deterioration and

pinching is used to model the reinforcing steel. The strength and stiffness deterioration in the reinforcing steel is captured by two material parameters, namely *Damage1* and *Damage2*, in *Hysteretic*. *Damage1* captures the degradation due to ductility based damage and *Damage2* captures degradation due to energy dissipation. The effect of these parameters on the strength and stiffness degradation is described in the OpenSees user's manual (OpenSees 2009). The degradation parameters of the material *Hysteretic* are calibrated by minimizing the residual sum of the squares to mimic the hysteresis data in seven selected columns tested by El-Bahy et al. (1999a,b) that were designed following the current Caltrans design specifications and hence comply with current seismic practices. The uniaxial fatigue material model, *Fatigue* (Patxi 2005), is used to monitor the fatigue damage in the steel. The material *Fatigue* can be used along with any other material to record fatigue damage in that material. The value of DI is recorded using the function *damage recorder*. *Fatigue* computes the value of DI for a given strain history by using a linear damage accumulation model shown in Eqs (2-14) and (2-15). The required values of c_1 and c_2 are provided by the user and are discussed in the next section.

2.4.2 Cyclic load tests of RC columns

In order to generate the data for the degradation in the curvature capacity of RC column sections, the columns are subjected to cyclic loading. The columns are subjected to cycles of constant amplitude equal to 2-4 times the yield displacement for the columns. The use of constant amplitude cycles does not limit the applicability of the model developed hereafter. This is because the degraded curvature and deformation capacity

does not depend on the past deformation histories if the current value of damage DI is known.

In the conducted virtual experiments, the value of DI is recorded after a specified number of cycles and then a static pushover is performed until the curvature in the bottom most section reaches ϕ_u'. A total of 800 such virtual experiments are conducted to generate the pairs of values of the reduced curvature capacity ϕ_u' and the corresponding DI in the longitudinal steel. Figure 2-2 is obtained by plotting the data such that the vertical axis represents the ratio ϕ_u'/ϕ_u and the horizontal axis represents DI. In the range $DI \le DI_{tr}$ (the initial horizontal part) ϕ_u'/ϕ_u is found to vary between 0.85 and 1.05. It is also found that at the end point of the curve (i.e., at DI =1.0) ϕ_u'/ϕ_u varies between 0.0 and 0.1. This observation is a deviation from the expected behavior shown in Figure 2-1. It is found that this deviation happens because of the existence of strains in the longitudinal steel at the beginning of the pushover (i.e., at column displacement = 0). Therefore, in the presence of these strains in the steel, ε_f does not exactly correspond to the strain amplitude that causes failure. This effect of strain in the longitudinal steel at

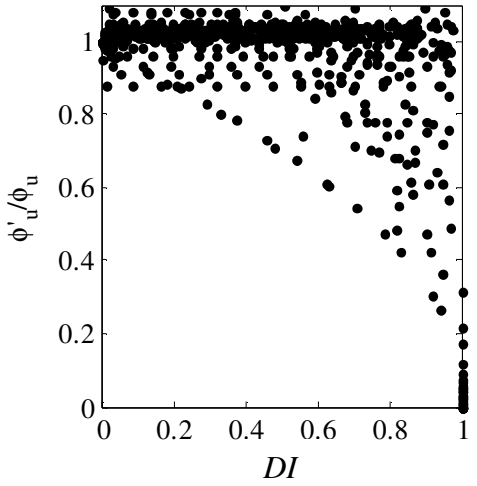

Figure 2-2. FE data for degradation in curvature capacity of RC column sections due to low-cycle fatigue of longitudinal steel

the beginning of pushover is considered to be insignificant in the calibration of the proposed model introduced in the next section. Furthermore, neglecting this effect allows keeping the model simple while maintaining a good accuracy. The model developed hereafter is a function of *DI* , therefore, its applicability is not limited by the drift histories used to induce the damage.

2.5 Proposed probabilistic model for deterioration in curvature capacity

Several mathematical functions can capture the behavior shown in Figure 2-2. However, a good mathematical model must be based on the underlying physical phenomena. The model form shown below is selected because it follows the fatigue formulation in Eq.(2-17) and thus can be justified based on the underlying fatigue phenomenon causing the deterioration.

$$\phi_u'\left(\mathbf{x}',\boldsymbol{\Theta}_\phi\right)=\phi_u\times\begin{cases}1.0 & 0.0\le DI<DI_{tr}\\ \left[\dfrac{1-DI}{1-DI_{tr}\left(\mathbf{x},\boldsymbol{\theta}_\phi\right)}\right]^{\eta}+\sigma_\phi\varepsilon_\phi & DI_{tr}\le DI\le 1.0\end{cases} \tag{2-18}$$

and

$$DI_{tr}\left(\mathbf{x},\boldsymbol{\theta}_\phi\right)=\sum_{i=1}^{n}\theta_{\phi i}h_{\phi i}\left(\mathbf{x}\right) \tag{2-19}$$

where $\boldsymbol{\Theta}_\phi=(\boldsymbol{\theta}_\phi,\eta,\sigma_\phi)$ is a vector of unknown model parameters, $\boldsymbol{\theta}_\phi=(\theta_{\phi 1},\theta_{\phi 2},...,\theta_{\phi n})$, $\mathbf{x}=$a vector of structural properties of the undamaged RC column, $\mathbf{x}'=$represents the damaged RC column, $h_{\phi i}(\mathbf{x})=$explanatory functions used to capture the dependency of DI_{tr} on $\mathbf{x}$, $n=$number of explanatory functions and $\sigma_\phi\varepsilon_\phi=$the model error, where $\sigma_\phi=$the standard deviation of the model error which is assumed not to depend on $\mathbf{x}$ (homoskedasticity assumption) and $\varepsilon_\phi=$a random variable with the standard normal distribution (normality assumption). Diagnostic plots of the data versus the individual regressors (Rao and Toutenburg 1997) are used to verify these two assumptions within the range of the data. The model in Eq. (2-18) shows that an RC column with lower values of DI_{tr} is more vulnerable to degradation by low-cycle fatigue than columns with higher values of DI_{tr}.

In order to develop the proposed model, the expression for $DI_{tr}(\mathbf{x},\boldsymbol{\theta}_\phi)$ in Eq. (2-19) is constructed starting from a complete second-order polynomial using the combinations of six functions: $\varepsilon_{cu}=$compressive strain at failure for concrete (negative in compression, e.g., -0.03), $\mu_c=$the ductility ratio, $H_c/D_c=$the aspect ratio,

$\rho_{sl}(\%)$ = the longitudinal reinforcement ratio, f_y / f_c' and ϕ_u / ϕ_y, where ϕ_y = curvature at yield of the longitudinal steel. All the functions are dimensionless so that the model can be used in any system of units.

We begin a model selection process to retain the minimum number of $h_{\phi i}(\mathbf{x})$ in Eq. (2-19) for an accurate, unbiased and parsimonious model. For this purpose, after a preliminary selection of terms using engineering judgment, a step-wise deletion process following Gardoni et al. (2002) is conducted to reduce the number of elements. In this method, the Bayesian updating rule (Box and Tiao 1992) is used to estimate $\boldsymbol{\Theta}_\phi$ in the model described by Eqs. (2-18) and (2-19) for a chosen set of $h_{\phi i}(\mathbf{x})$. Extensive description of Bayesian updating method to develop probabilistic models can be found in Gardoni et al. (2002). Bayesian updating is a highly effective tool for statistical regression equally applicable to linear and nonlinear models without any significant difference in the formulation. It can also be used to update an existing model using newly available data (Choe et al. 2007).

In the stepwise deletion process, in each step $\boldsymbol{\Theta}_\phi$ is estimated for a given set of $h_{\phi i}(\mathbf{x})$ and an element from the set is deleted such that σ_ϕ does not show a sudden increase. As the elements are deleted, σ_ϕ increases indicating that the model accuracy is decreasing. The deletion process is stopped when σ_ϕ is unacceptable. The functions retained in the model are the constant 1.0, ε_{cu}, ρ_{sl}, and $(\phi_u / \phi_y)(f_y / f_c')$. Therefore, the final expression for DI_{tr} is

$$DI_{tr}\left(\mathbf{x}_{\phi},\boldsymbol{\theta}_{\phi}\right)=\theta_{\phi 1}+\theta_{\phi 2}\varepsilon_{cu}+\theta_{\phi 3}\rho_{sl}+\theta_{\phi 4}\left(\frac{\phi_u}{\phi_y}\right)\left(\frac{f_y}{f_c'}\right) \tag{2-20}$$

Table 2-4 shows the posterior statistics of $\boldsymbol{\Theta}_{\phi}$ estimated using importance sampling and non-informative prior distribution (Gardoni et al. 2002). It can be seen from Eq. (2-20) that an increase in $|\varepsilon_{cu}|$ (that also leads to an increase in ϕ_u) decreases the value of DI_{tr} and a decrease in ρ_{sl} decreases the value of DI_{tr}. These observations are supported by the fact that ductile RC columns, which are well confined (i.e., high $|\varepsilon_{cu}|$) and under-reinforced (i.e., small ρ_{sl}), like seismically designed bridge columns, are vulnerable to low-cycle fatigue.

Figure 2-3 shows the comparison between the mean predictions from the probabilistic model and the observations in the virtual experiments. For a perfect model, the black dots (•) would line up along the dashed 1:1 line. However, all the black dots do not lie on the dashed 1:1 line indicating the presence of modeling error captured by $\sigma_{\phi}\varepsilon_{\phi}$. The error for a given predicted value is the vertical distance between the corresponding black dot and the 1:1 line. The dotted lines on both sides of the 1:1 line represent the prediction bounds and are drawn at a vertical distance $\pm\sigma_{\phi}$ from the 1:1 line.

Table 2-4. Posterior means and standard deviations of the unknown parameters in the probabilistic curvature capacity degradation model

Parameters	$\theta_{\phi 1}$	$\theta_{\phi 2}$	$\theta_{\phi 3}$	$\theta_{\phi 4}$	η	σ_{ϕ}
Mean	0.690	–30.176	0.031	–0.002	0.266	0.168
Standard Deviation	0.0143	3.277	0.007	0.0002	0.0210	0.010
Correlation Coefficient						
$\theta_{\phi 1}$	1.00					
$\theta_{\phi 2}$	–0.65	1.00				
$\theta_{\phi 3}$	–0.71	0.81	1.00			
$\theta_{\phi 4}$	–0.71	0.82	0.85	1.00		
η	0.10	–0.10	0.68	–0.11	1.00	
σ_{ϕ}	–0.46	0.26	0.10	0.26	–0.20	1.00

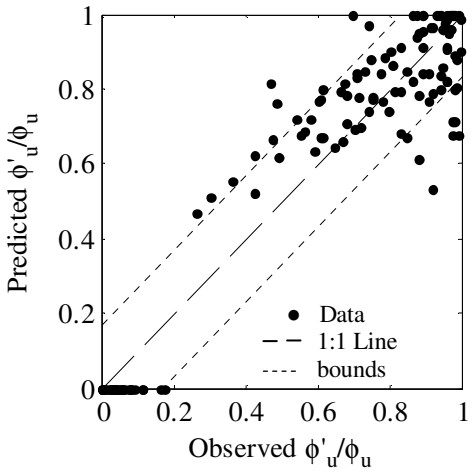

Figure 2-3. Predictions of the probabilistic model for degradation of curvature capacity

2.6 Degradation in the deformation capacity of RC columns and fragility estimates

The deformation capacity of an RC column is defined as the drift of the column at which either the concrete or the steel reaches its ultimate strain. This study proposes a deformation capacity model for degrading RC columns as a function of *DI* by incorporating the proposed model for ϕ_u' into the deformation capacity model of undamaged RC columns originally developed by Gardoni et al. (2002) and updated for additional data by Choe et al. (2007). Then, the proposed degraded deformation capacity model is used to assess the fragility of three example RC columns for given deformation demands.

2.6.1 Deformation capacity model

The probabilistic deformation capacity model for an undamaged RC columns as developed by Gardoni et al. (2002) and Choe et al. (2007) is as follows:

$$C_\delta(\mathbf{x},\boldsymbol{\Theta}_c) = \ln\left[\hat{\delta}_c(\mathbf{x})\right] + \gamma_c(\mathbf{x},\boldsymbol{\theta}_c) + \sigma_c\varepsilon_c \tag{2-21}$$

where $C_\delta(\mathbf{x},\boldsymbol{\Theta}_c)$ is the natural logarithm of deformation capacity, $\boldsymbol{\Theta}_c = (\boldsymbol{\theta}_c, \sigma_c)$ is a vector of model parameters calibrated using experimental data, and $\boldsymbol{\theta}_c = (\theta_{c,1}, \theta_{c,2}, ..., \theta_{c,j})$. The model consists of a deterministic model $\hat{\delta}_c(\mathbf{x})$, bias correction term $\gamma_c(\mathbf{x},\boldsymbol{\theta}_c)$, and model error $\sigma_c\varepsilon_c$. The deterministic model is given as

$$\hat{\delta}_c = \frac{\hat{\Delta}}{H} \tag{2-22}$$

$$\Delta = \hat{\Delta}_f + \hat{\Delta}_s + \hat{\Delta}_{sl} \tag{2-23}$$

where $\hat{\Delta}$ = the displacement capacity, $\hat{\Delta}_f$, $\hat{\Delta}_s$ and $\hat{\Delta}_{sl}$ = the flexural, shear and slip components in the displacement capacity, where

$$\hat{\Delta}_f = \hat{\Delta}_y + \hat{\Delta}_p \tag{2-24}$$

$$\hat{\Delta}_y = \frac{1}{3}\phi_y L_{eff}^2 \tag{2-25}$$

$$\hat{\Delta}_p = \left(\phi_u - \phi_y\right) L_p L \tag{2-26}$$

$L_{eff} = H_c + 0.022 f_y d_b$, d_b = diameter of the longitudinal bar, L_p = the length of plastic hinge, and $L = (H_c - L_p)$. In this study, the degradation in Δ_s and Δ_{sl} due to cyclic loading is not modeled. This is because the degradation model is developed for flexural RC columns which are most susceptible to low cycle fatigue. In flexure dominated columns, Δ_s and Δ_{sl} are insignificant compared to Δ_f. It is also noted that the effects of cyclic loading and low-cycle fatigue on Δ_s and Δ_{sl} is still not well understood.

The bias correction part $\gamma_c(\mathbf{x}, \boldsymbol{\theta}_c)$ is written as

$$\gamma_c\left(\mathbf{x}, \boldsymbol{\theta}_c\right) = \theta_{c1} + \theta_{c2}\frac{4V}{\pi D^2 f_t'} + \theta_{c3}\frac{\rho_s f_{yh}\left(D_c - 2cover\right)}{f_c' D_c} + \theta_{c4}\varepsilon_{cu} \tag{2-27}$$

where V = the shear force at yield of the column and f_t' = the rupture modulus of concrete given by $0.5\sqrt{f_c'}$ in MPa units. The statistics of the model parameters $\boldsymbol{\Theta}_\delta$ can be found in Choe et al. (2007). It can be seen that the capacity depends on the values of ϕ_u and ϕ_y Eq. (2-26) of the plastic hinge zone that develops at the base for a single bent bridge column. Writing $\boldsymbol{\Theta}_c' = (\boldsymbol{\Theta}_\phi, \boldsymbol{\Theta}_c)$, the degraded deformation capacity $C_\delta(\mathbf{x}', \boldsymbol{\Theta}_c')$ is

obtained by replacing ϕ_u by $\phi_u'(\mathbf{x}', \boldsymbol{\Theta}_\phi)$ (computed using Eq.(2-18)) in the formulation for $C_\delta(\mathbf{x}, \boldsymbol{\Theta}_c)$. The effect of degradation on ϕ_y is not considered in the model as it is found that the contribution of ϕ_y is insignificant compared to that of ϕ_u. Therefore the original value of ϕ_y is retained in the model.

2.6.2 Fragility estimates

Fragility is defined as the conditional probability of attaining or exceeding a specified limit state for a given set of boundary conditions. Following Gardoni et al. (2002), the predictive fragility of an RC column conditioned on the deformation demand D_δ is computed as

$$\hat{F}\left(DI, D_\delta\right) = \int P\left[g\left(\mathbf{x}', \boldsymbol{\Theta}_c', DI\right) \le 0 \middle| \boldsymbol{\Theta}_c', DI, D_\delta \right] f\left(\boldsymbol{\Theta}_c'\right) d\boldsymbol{\Theta}_c' \tag{2-28}$$

where

$$g\left(\mathbf{x}', \boldsymbol{\Theta}_c', DI\right) = C_\delta\left(\mathbf{x}', \boldsymbol{\Theta}_c'\right) - D_\delta \tag{2-29}$$

The fragility $\hat{F}(DI, D_\delta)$ captures the uncertainty in the random variables $\mathbf{x}$ and the model parameters $\boldsymbol{\Theta}_c'$. The values of the fragilities are computed using software FERUM (Haukaas et al. 2003) using the First Order Reliability Method (FORM) (Ditlevsen and Madsen 1996).

The fragilities are computed for 3 different example columns (A, B, and C) with basic and derived properties described in Table 2-5 and Table 2-6. This example studies the effects of ductility of seismically designed RC bridge columns. For this purpose all the basic structural properties, except ρ_{sv}, are kept same in all the three columns. As

shown in Table 2-6, the value of $|\varepsilon_{cu}|$ for Column A is four times larger than the values of $|\varepsilon_{cu}|$ for Columns C and twice as that of Column B due to the proportionally higher value of ρ_{sv}. The value of ϕ_u / ϕ_y for Column A is about four times the value for Column C and about three times that of Column B. This is a direct consequence of the differences in the values of $|\varepsilon_{cu}|$. Finally, based on Eq. (2-20) the values of DI_{tr} for Columns A, B and C are found to be 0.50, 0.80, and 0.90 respectively.

Table 2-5. Basic properties of the example columns for the fragility analysis

Parameter	Symbol	Column A	Column B	Column C	Units
Height	H_c	3.988	3.988	3.988	m
Diameter	D_c	0.443	0.443	0.443	m
Longitudinal reinforcement ratio	ρ_{sl}	2.0	2.0	2.0	%
Transverse reinforcement volumetric ratio	ρ_{sv}	1.0	0.6	0.3	%
Compressive strength of concrete	f_c'	20.00	20.00	20.00	MPa
Yield strength of steel	f_y	517.11	517.11	517.11	MPa
Ultimate strength of steel	f_u	689.47	689.47	689.47	MPa
Clear cover	$cover$	0.025	0.025	0.025	m
Axial load ratio	P_r	0.07	0.07	0.07	-

Table 2-6. Derived properties of the example columns for the fragility analysis

Parameter	Symbol	Column A	Column B	Column C
Ultimate concrete strain	ε_{cu}	–0.033	–0.018	–0.009
Ratio of ultimate to yield curvature	ϕ_u / ϕ_y	12.17	4.62	3.40
Ratio of yield s$V_y$trength of steel to compressive strength of concrete	f_y / f_c'	26.00	26.00	26.00
Transition point	DI_{tr}	0.50	0.80	0.90

For each column the fragilities are computed for different damage levels to show the effect of deterioration on the failure probability. The uncertainty in $\mathbf{x}$ is modeled by assuming that f_c', f_y and P_r are lognormally distributed random variables with means as shown in Table 2-5 and coefficient of variation (COV) equal to 10%, 5% and 25%. Figure 2-5 shows the fragility results for the three example columns. It can be seen that the fragilities do not change for *DI* values less than DI_{tr}. This is because for $DI \le DI_{tr}$, concrete governs the deformation capacity (i.e., $\phi_u' = \phi_u$). It is also found that once DI exceeds DI_{tr} the fragilities increase significantly with DI. Therefore, high values of DI_{tr} can help preserve the original fragility of the columns.

2.7 Conclusions

This section emphasizes the importance of considering the occurrence of more than one damaging earthquake in seismic design. We compute the probability of observing more than one damaging earthquake in a bridge's service life considering both main and after-shocks. We use a time-independent Poisson process to model the occurrence of the main shocks and a time-dependent Poisson process for the aftershocks. Furthermore, we develop probabilistic models for computing degraded curvature capacity of reinforced concrete (RC) sections and the deformation capacity for RC bridge columns as a function of cumulative low-cycle fatigue damage. These degradation models are developed based on cyclic load tests conducted using finite element (FE) models of RC columns.

It is found that the probability of observing more than one damaging earthquake in a bridge's life time is nearly equal to the probability of observing exactly one damaging earthquake. It is also noted that the probability of observing more than one damaging earthquake increases with the service life of a bridge. As sustainability continues to become central to the design of infrastructure systems due to the limited resources and the growing environmental concerns and the design life is expected to lengthen, design criteria for infrastructure systems based on performance objectives spanning more than one seismic event are needed. Furthermore, it is found that ductile bridge columns are vulnerable to low-cycle fatigue degradation. This is because it is found that the structural parameters that enhance ductility, in particular compressive strain at failure for concrete and the ratio between the ultimate curvature capacity and the curvature at yielding of the longitudinal steel, make the RC columns more vulnerable to degradation due to low-cycle fatigue.

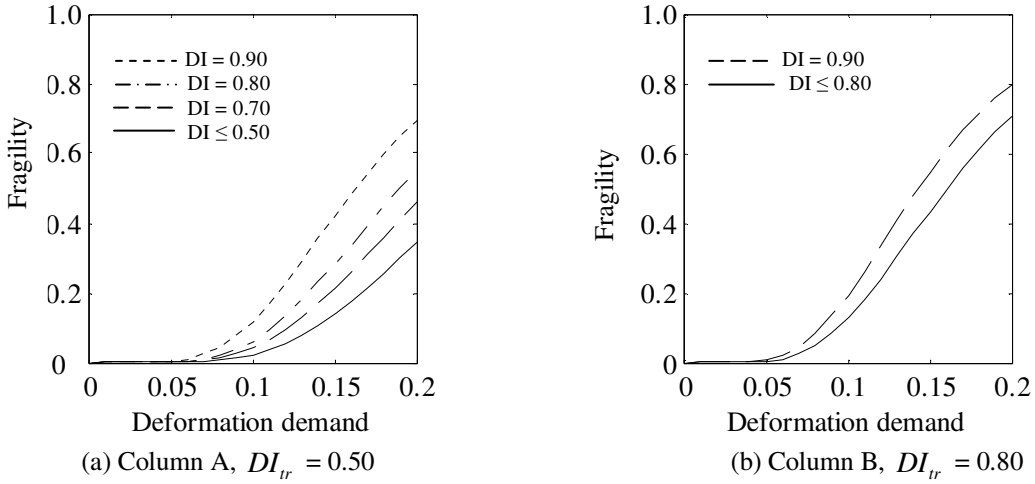

Figure 2-4. Predictive degrading fragilities of three example RC columns

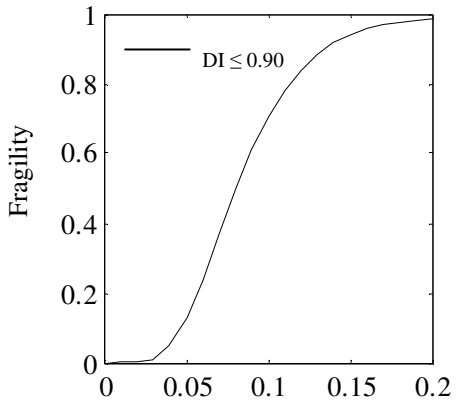

(c) Column C, DI_{tr} = 0.90

Figure 2-4, continued.

The proposed model for degradation in deformation capacity is used to assess the fragility of three example RC columns that are affected by low-cycle fatigue damage conditioning on the value of damage and deformation demand. It is found that, the fragilities of RC columns for given deformation demand increases significantly with the increase in the value of fatigue damage (here captured through a damage index). It is also seen that fragilities of ductile RC columns increase faster than the non-ductile columns. The proposed model computes the degraded deformation capacity as a function of Damage Index (*DI*) and the fragilities are conditioned on the values of *DI* and deformation demand. Therefore, further research must be conducted to estimate *DI* for a given earthquake.

3. SEISMIC DEGRADATION OF STATIC PUSHOVER PROPERTIES OF RC BRIDGE COLUMNS AND ITS EFFECT ON THE VULNERABILITY OF RC BRIDGES

3.1 Introduction

The previous section showed that it is important to assess the seismic vulnerability of seismically degraded structures because there is a considerable probability of multiple damaging earthquakes in a structure's service life. The section computed the increase in fragility of RC bridge columns due to low-cycle fatigue damage DI to longitudinal reinforcing steel. Low-cycle fatigue primarily affects the longitudinal steel and results in the degradation of deformation capacity of RC columns. However, cyclic seismic loads are also expected to affect the future seismic deformation demand which is not captured by the low-cycle fatigue model. Moreover the pervious section did not compute the value of DI resulting from an earthquake.

This section proposes the probabilistic models to predict the seismic degradation in RC bridge columns. The first model predicts the degradation in the static pushover properties of a column; in terms of the degradation in the lateral stiffness K and the shift in the yield point (Δ_y, V_y), where Δ_y is the displacement at yield, V_y is the shear force at yield and $V_y = K\Delta_y$. The prediction of static pushover properties of bridge columns is important because the change in seismic response of an RC bridge can be predicted by modeling the change in static pushover curve of the RC columns. The degradation of the static pushover curve is primarily due to the degradation in the

stiffness and the strength of concrete caused by its internal cracking. The second model predicts the value of *DI* in the longitudinal reinforcing steel resulting from an earthquake which is required to compute the degradation in deformation capacity of RC bridge columns.

The data required to develop the proposed models is generated by conducting virtual experiments, where nonlinear time-history analysis (NTHA) are conducted. In the NTHA, dynamic analyses of RC highway bridges are performed using a selected set of ground motion records in OpenSees (Mackenna and Fenves 2000). The generated data is then used in statistical regression using Bayesian updating method.

This section is organized into six major subsections including this introduction. The second subsection presents the design of virtual experiments. Here, we discuss the FE modeling of RC bridges, the procedure of selecting bridge parameters and the ground motion records and generation of degradation data using static pushover analysis and NTHA. The third subsection describes the development of the probabilistic models using Bayesian updating. Thereafter, the fourth subsection presents the formulation to estimate the seismic fragility of structures that have experienced degradation during past earthquakes. The fifth subsection presents an example estimation of the seismic fragility of an RC highway bridge that has experienced one earthquake in the past accounting for low-cycle fatigue damage and degradation of static pushover properties of the bridge column. Finally, the sixth subsection presents conclusions from this section.

3.2 Virtual experiments

To generate the degradation data, we conduct 1200 virtual experiments in which we perform NTHA of representative RC bridges for selected ground motions and static pushover analyses of the RC bridges before and after the NTHA. The analyses are conducted using the FE software OpenSees (Mackenna and Fenves 2000). The representative bridges and ground motions capture the variability in the structural properties, site properties and ground motion parameters. We use the experimental design in Table 3-1 developed by Huang et al. (2010) that represents RC bridges with one single-column bent designed as per Caltrans seismic design specifications (Caltrans 2006). This experimental design was originally created for developing the probabilistic seismic demand model for RC bridges with one single-column bent. The experimental design consists of 60 RC bridges with one single-column bent characterized by 12 independent parameters and 200 ground motions that are characterized by; site-to-source distance, magnitude of earthquake, type of soil and scaling of ground accelerations. The ground motions are assigned randomly to the bridges without reassigning the ground motions. The details regarding the ground motion records can be found in Huang et al. (2010).

Table 3-1. Range of bridge design parameters used in virtual experiments

Parameter	Symbol/ Formula	Range	Units
Skew angle	α^s	0 – 30	degrees
Shorter Span	L_1	18.0 – 55.0	m
Span ratio	L_2 / L_1	1.0 – 1.5	-
Column height	H_c	5.0 – 11.0	m
Ratio of column diameter to super structure depth	D_c / D_s	0.67 – 1.33	-
Yield strength of longitudinal steel	f_y	276 - 655	MPa
Compressive strength of concrete	f_c'	20.0 – 55.0	MPa
Longitudinal reinforcement ratio	ρ_{sl}	1.0 – 4.0	%
Volumetric ratio of transverse steel	ρ_{sv}	0.4 – 1.1	%
Additional bridge deadload	wt	10 – 75 % of self weight	-
Soil type†	Soil	A,B,C,D (USGS)	-
Abutment model	Abutment	A, B, C, D,E, F, G	-

† Refer to Huang et al. (2010) for soil classification

3.2.1 Finite element model of RC bridges with one single-column bent

Figure 3-1 shows the FE model of RC bridges considered in the virtual experiments. The figure shows an RC bridge consisting of 4 major parts: one single-column bent, one two-span deck, two abutments and one pile foundation. The column has height H_c and a circular cross-section of diameter D_c. The cross-section of the column is modeled using an uniaxial fiber-section model available in OpenSees to model RC sections. The cross-section is divided into an inner core and an outer concentric circular strip representing the cover region. Both the core and the cover region are divided into 20-40 radial segments based on the convergence of pushover results. The strain-displacement relations for the column are modeled using the element *nonlinearBeamColumn* which is based on Euler-Bernoulli beam theory. The shear and torsional behavior of the RC

column is modeled by coupling elastic shear and torsion with *nonlinearBeamColumn* using the object *section Aggregator*. The concrete in the core of the RC column is modeled using material model *concrete02*. The stress-strain values corresponding to yield and ultimate state for confined core concrete are computed using the constitutive model developed by Hoshikuma et al. (1997). The reinforcing steel is modeled using the bilinear model *Steel01*. The deck consists of two spans with L_1 and L_2 being the lengths of the shorter and the longer span. The deck is modeled as an elastic beam using *nonlinearBeamColumn* element and an elastic uniaxial material. The structural properties pertaining to torsion and shear of the deck are computed using the area of deck, the modulus of elasticity and the shear modulus of concrete. Seven different types of abutments are modeled using seven different abutment models following Huang et al. (2010). The abutment models are: a simple roller support model (Type A); Caltrans (2000) model (Type B), two models by Maroney et al (1994) with mass participation (Type C) and without mass participation (Type F), Wilson and Tan (1990) model (Type D), and two models by Zhang and Makris (2001) with mass participation (Type E) and without mass participation (Type G). The pile is modeled as an extension of the column into the soil strata. The materials, fiber section and the elements used for the column are also used for the pile. The soil around the pile is modeled using elastic-perfectly plastic springs. The soil stiffness used for springs can be found in Huang (2010). The topmost point of the column is considered as fixed to the deck and the lowermost point is fixed to the top of the pile. The lowermost point of the pile is connected to a pinned support.

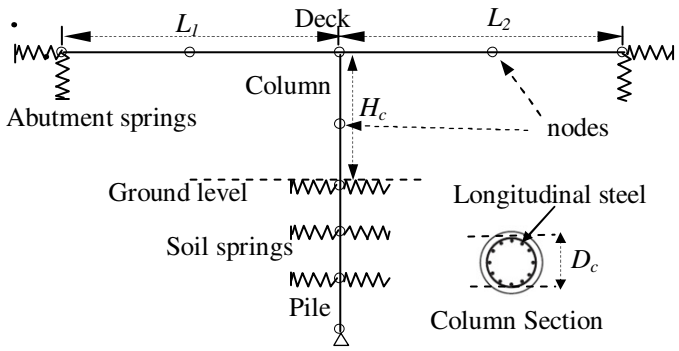

Figure 3-1. FE model of RC bridge with one single-column bent

3.2.2 Degradation data for static pushover properties and low-cycle fatigue

The developed FE models for RC bridges are subject to NTHA for the selected set of ground motions to induce seismic degradation. To obtain the degradation data for the static pushover properties, we conduct one static pushover analysis before and another immediately after the NTHA. From the results of two pushover analyses, the values of the ratios K'/K, V_y'/V_y and Δ_y'/Δ_y are obtained, where the prime sign in K', V_y' and Δ_y' indicates the post-earthquake state. The values of K, V_y, Δ_y, K', V_y' and Δ_y' are obtained by fitting an elastic-perfectly-plastic curve to the static pushover curves using the method of least squares. Figure 3-2, Figure 3-3 and Figure 3-4 show the

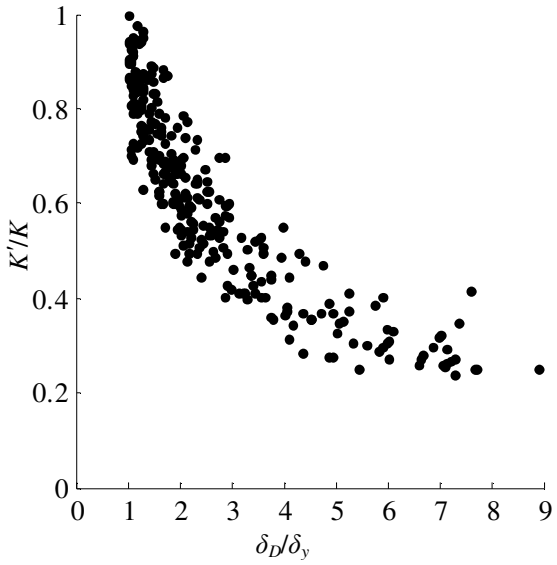

Figure 3-2. Data showing the value of K'/K with respect to δ_D/δ_y

values of K'/K, V_y'/V_y and Δ_y/Δ_y' (the reciprocal of Δ_y'/Δ_y) with respect to the seismic ductility demand δ_D/δ_y, where δ_D is the maximum drift (displacement to height ratio) during an earthquake and $\delta_y = \Delta_y/H$. Figure 3-2 and Figure 3-3 show that the values of K'/K and V_y'/V_y decrease with the increase in δ_D/δ_y. These phenomena are often termed as stiffness and strength degradation, respectively. Figure 3-4 shows that Δ_y/Δ_y' also decreases when δ_D/δ_y increases. This is a direct consequence of the well known relation $V_y = K\Delta_y$ and $V_y' = K'\Delta_y'$, and the fact that V_y'/V_y decreases less than K'/K as a function of δ_D/δ_y and remains close to 1.0, as shown in Figure 3-3. It can be seen in Figure 3-5 that the values of K'/K and Δ_y/Δ_y' are highly positively correlated. This is because V_y'/V_y remains close to 1.0. Note that the data are shown

only for $\delta_D / \delta_y > 1$ and we do not use the data corresponding to $\delta_D / \delta_y \leq 1$ to calibrate the degradation models. This is because in this range the column is theoretically in the elastic range but the measured values of K'/K, Δ_y / Δ_y' and V_y'/V_y show small random deviations from 1.0 resulting from the process of obtaining the least squares fit.

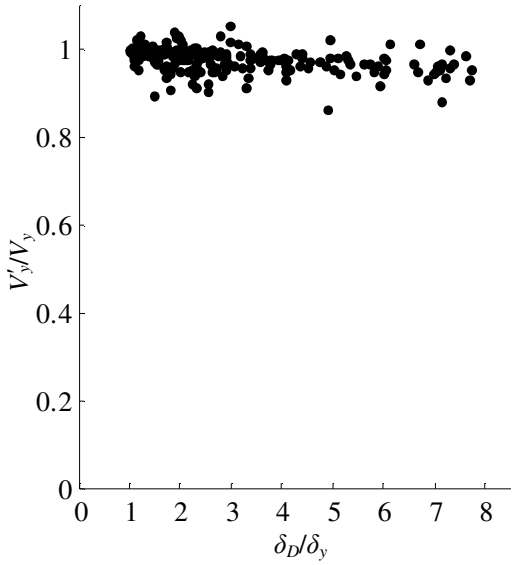

Figure 3-3. Data showing the value of in V'/V_y with respect to δ_D / δ_y

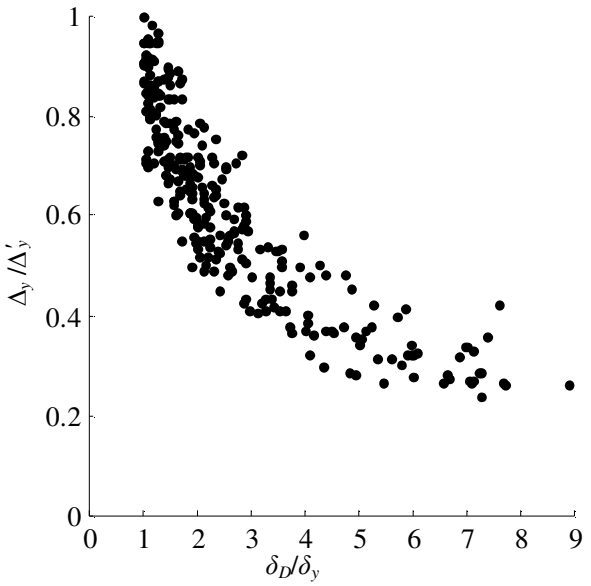

Figure 3-4. Data showing the change in Δ_y / Δ'_y with respect to δ_D / δ_y

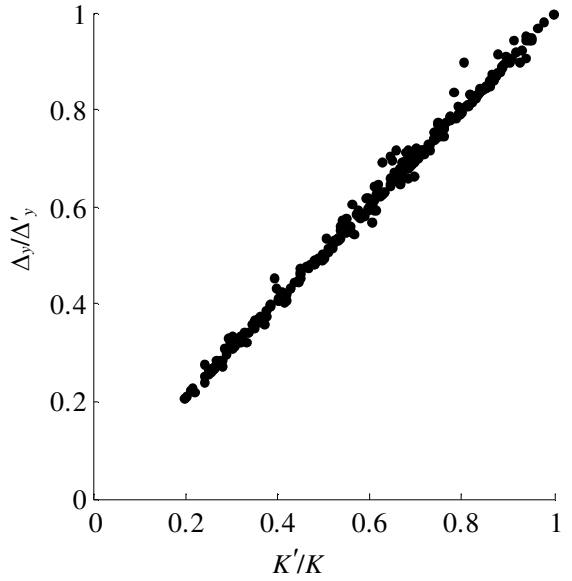

Figure 3-5. Data showing the relation between Δ_y / Δ'_y and K' / K

Next, we compute the value of DI from the structural response obtained from NTHA (Figure 3-6). To compute DI, we first obtain the number and amplitude of strain cycles in the longitudinal reinforcing steel using Rainflow Counting method (Downing and Socie 1982). Then, we use Eqs (2-14) and (2-15) to compute DI.

3.3 Probabilistic seismic degradation models

In this subsection, the generated data is used to develop the probabilistic models to predict the values of K'/K, V_y'/V_y, Δ_y/Δ_y' and DI based on the value of δ_D/δ_y. The models are developed using the Bayesian updating rule (Box and Tiao 1992). In this section, we estimate the model parameters using Markov-Chain Monte-Carlo or MCMC method () instead of importance sampling followed in Section 2. MCMC is an efficient method of sampling from complex multivariate distributions (Smith and Roberts 1993). In Bayesian updating, MCMC is particularly used because the posterior distribution is known only to a constant factor.

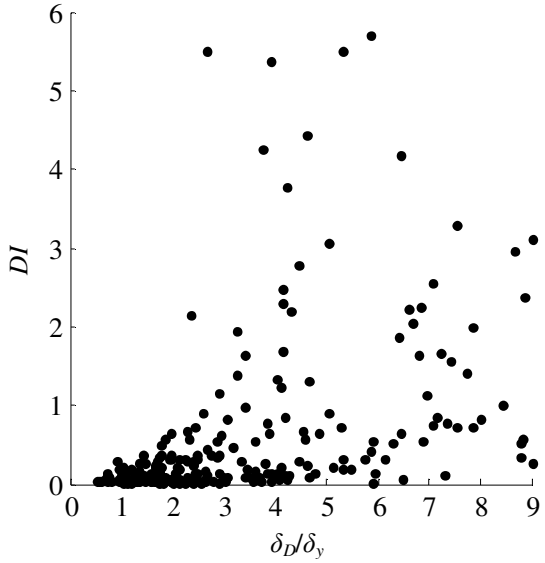

Figure 3-6. Low-cycle fatigue damage in longitudinal reinforcing steel due to an earthquake.

3.3.1 Probabilistic models for degradation of static pushover properties

To model the degradation in static pushover properties, it is sufficient to model any two of the quantities; K'/K, Δ_y'/Δ_y and V_y'/V_y. This is because the standard relation $K = V_y/\Delta_y$ must hold also for the deteriorated state i.e., $K' = V_y'/\Delta_y'$. Based on the obtained data, we propose the following linear probabilistic models model forms for predicting K'/K and Δ_y'/Δ_y:

$$\ln\left(K'/K\right) = \left[\sum_{i=1}^{n} \theta_{K,i} h_{K,i}\left(\mathbf{x}\right)\right] \ln\left(\delta_D/\delta_y\right) + \sigma_K \varepsilon_K \qquad \delta_D/\delta_y \geq 1 \qquad (3\text{-}1)$$

$$\ln\left(\Delta_y'/\Delta_y\right) = \theta_{\Delta,1} \ln\left(K'/K\right) + \sigma_\Delta \varepsilon_\Delta \qquad \delta_D/\delta_y \geq 1 \qquad (3\text{-}2)$$

where $\boldsymbol{\theta}_K = \{\theta_{K,1}, \theta_{K,2}, \ldots, \theta_{K,j}\}$, $\theta_{\Delta,1}$, σ_K and σ_Δ are unknown model parameters, $h_{K,i}(\mathbf{x})$ are explanatory terms, and ε_K and ε_Δ are correlated random variables having a bivariate normal distribution (normality assumption) with correlation coefficient $\rho_{K,\Delta}$.

The proposed model forms for K'/K and Δ_y'/Δ_y are selected for three reasons. First, the model form for K'/K is based on the observed data that suggests a power-law relation $K'/K = (\delta_D/\delta_y)^\zeta$, where ζ may depend on the properties of the column. Using the logarithmic model form, ζ can be assessed in the proposed linear regression model. Second, since V_y'/V_y remains nearly constant, there is a high correlation between K'/K and Δ_y'/Δ_y, which justifies the exclusion of explanatory terms other than K'/K in Eq. (3-2). Third, the logarithmic form is used to satisfy the homoscedasticity and normality assumptions. The homoscedasticity and normality assumptions can be verified using appropriate diagnostic plots (Rao and Toutenburg, 1997).

We choose $h_{K,i}(\mathbf{x})$ by developing functions that represent the global behavior of RC columns. First, we select a number of possible candidate functions. Then, we use a step-wise deletion process developed by Gardoni et al. (2002) to remove the functions that are unimportant developing the most parsimonious model. The selected candidate terms are: constant 1.0, $P_u/(f_c'A_g)$, where P_u is the axial load on the column due to the weight of the super structure and the column, f_c' is the compressive strength of concrete and A_g is the gross cross-sectional area of the column. The next term is

$T_n = 2\pi\sqrt{P_u / Kg}$ that is an approximation of the natural period of the first mode of vibration of the bridge (T_n is not exactly equal to the natural period of the bridge because the stiffness contribution from abutments is not included in K). The other terms are slenderness ratio H_c / D_c, drift at yield $\delta_y = \Delta_y / H_c$ and the normalized shear force at yield $V_y / (A_g f_c')$.

To develop a parsimonious model, first the model in Eq. (3-1) is assessed using all the candidate explanatory functions. We assess the unknown model parameters using Bayesian updating rule with non-informative priors (Gardoni et al. 2002) for the model parameters. The joint posterior distribution is computed using Markov-Chain Monte-Carlo (MCMC) simulations. After assessing the model parameters, the function that is multiplied by the model parameter with the highest coefficient of variation (c.o.v) is removed. The reduced model is then reassessed and a second explanatory function is removed. The deletion process is repeated until removing one explanatory function has a significant influence on the accuracy of the model as captured by the value of σ_K (Gardoni et al. 2002). Following this method, the terms $h_{K,1}(\mathbf{x}) = 1$, $h_{K,2}(\mathbf{x}) = P_u / (f_c' A_g)$ and $h_{K,3}(\mathbf{x}) = T_n$ are retained in the model. Table 3-2 shows the posterior statistics of $\boldsymbol{\theta}_K$, $\theta_{\Delta,1}$, σ_K, σ_Δ and $\rho_{K,\Delta}$. The comparison of the model predictions and the measured values is shown in Figure 3-7 through Figure 3-11. In the figures, the measured values are represented by horizontal axis and the predicted values are represented by the vertical axis. The dashed lines or bounds are drawn at a distance equal to ±1 standard deviation of the model error (i.e., measured – predicted) from the 1:1 line. Figure 3-7

and Figure 3-8 show the predictions of the model for K'/K in logarithmic and original spaces respectively. Figure 3-9 and Figure 3-10 show the model predictions for Δ_y'/Δ_y in the logarithmic and the original spaces.

Table 3-2. Posterior statistics of the parameters in the probabilistic degradation models

Parameters	$\theta_{K,1}$	$\theta_{K,2}$	$\theta_{K,3}$	$\theta_{\Delta,1}$	σ_Δ	σ_K	$\rho_{K,\Delta}$
Mean	−0.735	0.347	0.124	−0.967	0.050	0.120	−0.070
Std. dev	0.018	0.25	0.033	0.0029	0.005	0.0053	0.066
				Correlation			
$\theta_{K,1}$	1.00	−0.45	−0.37	0.28	−0.032	0.16	−0.09
$\theta_{K,2}$	−0.45	1.00	−0.61	−0.063	−0.016	−0.0085	−0.13
$\theta_{K,3}$	−0.37	−0.61	1.00	−0.14	0.062	−0.15	0.21
$\theta_{\Delta,1}$	0.28	−0.06	−0.14	1.00	0.20	0.014	−0.167
σ_Δ	−0.03	−0.016	0.062	0.20	1.00	0.088	−0.028
σ_K	0.16	−0.0085	−0.15	0.01	0.089	1.00	−0.147
$\rho_{K,\Delta}$	−0.09	−0.1349	0.21	−0.17	−0.028	−0.147	1.00

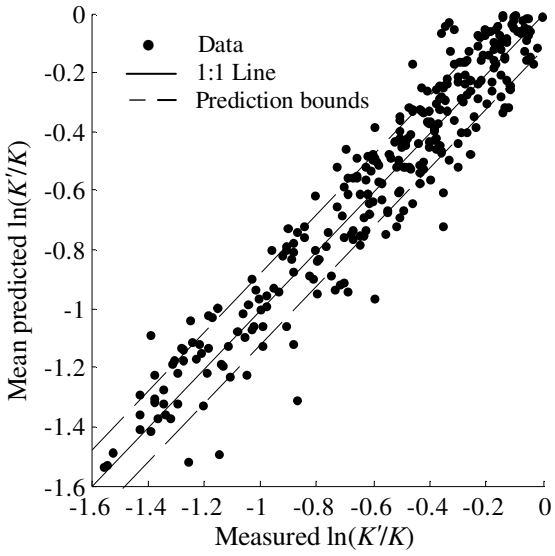

Figure 3-7. Predicted versus measured values of $\ln(K'/K)$

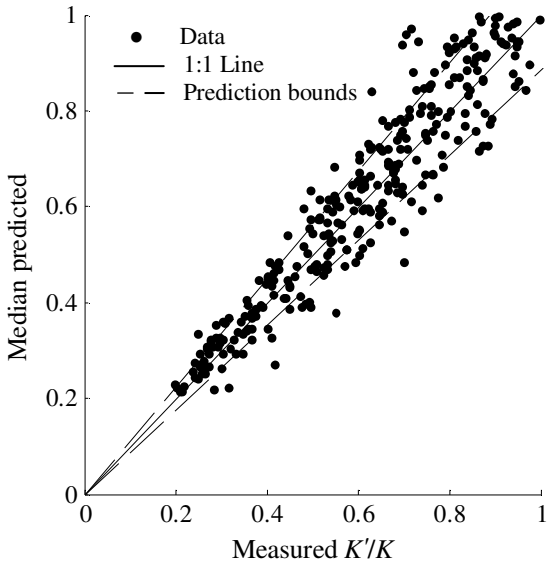

Figure 3-8. Predicted versus measured values of K'/K

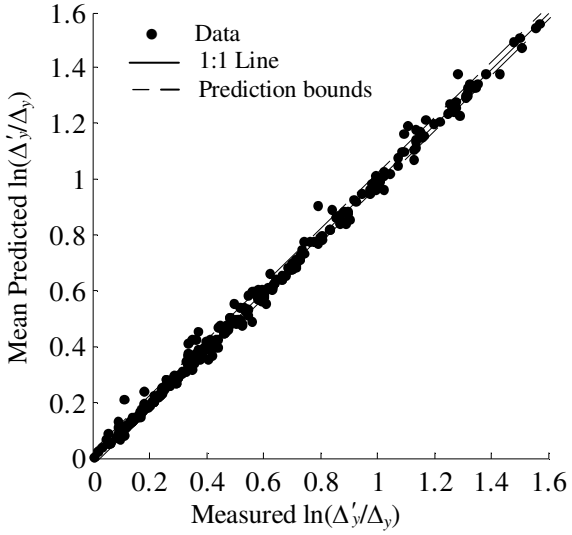

Figure 3-9. Predicted versus measured values of $\ln(\Delta_y'/\Delta_y)$

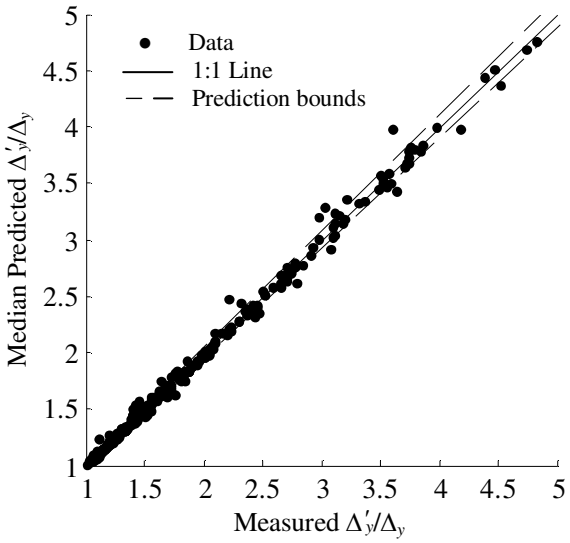

Figure 3-10. Predicted versus measured values of Δ_y' / Δ_y

3.3.2 Probabilistic model of low-cycle fatigue damage DI

Based on the mathematical formulation of low-cycle fatigue damage the valid theoretical range for DI is 0 to ∞, where $DI \geq 1.0$ indicates the failure of a reinforcing bar. To model DI, we develop a linear regression model of $\ln(DI)$.

$$\ln\left(DI\right) = \sum_{i=1}^{n} \theta_{DI,i} h_{DI,i}\left(\mathbf{x}\right) + \sigma_{DI}\varepsilon_{DI} \tag{3-3}$$

where $\boldsymbol{\theta}_{DI} = (\theta_{DI,1},\ldots,\theta_{DI,n})$ are the model parameters, and $\sigma_{DI}\varepsilon_{DI}$ is the model error, in which ε_{DI} is a standard normal random variable (normality assumption) and σ_{DI} is the standard deviation of the model error assumed to be constant (homoscedasticity assumption.) The logarithmic transformation is used to satisfy the homoscedasticity and normality assumption of the model error and so that a linear regression model can be developed since $\ln(DI)$ now ranges from $-\infty$ to ∞. The candidate explanatory

functions considered, $h_{DI,i}(\mathbf{x})$, are: the pseudo-spectral acceleration corresponding to T_n and 5% viscous damping, S_a; the ratio of peak ground velocity $v_{\max}$ to peak ground acceleration $a_{\max}$, $v_{\max}/a_{\max}$; the normalized energy $E_H/(V_y\Delta_y)$, where $E_H=[m(S_a/\omega_n)^2]/2$, $\omega_n=2\pi/T_n$ and $m=P_u/g$ (in which E_H is the maximum energy of an elastic system with natural period T_n and mass m and does not equal the hysteretic energy dissipated by the inelastic system); and the equivalent number of cycles N_e at the maximum displacement $\delta_D H_c$ given by $\sum_{i=1}^{N_c}[\Delta_i/(\delta_D H_c)]^2$, where Δ_i is the displacement in the i^{th} half-cycle and N_c is the total number of cycles in an earthquake. The most parsimonious model obtained using the previously described stepwise deletion method is

$$\ln(DI)=\theta_{DI,1}+\theta_{DI,2}\ln\left(\delta_D/\delta_y\right)+\theta_{DI,3}\ln(T_n)+\sigma_{DI}\varepsilon_{DI} \tag{3-4}$$

Table 3-3 shows the estimates for $\boldsymbol{\theta}_{DI}$ and σ_{DI}. Figure 3-11 and Figure 3-12 show the model predictions for DI in the logarithmic and original space.

Table 3-3. Parameters for low-cycle fatigue damage accumulation model

Parameters	$\theta_{DI,1}$	$\theta_{DI,2}$	$\theta_{DI,3}$	σ_{DI}
Mean	5.816	2.395	–2.074	1.44
Std.dev	0.271	0.080	0.111	0.076
		Correlation		
$\theta_{DI,1}$	1.00	0.930	–0.22	0.013
$\theta_{DI,2}$	0.930	1.00	–0.52	0.017
$\theta_{DI,3}$	–0.22	–0.52	1.00	–0.012
σ_{DI}	0.013	0.017	–0.012	1.00

This model can be used to predict the degradation in curvature capacity of an RC section due to an earthquake using the curvature capacity model conditioned on the value of DI developed in the previous section. The curvature capacity can be used to compute the degraded deformation capacity of an RC column.

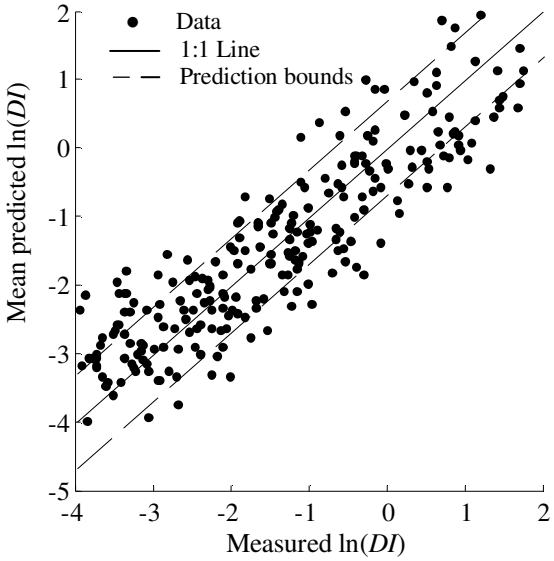

Figure 3-11. Predicted versus measured values of $\ln(DI)$

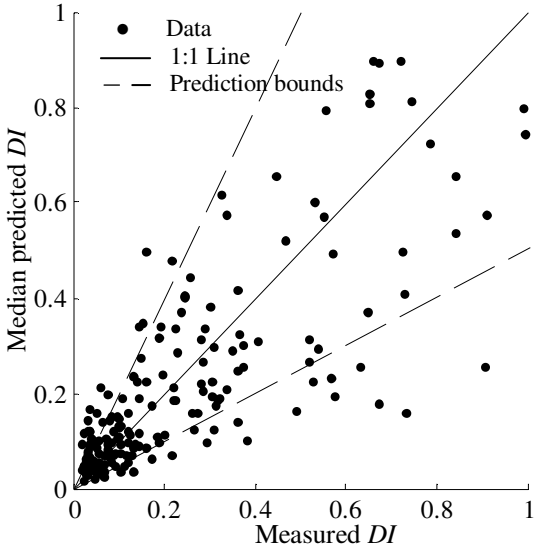

Figure 3-12. Predicted versus measured values of DI

3.4 Seismic fragility of seismically degraded structures

Seismic fragility is defined as the conditional probability of exceeding a specified performance level during an earthquake conditioned on the values of selected seismic intensity measures (Gardoni et al. 2003). In general, the seismic fragility of a structure, that has experienced m earthquakes in the past, can be written as follows conditioning on the pseudo-spectral acceleration of the past and future earthquakes:

$$\tilde{F}\left[\mathbf{S}_{\mathbf{a}}^{(m)}, S_a^{(m+1)}\right] = P\left\{\bigcup_j \left\{C_j\left[\mathbf{x}^{(m)}\left(\mathbf{S}_{\mathbf{a}}^{(m)}\right)\right] - D_j\left[\mathbf{x}^{(m)}\left(\mathbf{S}_{\mathbf{a}}\right), S_a^{(m+1)}\right] \le 0 \middle| \mathbf{S}_{\mathbf{a}}^{(m)}, S_a^{(m+1)}\right\}\right\} \quad (3\text{-}5)$$

where $\mathbf{S}_{\mathbf{a}}^{(m)} = \{S_a^{(1)}, S_a^{(2)}, \ldots, S_a^{(m)}\}$ is the vector of pseudo-spectral accelerations of the past m earthquakes, $S_a^{(m+1)}$ is the pseudo-spectral acceleration of the future earthquake, $\tilde{F}[\mathbf{S}_{\mathbf{a}}^{(m)}, S_a^{(m+1)}]$ is the predictive seismic fragility (Gardoni et al. 2002) considering all the failure modes, $P[A \mid B]$ is the conditional probability of event A given B, $\mathbf{x}^{(m)}(\mathbf{S}_{\mathbf{a}})$ are

the properties that describe the current state of the bridge after experiencing m past earthquakes, $C_j[\mathbf{x}^{(m)}(\mathbf{S_a})]$ and $D_j[\mathbf{x}^{(m)}(\mathbf{S_a}), S_a^{(m+1)}]$ are the capacity of the existing structure and the seismic demand, respectively, corresponding to mode j due to the future earthquake. For the as-built state, i.e., $m=0$, we write $\mathbf{S}_\mathbf{a}^{(0)}=\{\}$ (an empty set), $\mathbf{x}^{(0)}(\mathbf{S_a})=\mathbf{x}$ (properties of the as-built state) and $\tilde{F}[\mathbf{S}_\mathbf{a}^{(m)}, S_a^{(m+1)}]=\tilde{F}[\{\}, S_a^{(1)}]$. Predictive fragilities are computed accounting for the uncertainty in the structural properties, and the model parameters and the model errors in the models used to estimate $C_j[\mathbf{x}^{(m)}(\mathbf{S}_\mathbf{a}^{(m)})]$ and $D_j[\mathbf{x}^{(m)}(\mathbf{S}_\mathbf{a}^{(m)}), S_a^{(m+1)}]$.

The effect of seismic degradation on seismic fragility is explained in Figure 3-13. The seismic fragility of a structure degrades with each passing earthquake (i.e., $m=1,2,...$) as shown in thick dotted lines with the seismic fragility of the structure in the as-built state (i.e., $m=0$ shown in thick solid line). The horizontal axis represents $S_a^{(m+1)}$ and the vertical axis represents $\tilde{F}[\mathbf{S}_\mathbf{a}^{(m)}, S_a^{(m+1)}]$. The $\tilde{F}[\mathbf{S}_\mathbf{a}^{(m)}, S_a^{(m+1)}]$ plots are shown for $m=0,1,2,...$ and an example sequence $\mathbf{S}_\mathbf{a}^{(m)}=[0.1g, 0.3g, 0.2g, \ldots 0.1g]$ is considered. It is shown that $\tilde{F}[\mathbf{S}_\mathbf{a}^{(m)}, S_a^{(m+1)}]$ increases monotonically for a given value of

$S_a^{(m+1)}$ for increasing values of m. It is expected in general owing to expected decrease in capacity and increase in demand. However, this necessarily may not be the case always because the change in seismic demand due to degradation depends on the value of T_n, the change in T_n due to degradation and the shape of the response spectrum of ground motions. The figure also compares the values of seismic fragilities for different values of m but for a given ground motion GM (not necessarily included in $\mathbf{S}_\mathbf{a}^{(m)}$). A ground motion is a more concrete basis than just the pseudo-spectral acceleration to compare seismic fragilities of different degraded states of a structure because pseudo-spectral acceleration depends on T_n which changes with degradation. For this purpose, we need to compute $\tilde{F}\{\mathbf{S}_\mathbf{a}^{(m)}, S_a'[GM, T_n^{(m)}]\}$, where $S_a'[GM, T_n^{(m)}]$ is the pseudo-spectral acceleration for GM corresponding to period $T_n^{(m)}$ that corresponds to the structure that has experienced $\mathbf{S}_\mathbf{a}^{(m)}$ in the past. The figure shows the differences in seismic fragilities for $m = 0$ (as-built) and for $m = 1$, where $\Delta_1\tilde{F}$ corresponds to the difference for a given pseudo-spectral acceleration $S_a'(T_n, GM)$ and $\Delta_2\tilde{F}$ corresponds to the difference considering a given ground motion GM.

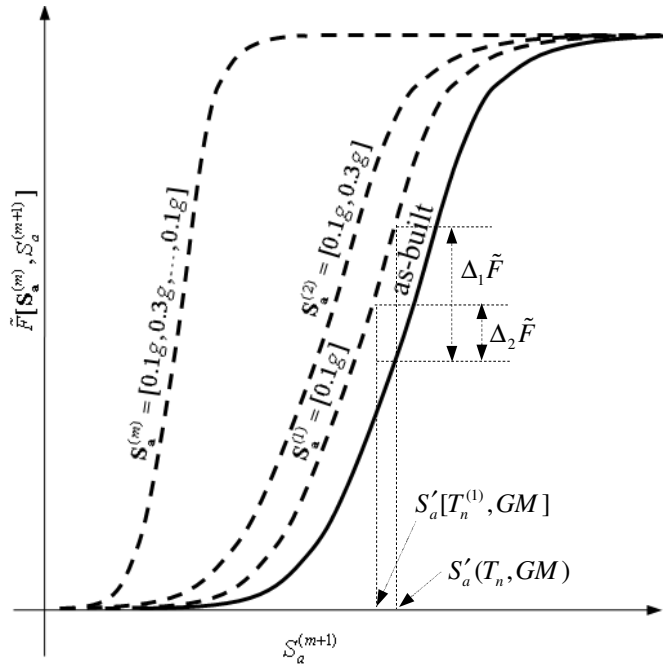

Figure 3-13. Increment in fragility due to multiple past earthquakes

3.5 Seismic fragility of an example RC bridge subjected to one earthquake in the past

In this section, we compute the seismic fragility of an example RC bridge that has experienced one earthquake in the past. The bridge is a typical bridge representative of California's current design specifications. It has one single-column bent with natural period $T_n = 0.84$ s. With reference to Figure 3-1, Table 3-4 shows the values of the design parameters of the example bridge. We consider the failure modes; shear ($j = v$) and deformation ($j = \delta$) of the bridge column in the fragility estimation. The seismic fragility are conditioned on the values pseudo-spectral acceleration of the past and future earthquakes.

Table 3-4. Structural properties of the example bridge

Parameter	Value/Mean	Distribution	c.o.v (%)
α^s	30°	constant	-
L_1	29.45 m	Lognormal	1.0
L_2 / L_1	1.36	constant	-
H_c	8.5 m	Lognormal	1.0
D_c	1.5 m	Lognormal	2.0
cover	0.040 m	Lognormal	10.0
f_y	642.15 MPa	Lognormal	5.0
f_{yh}	642.15 MPa	Lognormal	5.0
f_c'	40.55 MPa	Lognormal	10.0
ρ_{sl}	0.022	constant	-
ρ_{sv}	0.009	constant	-
w_t	0.60	Normal	25.0
Soil	Type D†	constant	-
Abutment	Type C	constant	-

† Refer to Huang et al. (2010) for soil classification

For one past earthquake, Eq. (3-5) is written as follows:

$$\tilde{F}\left[S_a^{(1)}, S_a^{(2)}\right] = P\left\{\bigcup_j \left\{C_j\left[\mathbf{x}^{(1)}\left(S_a^{(1)}\right)\right] - D_j\left[\mathbf{x}^{(1)}\left(S_a^{(1)}\right), S_a^{(2)}\right] < 0 \middle| S_a^{(1)}, S_a^{(2)}\right\}\right\} \quad (3\text{-}6)$$

where $S_a^{(1)}$ is the pseudo-spectral acceleration of the past earthquake, $S_a^{(2)}$ is the pseudo-spectral acceleration of the future earthquake. The predictive seismic fragility in Eq. (3-6) can be computed using either Monte-Carlo simulations for more than one mode of failure or reliability methods such as First Order Reliability Method (FORM) and Second Order Reliability Method (SORM) for single mode of failure (Ditlevsen and Madsen 1996; Haldar and Mahadevan 2000).

Figure 3-14 shows an example comparison of $\tilde{F}[S_a^{(1)}, S_a^{(2)}]$ with the as-built seismic fragility. The figure shows a monotonous increase in fragility values with

increase in $S_a^{(1)}$ for a given value of $S_a^{(2)}$. However, this necessarily may not be the case as explained earlier. The figure also shows a comparison of the seismic fragilities for two different states of structure but for a given ground motion GM.

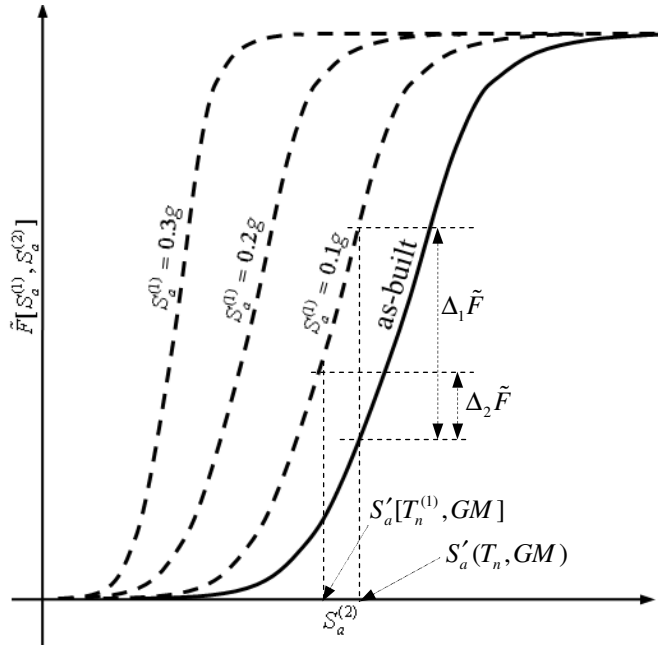

Figure 3-14. Fragility increments with respect to intensity of past earthquake

3.5.1 Residual capacity and demand of the degraded RC bridge columns

To completely define the terms in Eq. (3-6) we need to compute $C_j\{\mathbf{x}^{(1)}[S_a^{(1)}]\}$ and $D_j\{\mathbf{x}^{(1)}[S_a^{(1)}], S_a^{(2)}\}$ for given values of $S_a^{(1)}$ and $S_a^{(2)}$ considering the deformation mode ($j = \delta$) and shear mode ($j = v$). In following, we describe the methodology used in this paper to compute $C_j\{\mathbf{x}^{(1)}[S_a^{(1)}]\}$ and $D_j\{\mathbf{x}^{(1)}[S_a^{(1)}], S_a^{(2)}\}$.

1. Computation of degraded deformation and shear capacity. Section 2 proposed the degraded curvature capacity $\phi_u'(\mathbf{x}, \boldsymbol{\Theta}_\phi, DI)$. We obtain $C_\delta\{\mathbf{x}^{(1)}[S_a^{(1)}]\}$ and $C_\nu\{\mathbf{x}^{(1)}[S_a^{(1)}]\}$ by substituting the degraded structural properties $\phi_u'(\mathbf{x}, \boldsymbol{\Theta}_\phi, DI)$ for $\phi_u(\mathbf{x})$ and (K', Δ_y', V_y') for (K, Δ_y, V_y) in the deformation and shear capacity models developed by Choe et al. (2007). These degraded structural properties are obtained using Eqs. (2-18) to (2-20) and Eqs. (3-1) to Eqs. (3-4).

2. Computation of seismic demands on degraded RC column. The seismic demands $D_\delta\{\mathbf{x}^{(1)}[S_a^{(1)}], S_a^{(2)}\}$ and $D_\nu\{\mathbf{x}^{(1)}[S_a^{(1)}], S_a^{(2)}\}$ can be obtained using the probabilistic demand models proposed by Gardoni et al. (2003). These demands are primarily governed by the static pushover curve characterized by static pushover properties (K, Δ_y, V_y). We compute the seismic demands for the future earthquakes by using the properties (K', Δ_y', V_y') in models proposed by Gardoni et al. (2003).

3.5.2 Results and discussions

Figure 3-15 shows the contours plot for $\tilde{F}[S_a^{(1)}, S_a^{(2)}]$ for failure modes δ and ν. In the figure, the horizontal axis represents $S_a^{(2)}$ and the vertical axis represents $S_a^{(1)}$. The dashed contour lines represent the $\tilde{F}[S_a^{(1)}, S_a^{(2)}]$ values corresponding to the deformation mode only and the solid contour lines represent the fragilities for failure in either shear or deformation mode. The fragility contours indicate that the contribution of the shear mode to the seismic fragility is small compared to that of the deformation mode. This is typical of RC columns designed per Caltrans' specifications (Caltrans 2006). As

expected, it is found that $\tilde{F}[S_a^{(1)}, S_a^{(2)}]$ increases with increase in the values of $S_a^{(1)}$ and $S_a^{(2)}$. The values of $\tilde{F}[S_a^{(1)}, S_a^{(2)}]$ are found to remain approximately constant for $S_a^{(1)} \leq 0.2g$ and increase at a faster rate as $S_a^{(1)}$ increases beyond $0.2g$. This is because the RC column is in elastic range for approximately $0 < S_a^{(1)} \leq 0.2g$ and hence does not experience degradation within that range. It is found that the values of seismic fragility of a bridge that has degraded due to a past earthquake is significantly greater than that of the bridge in its as-built condition.

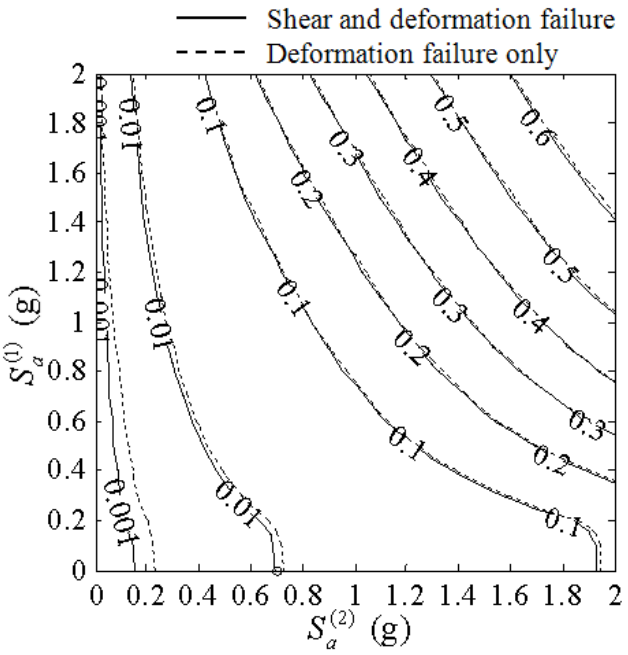

Figure 3-15. Fragility contours showing the effect of past earthquake on the seismic fragility of an RC bridge

In addition to the seismic fragility with respect to the second earthquake of the degraded bridge, we also compute the probability of failure in a sequence of two earthquakes conditioning on the values of their pseudo-spectral acceleration. These values are computed as follows:

$$P_f\left[S_a^{(1)}, S_a^{(2)}\right] = \tilde{F}\left[0, S_a^{(1)}\right] + \left\{1 - \tilde{F}\left[0, S_a^{(1)}\right]\right\} \tilde{F}\left[S_a^{(1)}, S_a^{(2)}\right] \qquad (3\text{-}7)$$

Figure 3-16 shows the contour plot for $P_f[S_a^{(1)}, S_a^{(2)}]$ (dotted lines) as compared to $\tilde{F}[S_a^{(1)}, S_a^{(2)}]$ (solid lines). The abscissa represents $S_a^{(2)}$ and the ordinate represents $S_a^{(1)}$. The figure shows, as expected that $P_f[S_a^{(1)}, S_a^{(2)}]$ increases with increase in the values of $S_a^{(1)}$ and $S_a^{(2)}$. This is because of increase in failure probability in each earthquake due greater pseudo-spectral accelerations and the increase in failure probability in second earthquake due to higher degradation in the first earthquake. In addition, it is observed that $P_f[S_a^{(1)}, 0] = P_f[0, S_a^{(2)}] = \tilde{F}[0, S_a^{(2)}\}]$ for $S_a^{(1)} = S_a^{(2)}$. This is because the cases with either $S_a^{(1)}$ or $S_a^{(2)}$ equal to 0 is equivalent to the case with just one earthquake.

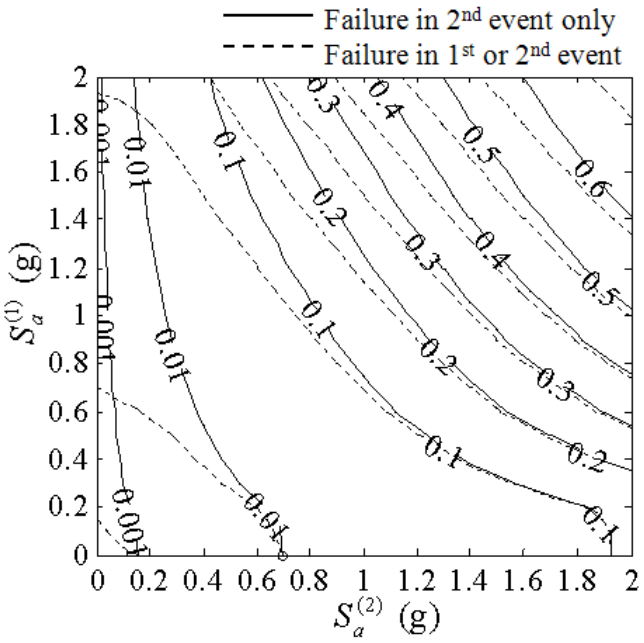

Figure 3-16. Contour plot for probability of failure in two consecutive earthquakes.

3.6 Conclusions

In seismic regions, structures are likely to experience multiple seismic events during their service lives. With each passing earthquake, the performance of structures may degrade due to seismic degradation. In order to develop optimal design and repair strategies it is important to consider the effect of seismic degradation on the structural performance.

This work investigates the seismic degradation of RC bridge columns and the effect of such degradation on the seismic fragility of reinforced concrete (RC) highway bridges. The seismic response and performance of RC bridges is affected by the properties of the bridge columns and their steel reinforcement. For this reason, we develop models to predict the degradation of the static pushover properties and the low-

cycle fatigue damage in the longitudinal reinforcing steel of the RC columns. The developed degradation models are used to assess the reliability of RC bridges subject to multiple earthquakes. As an example, the proposed method is applied to an example RC highway bridge. The results show that seismic degradation causes significant increase in seismic fragilities of the bridge. The developed fragility curves and more generally the proposed method can be used either to design more durable structures to reduce repair costs or to make decisions regarding post-earthquake repairs.

4. STOCHASTIC SEMI-ANALYTICAL APPROACH OF MODELING OF DETERIORATION IN ENGINEERING SYSTEMS

4.1 Introduction

Engineering systems deteriorate while in service due to exposure to extreme conditions (e.g., excessive loading and harsh environment) and routine use. Deterioration is a serious concern because it can considerably reduce the service life and reliability of systems. Moreover, the process of deterioration is highly unpredictable and often invisible. Therefore, systems must be designed accounting for deterioration processes and the various associated uncertainties.

A deterioration process can be of two distinguishable types; shocks and gradual deterioration. A shock is an instantaneous change in a system's properties due to the action of external loads (e.g., sudden deterioration of a bridge due to an earthquake). Gradual deterioration is associated to the wear and decay of the system due to prolonged use (e.g., fatigue in machine parts during regular operation), aging, and exposure to unfavorable environment (e.g., corrosion of steel reinforcement bars in RC structures due to exposure to chlorides).

Researchers have conducted various studies on the reliability of deteriorating systems. These studies can be broadly classified into two categories. The first category includes time-dependent reliability analyses. This type of research is primarily aimed at computing the change in the reliability of a deteriorating system with respect to time (Stewart 2001; Val 2005; Melchers 2005; Choe et al. 2009; Pillai et al. 2010) obtained by performing a reliability analysis of the deteriorating system at different points in time

using standard methods like the First Order Reliability Method (FORM), the Second Order Reliability Method (SORM), and Monte Carlo simulations. Such studies often use experimental data and sophisticated computational tools (e.g., Finite Element Method) to model the behavior of the deteriorated system. However, these analyses cannot be extended to estimate critical life-cycle quantities such as time to failure or to compute survival and hazard functions.

The second category of studies includes stochastic modeling of deterioration processes. This type of research is primarily focused at developing a general framework to perform life-cycle analysis of deteriorating systems (e.g., Klutke and Yang 2002; Noortwijk et al. 2005; Sanchez-Silva 2011; Mori and Ellingwood 1994; Esary and Marshall 1994; Wortman et al. 2006). Depending on the objective, a life-cycle analysis may involve computation of life-time distributions, hazard and survival functions, life-cycle costs and, repair and maintenance strategy. In this type of research, stochastic processes are used because they can model the random nature of deterioration processes and random occurrences of loading and failure events. A general framework is helpful for systematically understanding and studying deteriorating systems in the terms of important variables that determine their life-cycles.

In the existing literature on stochastic frameworks, there are two distinct approaches depending on the type of failure. System failures can be of two types: 1) Excessive demand and 2) Excessive deterioration. Failure due to excessive demand takes place during the occurrence of a load when the imposed demand exceeds the capacity of the system (Mori and Ellingwood 1994; Ellingwood and Mori 1993; Stewart

2001; Val 2005). Failure due to excessive deterioration occurs when the total deterioration in a system, not necessarily during the occurrence of a load, exceeds a maximum allowable value (Esary et al 1973; Klutke and Yang 2002; Wortman et al. 2006; Sanchez-Silva et al. 2011). For example, a bridge column might fail during an earthquake due to excessive deformation demand. It may also be considered unusable due to excessive deterioration in deformation capacity caused by corrosion. In reality, many systems exhibit both the failure types. Ignoring either of the failure types may cause inaccuracy in the prediction of failure probabilities and the life-span of a system. Therefore, a general framework must be able to account for both types of failures. Often, however, either only one failure type is considered or simplifications are made in order to account for both failure types. This section proposes a stochastic model for deterioration named SSA that addresses the following important issues, one or more of which are not addressed in the existing literature:

1. Modeling the effect of deterioration on capacity
2. Modeling the dependence between the deterioration process and demand
3. Modeling the combination of shock and gradual deterioration process
4. Accounting for failures due to excessive demand and excessive deterioration
5. Proposing accurate, time-efficient and convenient solution strategies.

This section is organized into six subsections including this introduction. The second subsection describes a general deterioration process and discusses issues related to the stochastic modeling of deterioration processes. The third subsection proposes the SSA model for deterioration in engineering systems along with two possible solutions

strategies. The fourth subsection presents two numerical examples to illustrate the proposed stochastic model. Thereafter, the fifth subsection presents a case study to analyze different deterioration scenarios. Finally, the sixth subsection presents the conclusions from this section.

4.2 The deterioration process

Figure 4-1 illustrates a general deterioration process and the failure of a deteriorating system. During the service life, a system is subject to a sequence of loads $\{S_{t_n}\}$ at times $\{t_n\}$, where $n = 1, 2, \ldots$. At time $t = t_n$, the external load S_{t_n} imposes a demand $D_{t_n} = D(\mathbf{x}_{t_n}, S_{t_n})$ on the system, where $\mathbf{x}_{t_n}$ represents the properties of the system at time t_n and $D(\mathbf{x}_{t_n}, S_{t_n})$ is a function of $\mathbf{x}_{t_n}$ and S_{t_n}. It is shown that the system experiences a shock deterioration at $t = t_{n-1}$ and t_n, and gradual deterioration in the interval (t_{n-1}, t_n) and for $t > t_n$. The capacity C_t gradually changes from $C_{t_{n-1}^+}$ to $C_{t_n^-}$ and instantaneously changes from $C_{t_{n-1}^-}$ to $C_{t_{n-1}^+}$ and $C_{t_n^-}$ to $C_{t_n^+}$ (where t_i^- and t_i^+ are the time instants immediately before and after t_i.).

As previously discussed, the failure of a system can be of two types: 1) excessive demand 2) excessive deterioration. The failure due to excessive demand can be written as the event $(C_{t_n^-} - D_{t_n}) < 0$, and the failure due to excessive deterioration can be written as the event where the total deterioration W_t at time t exceeds a specified threshold w_a, that is $W_t > w_a$.

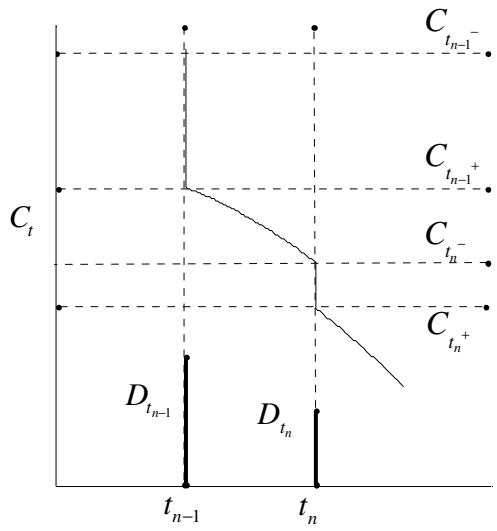

Figure 4-1. The effect of deterioration process on capacity

This section discusses the following important issues in modeling a deterioration process and subsequently proposes a model that addresses these issues.

1. *Modeling the effect of deterioration on capacity*. Reduction in capacity due to deterioration is the most widely acknowledged and addressed issue in the modeling of deteriorating systems. The reduction in capacity has been modeled in the past using random and deterministic functions of time (Ellingwood and Mori 1993; Klutke and Yang 2002; Sanchez-Silva et al. 2011).
2. *Modeling the dependence between the deterioration process and demands*. This issue consists of two parts. First, shock deterioration is dependent on the process $\{D_{t_n}\}$ because shock deterioration process and $\{D_{t_n}\}$ are generated due the same loading events. Second, the process $\{D_{t_n}\}$ is not necessarily a stationary process

for deteriorating systems. This is because the deterioration process may change $\mathbf{x}$ such that the same load can impose different demands on the system during two different events. Consequently, significant errors can be introduced in the estimates by ignoring the inter-dependence between deterioration process and $\{D_{t_n}\}$. Here, it is important to note that some studies relate deterioration process to change in capacity only (Klutke and Yang 2002), or both capacity and demand but only of gradual deterioration (Gardoni and Rosowsky 2011). However, in most systems the effect of deterioration is observed in both capacity and demand (e.g., change in deformation demand due to change in natural period of vibration of bridges due to deterioration). The inter-dependence between deterioration process and $\{D_{t_n}\}$ has not been addressed adequately in literature.

3. *Modeling the combination of shock and gradual deterioration process.* The problem of combined effect of shock and gradual deterioration is important because most engineering systems experience both types of deterioration. This issue has been addressed in some of the past works using a Gamma process (Noortwijk et al. 2005) and combinations of compound Poisson processes and deterministic functions of time (Esary et al. 1973; Klutke and Yang 2002; Sanchez-Silva 2011).

4. *Accounting for different failure types.* In the existing literature, generally only one failure type, either excessive demand or excessive deterioration, is considered. However, in general a system can experience either type of failure in its life time. In some studies (Noortwijk et al. 2005), simplifying assumptions like

mutual independence between the deterioration process and $\{D_{t_n}\}$ are used to manage the different failure types.

5. *Proposing accurate, time-efficient and convenient solution strategies*. Some studies (Kumar et al. 2009) account for some of the above-mentioned issues but the modeling process is not general but specific to one hazard and system type. Moreover, the failure probabilities are computed by simulating scenarios of failure and no failure. This is a purely simulation approach and is not suitable for computing failure probability of engineering systems with very low failure probabilities.

4.3 Proposed SSA model for deterioration processes

In this subsection, we propose a general stochastic model named SSA that addresses the critical issues associated to modeling of deterioration processes and provides computationally efficient semi-analytical solutions to compute the time to failure. In order to develop the proposed SSA model, we make the following assumptions:

1. The total effect of shock and gradual deterioration process on the capacity and demand of a system is the sum of the effects of the individual deterioration processes.
2. The shock and the gradual deterioration process are independent of each other.
3. The shock deterioration process is composed of statistically independent and identically distributed (SIID) shocks but each shock is dependent on the corresponding demand on the system.

4.3.1 Capacity of a deteriorating system

Assuming that shock and gradual deterioration processes are mutually independent, the time-dependent capacity of a system can be written in the following additive form:

$$C_t = C_0 + \sum_{i=1}^{N(t^-)} \Delta C^s_{t_i} + R_C(t) \tag{4-1}$$

where C_0 is the initial capacity, $N(t) = \max\{n : t_n \le t\}$ is the number of occurrences of loads or shocks in time t and $\Delta C^s_{t_i} = C_{t_i^+} - C_{t_i^-}$ is the value of shock deterioration in capacity at time t_i and $R_C(t) = \int_0^t [(dC_t / dt)_{t \ne t_i}]dt$ is the gradual capacity deterioration process.

4.3.2 Demands on a deteriorating system

The distribution of D_{t_n} depends on the deterioration process and it is a function of both $\mathbf{x}_{t_n}$ and S_{t_n}. Therefore, the process $\{D_{t_n}\}$ cannot be modeled as a SIID sequence for deteriorating systems. The following model is proposed to capture the effect of deterioration on demands:

$$D_{t_n} = Y_{t_n} + \alpha_{t_n} \tag{4-2}$$

where $\{Y_{t_n}\}$ is a SIID sequence independent of the deterioration process and $\alpha_t = \alpha(\mathbf{x}_t)$ captures the effect of deterioration on $\{D_{t_n}\}$. Adopting an additive form, the changes in α_t due to deterioration can be written as follows:

$$\alpha_t = \alpha_0 + \sum_{i=1}^{N(t^-)} \Delta\alpha^s_{t_i} + R_\alpha(t) \tag{4-3}$$

where $\Delta\alpha^{s}_{t_i} = \alpha_{t_i^+} - \alpha_{t_i^-}$ is the value of shock and $R_\alpha(t) = \int_0^t [(d\alpha_t / dt)_{t \neq t_i}]dt$ is the gradual deterioration process. Accounting for the deterioration effects, D_{t_n} is written as follows using Eqs. (4-2) and (4-3):

$$D_{t_n} = Y_{t_n} + \alpha_0 + \sum_{i=1}^{N(t^-)} \Delta\alpha^{s}_{t_i} + R_\alpha(t_n) \tag{4-4}$$

Figure 4-2 illustrates the effect of deterioration on demand as expressed in Eq. (4-4).

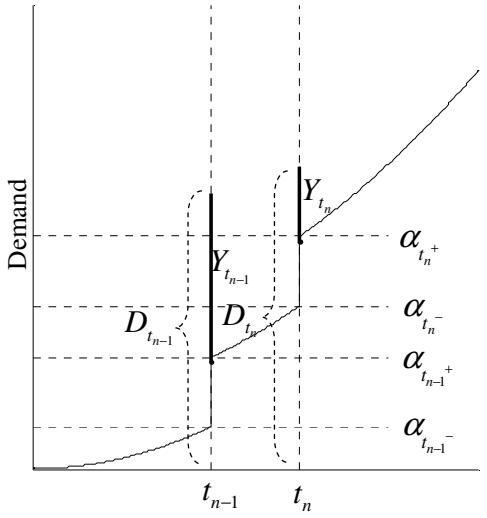

Figure 4-2. Effect of deterioration on demand

4.3.3 Failure of the system

1. *Failure due to excessive demand.* Failure due to excessive demand is observed at the n^{th} load if $(C_{t_n^-} - D_{t_n} < 0)$, where $(C_{t_n^-} - D_{t_n})$ can be written as

$$C_{t_n^-} - D_{t_n} = (C_0 - \alpha_0) - Y_{t_n} + \sum_{i=1}^{N(t^-)} \left(\Delta C^s{}_{t_i} - \Delta \alpha^s{}_{t_i}\right) + \left[R_C(t_n) - R_\alpha(t_n)\right] \qquad (4\text{-}5)$$

Normalizing Eq. (4-5) with $u_0 = (C_0 - \alpha_0)$ and by writing $\hat{Y}_{t_n} = Y_{t_n} / u_0$

$$\frac{C_{t_n} - D_{t_n}}{u_0} = 1 - \hat{Y}_{t_n} + \sum_{i=1}^{N(t^-)} \frac{\left(\Delta C^s{}_{t_i} - \Delta \alpha^s{}_{t_i}\right)}{u_0} + \left[\frac{R_C(t_n) - R_\alpha(t_n)}{u_0}\right] \qquad (4\text{-}6)$$

Writing the changes in the system during the i^{th} shock as Z_{t_i} and due to gradual deterioration in time $[0,t]$ as $R(t)$, the following is obtained

$$\frac{C_{t_n} - D_{t_n}}{u_0} = 1 - \hat{Y}_{t_n} + \sum_{i=1}^{N(t^-)} Z_{t_i} + R(t_n) \qquad (4\text{-}7)$$

Now defining g_{t_n} as follows:

$$g_{t_n} = \hat{Y}_{t_n} + \sum_{i=1}^{N(t^-)} Z_{t_i} + R(t_n) \qquad (4\text{-}8)$$

the number of shocks until failure is given by $n_F = \min\{n : g_{t_n} > 1\}$ and the time until failure $t_F = t_{n_F}$ assuming failure due to excessive demand only.

2. *Failure due to excessive deterioration*. The total deterioration in the system at time t is given as follows:

$$W_t = \sum_{i=1}^{N(t^-)} Z_{t_i} + R(t) \qquad (4\text{-}9)$$

The total deterioration W_t is an important indicator of the state of the system. The important properties of W_t are as follows:

(i) W_t captures all the changes in a system that determine its failure.

(ii) Increase in W_t reduces the life of a system.

(iii) If $W_t \geq w_a$ then at $i = N(t)+1$ any demand having $Y_{t_i} > 1 - w_a$ causes failure of the type excessive demand. The value of w_a can computed such that an insignificantly small Y_{t_i} results in failure of the type excessive demand. The time until failure considering both excessive demand and excessive deterioration is given by $t_F = \min\{t_{n_F}, \min\{t : W_t \geq w_a\}\}$.

It can be seen that instead of the additive form used in Eqs. (4-1) to (4-4), a multiplicative form can be also be used as following to express the changes due to deterioration:

$$\Gamma_{C,t_n} C_0 - \Gamma_{D,t_n} Y_{t_n} \leq 0 \tag{4-10}$$

Γ_{C,t_n} is the change in the capacity in time t and Γ_{D,t_n} accounts for the effect of deterioration on demands. By rearrangement of terms in the multiplicative form in Eq. (4-10), we have $n_F = \min\{n : g_{t_n} = \hat{Y}_{t_n} + W_{t_n} > 1\}$, where $\hat{Y}_{t_n} = Y_{t_n} / C_0$, $W_t = [1 - \Gamma_{C,t} / \Gamma_{D,t}]$. The multiplicative form is more or less similar to the additive form but can be more suitable than additive form for some cases. The stochastic process W_t for both additive and multiplicative form can be modeled as a combination of shock and gradual process as shown in Eq. (4-9).

4.3.4 Semi-analytical estimation of n_F and t_F

As discussed earlier, the process W_t consists of shocks $\{Z_{t_n}\}$ and a gradual process $R(t)$. The magnitudes of Z_{t_n} and $\hat{Y}_{t_n}$ are correlated because both are caused during the same

loading events S_{t_n}. A purely analytical solution to compute n_F and t_F is not available owing to the dependence between Z_{t_n} and $\hat{Y}_{t_n}$. Therefore, a novel simulation-based approach is proposed to estimate n_F and t_F. The traditional method of simulating scenarios of failure and no failure is unsuitable for computing small failure probabilities (as is commonly observed for well-designed engineering systems). This is because such a method computes failure probability by estimating the expectation of a Bernoulli random variable (i.e., 1 for failure and 0 for no failure) which requires a large number of simulations as compared to the estimation for a continuous random variable. Therefore, a semi-analytical approach is proposed that estimates the expectation of a continuous random variable chosen such that its expectation is equal to the failure probability of the system.

The proposed semi-analytical solution is based on the dependence between Z_{t_n} and $\hat{Y}_{t_n}$. The dependence can be modeled in several ways, e.g., by developing the joint probability density function (PDF) $f_{Z\hat{Y}}(z, y)$ for Z_{t_n} and $\hat{Y}_{t_n}$ or the conditional PDF $f_{Z|\hat{Y}}(z|\hat{Y}_{t_n})$ of Z_{t_n} given the value of $\hat{Y}_{t_n}$. The proposed framework has the flexibility to incorporate any kind of dependence between Z_{t_n} and $\hat{Y}_{t_n}$ as long as $F_{\hat{Y}|Z}(y|Z_{t_n})$ the CDF of $\hat{Y}_{t_n}$ given the value of Z_{t_n} can be computed. The proposed semi-analytical solution to estimate n_F and t_F is explained in the following:

1. *Number of shocks to failure*, n_F. The probability that failure has not occurred in $[0, t_n]$ is

$$P(n_F > n) = P\left[\bigcap_{i=1}^{n}\left(W_{t_i} + \hat{Y}_{t_i} \le 1\right)\right] \tag{4-11}$$

By conditioning on the value of $\{Z_{t_i}\}$ and $\{t_i\}$ for $i \ge 1$, the failures due to each S_{t_i} can be treated as independent events. Therefore,

$$P\left(n_F > n \middle| \{Z_{t_i}\}_{i\ge1}, \{t_i\}_{i\ge1}\right) = \prod_{i=1}^{n} P\left[\hat{Y}_{t_i} \le 1 - W_{t_i} \middle| \{Z_{t_i}\}_{i\ge1}, \{t_i\}_{i\ge1}\right] \tag{4-12}$$

Now taking the expectation of the expression in Eq. (4-12) over the distributions of $\{Z_{t_i}\}$ and $\{t_i\}$, we get

$$P(n_F > n) = E\left[\prod_{i=1}^{n} P\left[\hat{Y}_{t_i} \le 1 - W_{t_i} \middle| \{Z_{t_i}\}_{i\ge1}, \{t_i\}_{i\ge1}\right]\right] \tag{4-13}$$

where $E[\cdot]$ is the expected value. Now, since $\hat{Y}_{t_i}$ depends only on Z_{t_i}, we have

$$P\left(\hat{Y}_{t_i} \le 1 - W_{t_i} \middle| \{Z_{t_i}\}_{i\ge1}, \{t_i\}_{i\ge1}\right) = F_{\hat{Y}|Z}\left(1 - W_{t_i} \middle| Z_{t_i}\right) \tag{4-14}$$

If $N(t)$ is a Poisson process with rate ν, then t_i has gamma distribution with parameters ν and i, where the mean is i/ν.

2. *The time to failure,* t_F. Assuming only failures due to excessive demand, the probability that failure has not occurred by time t is

$$P(t_F > t) = E\left[\prod_{i=1}^{N(t)} P\left(\hat{Y}_{t_i} \le 1 - W_{t_i} \middle| Z_{t_i}\right)\right] \tag{4-15}$$

Using Eq.(4-14), we have

$$P\left(t_F > t\right) = E\left[\prod_{i=1}^{N(t)} F_{\hat{Y}|Z}\left(1 - W_{t_i} \middle| Z_{t_i}, \{t_i\}_{i\geq 1}\right)\right] \tag{4-16}$$

If $N(t)$ is a Poisson process with rate ν, then

$$P\left(t_F > t\right) = \sum_{n=0}^{\infty} \frac{(\nu t)^n e^{-\nu t}}{n!} E\left[\prod_{i=1}^{n} F_{\hat{Y}|Z}\left(1 - W_{t_i} \middle| Z_{t_i}, \{\tau_{n,i}\}_{1\leq i\leq n}\right)\right] \tag{4-17}$$

where $\{\tau_{n,i}\} = \{tU_{n,i}\}$ and $U_{n,1} < U_{n,2} < ..... < U_{n,n}$ are the order statistics of random uniform $[0,1]$ sample of size n. Considering both failures due to excessive demand and excessive deterioration, we have

$$P\left(t_F > t\right) = P\left[\{n_F > N(t)\} \cap \{W_t < w_a\}\right] = E\left[1_{W_t \leq w_a} \prod_{i=1}^{N(t)} F_{\hat{Y}|Z}\left(1 - W_{t_i} \middle| Z_{t_i}, \{t_i\}_{i\geq 1}\right)\right] \tag{4-18}$$

and if $N(t)$ is a Poisson process, then

$$P\left(t_F > t\right) = \sum_{n=0}^{\infty} \frac{(\nu t)^n e^{-\nu t}}{n!} E\left[1_{W_t \leq w_a} \prod_{i=1}^{n} F_{\hat{Y}|Z}\left(1 - W_{t_i} \middle| Z_{t_i}, \{\tau_{n,i}\}_{1\leq i\leq n}\right)\right] \tag{4-19}$$

where $1_X = 1$ if X is true and 0 otherwise. Using Eq. (4-18), we can also compute the probability distribution for W_t conditioned at any given time during the service life of the systems. This is given by $P[W_t < w \mid t_F > t] = P[W_t < w \cap n_F > N(t)] / P[W_t < w_a \cap n_F > N(t)]$ for $w < w_a$. As Eqs. (4-13) through (4-19) require the computation of expectations using simulations, errors arising out of these simulations must be reported. For computing simulation errors the variance of the quantity estimated through simulations can be computed. This variance can be used to compute upper and lower bounds on the estimate. We use $\bar{X} \pm 2\sigma_{\bar{X}}$ as

upper and lower bounds, where $\bar{X}$ is the sample mean for the simulation, $\sigma_{\bar{X}}^2 = \hat{\sigma}_X^2 / N_{sim}$ is the variance of $\bar{X}$, $\hat{\sigma}_X^2$ is the sample variance of X and N_{sim} is the number of simulations.

4.3.5 Approximate estimation of t_F

Now, we develop an approximate solution for estimating t_F considering only the failure due to excessive demand. The solution is based on the assumption that W_t is independent of $N(t)$. This approach can also yield closed-form solutions in some cases where closed-forms for required convolutions and integrations are possible.

The conditional probability $P_f(t)$ of observing a failure at t conditioning on the occurrence of a load is given by

$$P_f(t) = P\left[W_t + \hat{Y}_{t_i} > 1\right] = P\left[\hat{Y}_{t_i} > 1 - W_t\right] \tag{4-20}$$

Defining, $N'(t) = \sum_{i=1}^{N(t)} 1_{\{\hat{Y}_{t_i} + W_{t_i} > 1\}}$, (i.e., $N'(t)$ is the number of times the event $(\hat{Y}_{t_i} + W_{t_i} > 1)$ is observed in the interval $[0, t]$) we have

$$P(t_F > t) = P\left[N'(t) = 0\right] \tag{4-21}$$

Assuming, W_t and $N(t)$ are mutually independent, if $N(t)$ is a Poisson process then we have

$$P\left[N'(t) = 0\right] = exp\left[-\nu \int_0^t P_f(s)\, ds\right] \tag{4-22}$$

The probability $P_f(t)$ can be found analytically as follows:

$$P\left[\hat{Y}_{t_i} > 1 - W_t\right] = \int_0^{\infty} \left[1 - F_{\hat{Y}}\left(1-w\right)\right] f_{Wt}\left(w,t\right) dw \tag{4-23}$$

where $f_{Wt}(w,t)$ is the PDF of W_t. The CDF $F_{Wt}(w,t)$ of W_t is found as follows:

$$P\left(W_t < w\right) = \sum_{n=0}^{\infty} \frac{\left(\nu t\right)^n e^{-\nu t}}{n!} F_Z{}^n\left[w - R\left(t\right)\right] \tag{4-24}$$

where $F_Z{}^n(z)$ is the CDF of $(Z_1 + Z_2 + \ldots + Z_n)$. If an analytical solution is not available then simulations can be used to compute $P_f(t)$. It is expected that the estimate for $P(t_F > t)$ using the approximate solution is a lower bound to that estimated using the semi-analytical solution. This is because of the assumption of independence between W_t and $N(t)$ which implies that for a given value of $N(t)$, $W_t = R(t) + Z_1 + Z_2 + \ldots + Z_n$, where n can be large with a positive probability resulting in the overestimation of $P_f(t)$. This approximate solution can be used to only to estimate $P(t_F > t)$ for failures due to excessive demand.

4.4 Numerical examples

In this section, we illustrate the proposed model with two examples. The objective of the first example is to illustrate the steps in the computation of n_F and t_F. For this example, we choose distributions such that the computation process is simplified. The second example illustrates the application of the model to a more realistic case.

4.4.1 Example 1

We assume that $\hat{Y}_{t_n}$ has a Pareto distribution and $Z_{t_n} = \xi_{t_n} \hat{Y}_{t_n}$, where ξ_{t_n} is uniformly distributed over the interval $[0,1]$. The probability distributions required to implement the semi-analytical solution are

$$F_{\hat{Y}}(y) = \left[1 - \left(\hat{Y}_{\mathrm{m}} / y\right)^{k}\right] 1_{y > \hat{Y}_{\mathrm{m}}} \tag{4-25}$$

and

$$F_{Z|\hat{Y}}\left(z \middle| \hat{Y}_{t_n} = y\right) = 1/y \qquad 0 < z \le y \tag{4-26}$$

where $F_{\hat{Y}}(y)$ is the CDF for $\hat{Y}_{t_n}$, $\hat{Y}_m$ is the minimum value of $\hat{Y}_{t_n}$ and k is a distribution parameter. Equations (4-25) and (4-26) are used to derive the following expression:

$$F_{\hat{Y}|Z}\left(y \middle| Z_{t_n} = z\right) = \left[1 - \left(\hat{Y}_{\mathrm{m}} / y\right)^{k+1}\right] 1_{y > \max(\hat{Y}_{\mathrm{m}}, z)} \tag{4-27}$$

Table 4-1. Description of different variables in the process for Example 1

Variable/ Function	Value/ Description	Distribution	Distribution Parameters	
			Symbol	Value
$\hat{Y}_{t_n}$	-	Pareto	$\hat{Y}_m$, k	0.05, 1.33
$R(t)$	$\min\{(t/75)^2, 1\}$			
$N(t)$	Poisson process		ν	0.20/year

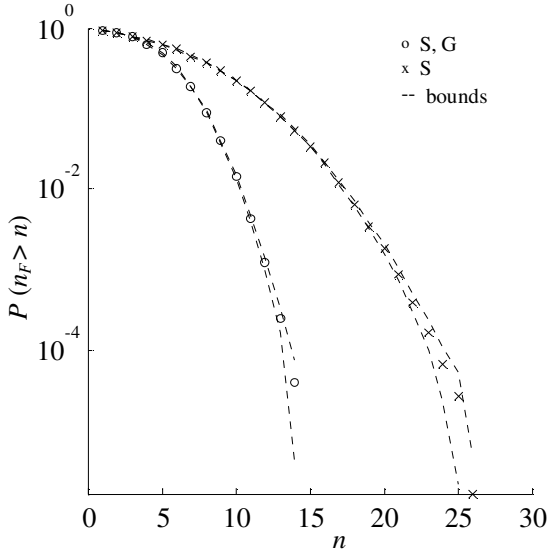

Figure 4-3. Probability distribution for n_F

Table 4-1 provides the description for the different processes and variables involved. Figure 4-3 shows the plots for $P(n_F > n)$ using the semi-analytical solution for two cases; considering both shocks and gradual deterioration (labeled as S, G) and considering shocks only (labeled as S). The figure also shows the bounds on the estimate of $P(n_F > n)$. As expected, the figure shows that the system is expected to reach failure in less number of shocks in the case (S,G) as compared to the case (S). Figure 4-4 shows the plots for $P(t_F > t)$ for three cases; shocks and gradual deterioration assuming failures due to both excessive demand and excessive deterioration (labeled as S, G, F_{dmd}, F_{det}), shocks and gradual deterioration assuming failure due to excessive demand only (labeled as S, G, F_{dmd}), and shocks only also assuming failure due to excessive demand only (labeled as S, F_{dmd}). The figure shows that the system is expected to fail earlier in the case (S, G, F_{dmd}, F_{det}) compared to the

other two cases. This figure does not show the bounds on the estimates because the bounds are found to be indistinguishable from the actual estimate which implies that the simulations errors are insignificantly small.

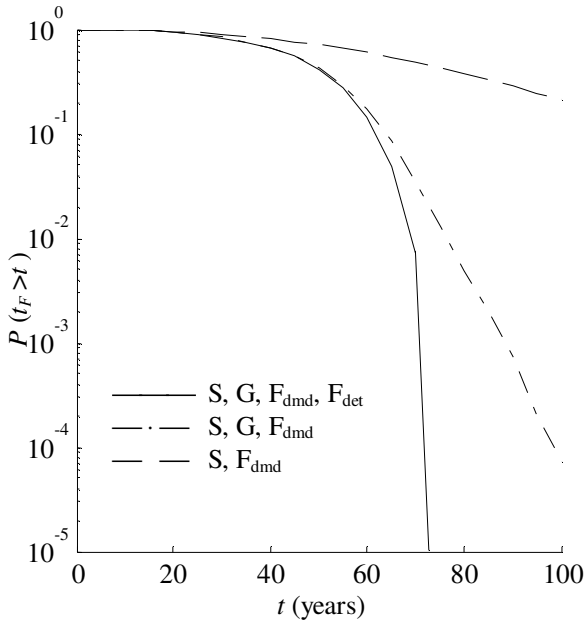

Figure 4-4. Probability distribution for t_F

Figure 4-5 compares the estimates for $P(t_F > t)$ obtained using the semi-analytical solution and the approximate solution. As explained earlier, the estimates of the approximate solution are a lower bound to the estimates of semi-analytical solution due to the assumption of independence between W_t and $N(t)$. This assumption implies that there is a positive probability of having more than $N(t)$ number of shocks in W_t resulting in the underestimation of $P(t_F > t)$. However, it is found that the approximate solution yields accurate results for early part of the life time (i.e., $t < 20\,years$). This is

because the probability of observing a large number of shocks within the early part of life time is small for $\nu = 0.2/\,year$.

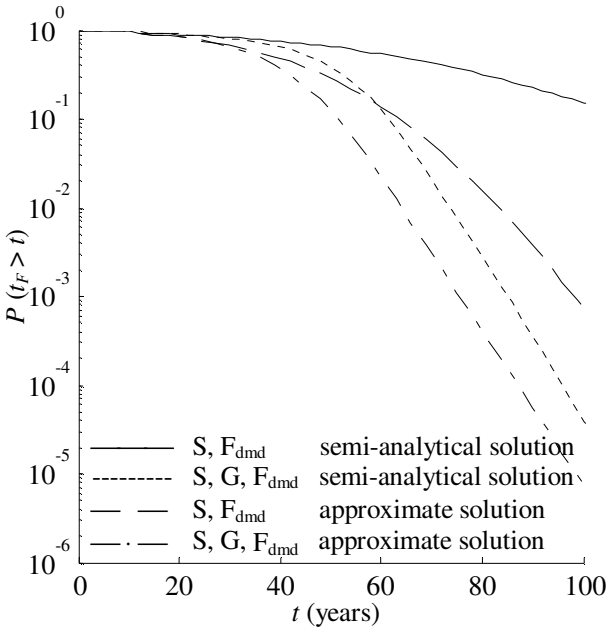

Figure 4-5. Comparision of estimates using semi-analytical and approximate solution for Example 1

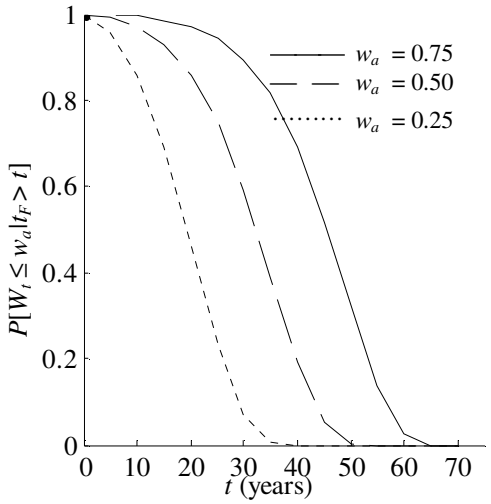

Figure 4-6. Plots for $P[W_t \le w_a | t_F > t]$

Figure 4-6 shows the plot for $P[\{W_t < w_a\} \bigcap \{n_F > N(t)\}]$ the probability of damage being less than w_a for $w_a = 0.25$, 0.50 and 0.75. As expected, at any given time, the probability of being less than w_a is higher for higher values of w_a. Also it is seen that the probability of being less than w_a decreases with increase in time. The results in Figure 4-6 can also be used to compute $P[\{W_t < w_a\} | \{n_F > N(t)\}]$ by dividng $P[\{W_t < w_a\} \bigcap \{n_F > N(t)\}]$ with $P[n_F > N(t)] = P[t_F > t]$ assuming failure due to excessive demand only.

4.4.2 Example 2

In this example we apply the framework to model a deteriorating system with a more realistic damage mechanism as compared to Example 1. It is commonly observed in engineering systems that there is no damage for D_{t_n} less than a certain threshold value l. We model this damage process by assuming that the damage is a random linear

function of D_{t_n}. However, for simplicity we assume that $\alpha_{t_n^-} \approx \alpha_0$ in the expression for Z_{t_n}. The damage process is then written as

$$Z_{t_n} = \xi_{t_n} \frac{\left(D_{t_n} - l\right)_+}{u} \approx \xi_{t_n} \left(\hat{Y}_{t_n} - h\right)_+ \tag{4-28}$$

where $(D_{t_n} - l)_+$ is the positive part of $(D_{t_n} - l)$, $h = (l - \alpha_0)/u$ and ξ_{t_n} are SIID random variables independent of $\{D_{t_n}\}$. The conditional CDF $F_{\hat{Y}|Z}(y \mid Z_{t_n} = z)$ for this case is given as follows:

$$\begin{aligned} F_{\hat{Y}|Z}\left(y \middle| Z_{t_n} = z\right) = F_{\hat{Y}|\hat{Y} \le c}\left(y\right) &= \frac{F_Y\left(uy\right)}{F_Y\left(uh\right)}, && z = 0,\ y \le h \\ &= \frac{1}{f_{Z|Z\neq 0}\left(z\right)} \int_c^y \left[\frac{1}{y+h}\right] f_\xi \left[\frac{z}{y+h}\right] f_{\hat{Y}|\hat{Y}>h}\left(y \middle| \hat{Y}_n > h\right) dy && \\ & && z \neq 0,\ y > h \end{aligned} \tag{4-29}$$

where $F_Y(y)$ is the CDF of Y_{t_n}, $f_{\hat{Y}|\hat{Y}>h}(y \mid \hat{Y} > h) = u[f_Y(uy)]/[1 - F_Y(uh)]$ and,

$$f_{Z|Z\neq 0}(z) = \int_h^\infty \left(\frac{1}{y-h}\right) f_\xi \left(\frac{z}{y-h}\right) f_{\hat{Y}|\hat{Y}>h}\left(y \middle| \hat{Y} > h\right) dy \tag{4-30}$$

The different variables of the system are described in Table 4-2. To implement the semi-analytical solution we first obtain the conditional CDF $F_{\hat{Y}|Z}(y \mid Z_{t_n} = z)$. The CDF has a closed-form expression for $z = 0$. For $z \neq 0$, we obtain the CDF by numerically performing the integrations in Eqs. (4-29) and (4-30). Figure 4-7 shows the conditional CDF $F_{\hat{Y}|Z}(y \mid Z_{t_n} = z)$ for $z \neq 0$.

Table 4-2. Description of different variables in the process

Variable/ Function	Value/ Description	Distribution	Distribution Parameters
C_0	1.00	-	-
α_0	0.00	-	-
l	0.05	-	-
Y_{t_n}	-	Exponential	0.2 (mean)
ξ_{t_n}	-	Beta	3.0, 6.0 (shape)
$R(t)$	$\min\{(t/75)^2, 1\}$		
$N(t)$	Poisson process		0.2/year (rate)

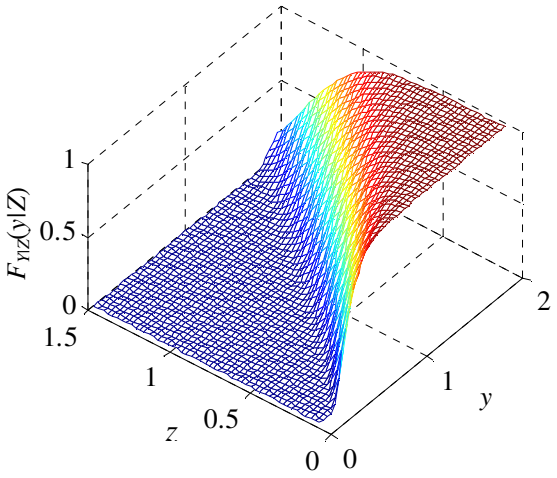

Figure 4-7. Plot for $F_{\hat{Y}|Z}(y|Z)$ for $z \neq 0$ obtained numerically

Figure 4-8 shows the plots for $P(n_F > n)$ for the cases (S,G) and (S). The figure also shows the bounds on the estimates of $P(n_F > n)$. The probability $P(n_F > n)$ is found to be greater for the case (S) than for case (S,G). This result is expected because in the second case the deterioration process is faster. Figure 4-9 compares the estimates obtained using semi-analytical and approximate solution.

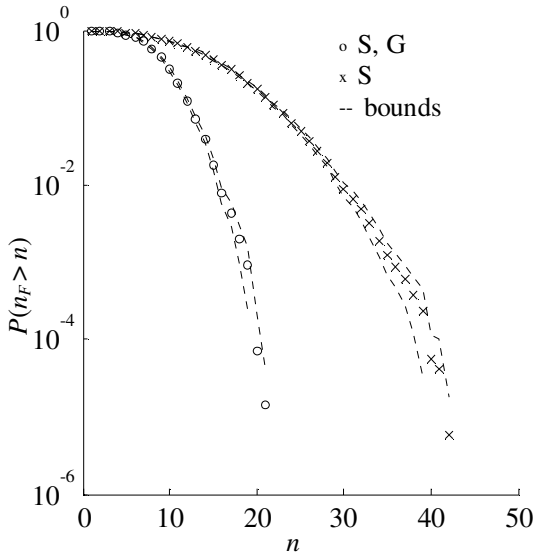

Figure 4-8. Plots of probability distribution for n_F

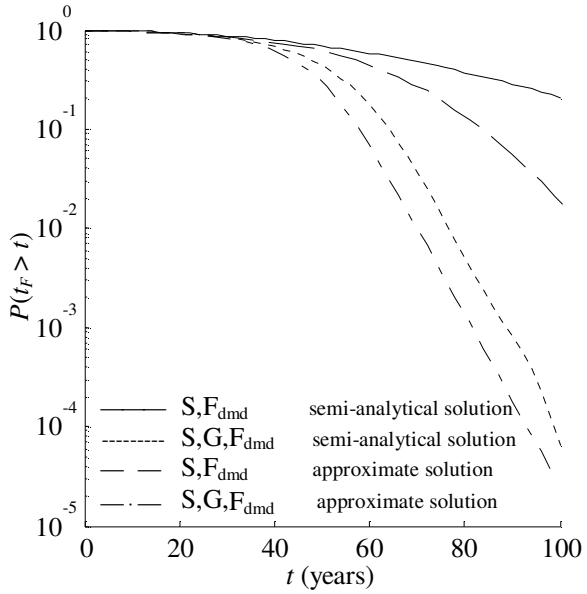

Figure 4-9. Comparision of estimates using semi-analytical and approximate solution for Example 2

As already explained in Example 1, the estimates of approximate solution are a lower bound to the estimates of semi-analytical solution. Figure 4-10 shows the plots for $P(t_F > t)$ that are obtained for cases with shocks only and with both shocks and gradual process. As expected and already seen in Example 1, the figure shows that the system is expected to fail earlier in the case (S, G, F_{dmd}, F_{det}) as compared to the other two cases. Figure 4-11 shows the probability of damage being less than $w_a = 0.25,\ 0.50,\ 0.75$ at various points of time in the service life of the system. The results are similar to those obtained in Example 1. Figure 4-10 and Figure 4-11 do not show the bounds because the simulation errors are found to be insignificantly small.

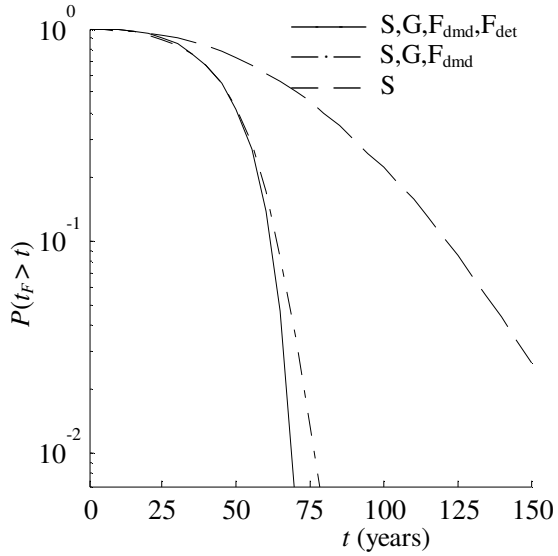

Figure 4-10. Plots of probability distribution for t_F

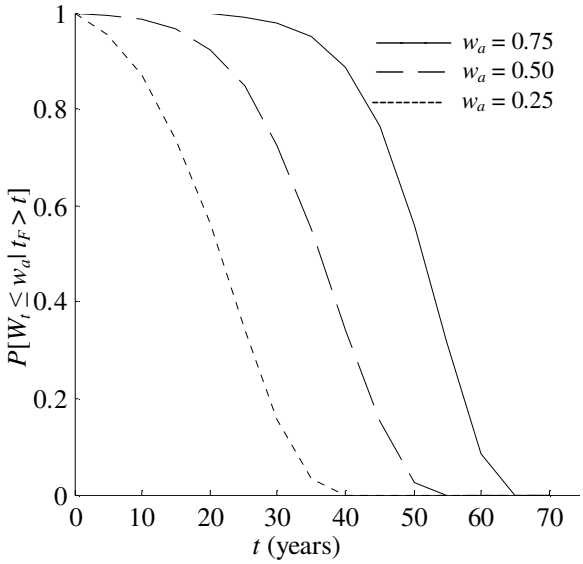

Figure 4-11. Plots for $P[W_t \leq w | t_F > t]$

4.5 Case study

In this section we use the system in Example 2 to study the effect of various deterioration scenarios. We develop four cases as described in Table 4-3 and Table 4-4. The cases are developed by combining different rates of shock and gradual deterioration process. The rate of shock deterioration is governed by several variables (e.g., $E[\hat{Y}_{t_n}]$, ν and $E[\xi_{t_n}]$). We choose to vary the distribution parameters of ξ_{t_n} to develop the cases. The rate of gradual deterioration is varied by changing the coefficient of t^2 in $R(t)$.

Table 4-3. Deterioration scenarios for case study

Gradual deterioration	Shock deterioration	
	Slow	Fast
Slow	Case I	Case II
Fast	Case III	Case IV

Table 4-4. Rates of deterioration process for case study

Deterioration process	Variable	Slow	Fast
Shock	ξ_{t_n}	Beta(3,6)	Beta(3,3)
Gradual	$R(t)$	$\min(0.01t^2,1)$	$\min(0.02t^2,1)$

The results from the case study are shown in Figure 4-12. The figure shows that in this case study, the deterioration process in the four cases is ordered in terms of increasing rate as I, III, II and IV. Cases I and III have slow shock deterioration process and cases II and IV have fast shock deterioration process. This implies that for this case study, shock deterioration process has more influence on the total deterioration rate than the gradual deterioration process. It is seen that even though one type of deterioration process is more influential than other, the combined effect of the two processes cannot be underestimated. Using this framework, similar case studies can be built to study the influence of various factors in the deterioration process.

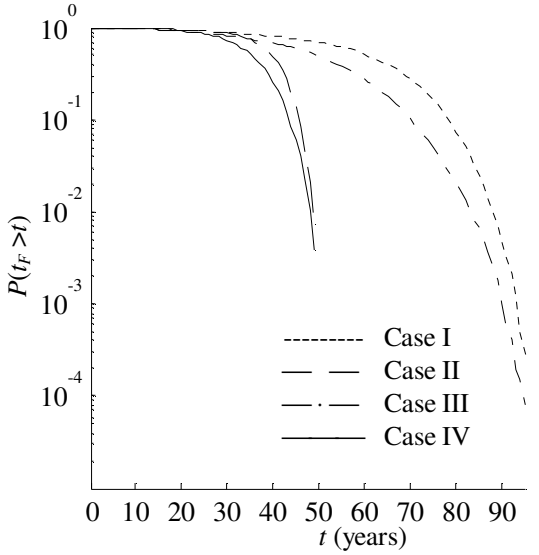

Figure 4-12. Plots showing effect of different deterioration scenarios

4.6 Conclusions

Deterioration is a serious concern in engineering because it can considerably reduce the service life and reliability of systems. In this paper we developed a novel stochastic framework to model deteriorating systems, consisting of shocks and a gradual deterioration process. We model the shock deterioration process accounting for the dependence between the shocks and the demands imposed by loading events. We use a deterministic function of time to model the gradual deterioration process. The developed framework addresses the following important issues in modeling deteriorating systems:

1. Modeling the effect of deterioration on both capacity;
2. Modeling the dependence between the deterioration process and demands;
3. Modeling the combination of shock and gradual deterioration process;
4. Accounting for different failure types; and

5. Proposing accurate, time-efficient and convenient solution strategies.

The proposed framework provides the flexibility for incorporating different types of damage mechanisms. Furthermore, we derived estimates of important quantities such as time to failure, number of shocks to failure, and accumulated damage that are essential for life-cycle analysis of systems. The proposed framework can be used in future research for conducting comprehensive life-cycle cost analysis accounting for various types of performance criteria.

5. RENEWAL THEORY BASED LIFE-CYCLE ANALYSIS OF DETERIORATING ENGINEERING SYSTEMS

5.1 Introduction

Deteriorating engineering systems have to be operated in a strategic manner in order to maximize the safety of, and the benefits to the users and owner. Such operation strategies can be effectively devised only by conducting a life-cycle analysis (LCA) of the deteriorating system. In general, a LCA study includes the prediction of the reliability of a system over its entire life-span and the costs and benefits associated to the operation of the system (Rackwitz 2000). LCA must factor in the uncertainties in the operating conditions (e.g., environmental conditions, intensity and time of occurrence of loads) and the process of deterioration of the system. Furthermore, LCA should be able to account for the influence of occasional repairs and maintenances on the reliability of the deteriorating system and costs associated to its operation. The LCA of most deteriorating engineering systems is a complex problem owing to the number of involved variables, the associated uncertainties and the propagation of uncertainties in time.

Research in the field of LCA has advanced over past few years and has found applications in various fields of engineering. Several types of LCA studies have been conducted based on the engineering system under consideration and the objective of the study. Wen and Kang (2001a,b) computed the losses due to building failures in a multiple hazard scenario but without considering the deterioration of the buildings over time. Yang (1976) computed the expected cost of inspecting and repairing service cracks in aircrafts considering the growth of cracks with time. While this formulation considers

the time-dependent condition of the system, it only includes serviceability failures. A serviceability failure is the failure of a system to meet a pre-collapse or pre-breakdown performance level related to safety and damage/repair costs (e.g., maximum acceptable crack size). However, a LCA study should also include the analysis of ultimate failures, where a system fails because of an extreme event resulting in a complete collapse or breakdown of the system. Ultimate failures are generally rare but they should be included in LCA because the corresponding losses are high. Typically a serviceability failure is an excessive deterioration type failure and ultimate failure is an excessive demand type failure as described in Section 4. Oswald and Schullër (1984) and Mori and Ellingwood (1993) estimated the reliability and the time to failure of an infrastructure system with time-dependent capacity deterioration. The methodology can be applied to serviceability or ultimate failures but only one type of failure can be considered at a time in the analysis. Moreover, the study does not consider repairs and replacements following failures and also does not include life-cycle cost analysis. Rackwitz (2000) estimated the life-cycle cost of deteriorating systems considering only the immediate replacement of the system after failures. The methodology is again applicable only to one type of failure (serviceability or ultimate). Also, repairs for intermediate levels of deterioration not requiring complete replacement are not considered. Noortwijk and Frangopol (2004), Neves and Frangopol (2005) and Kim et al. (2011) used deterministic functions of time representing the reliability of a deteriorating system in order to compute the maintenance and failure costs. The adopted methodologies consider both serviceability and ultimate failures. However, the method of using the deterministic time-dependent

reliability functions for LCA, typically considers only the gradual time–continuous deterioration processes and ignores the discrete shock type deterioration in a system caused by loads. Sanchez-Silva et al. (2011) computed the number of repairs/replacements per year required to maintain a system above the target safety level. The study considers both gradual and shock type deterioration and can be used for both serviceability and ultimate failures. However, the study the study did not include life-cycle cost analysis and is limited only to a specific criterion for conducting repairs and hence cannot be used to study the influence other types of operation strategies. A LCA formulation should be applicable to a wide variety of operation strategies in order to arrive at an optimum solution.

This section proposes a novel probabilistic formulation for LCA of deteriorating systems named Renewal Theory-based Life-cycle Analysis (RTLCA). As the name suggests, the formulation is based on renewal theory (Grimmett and Stirzaker 2001). The proposed formulation develops analytical equations to estimate the life-cycle variables such as the time lost in repairs, the age and reliability of the system and cost of operation and failures. Both serviceability and ultimate failures can be considered simultaneously in the formulation and it is applicable for a wide variety of repair and maintenance strategies. Furthermore, RTLCA formulation is not dependent on any particular deterioration model which increases makes it easily transferable to analyses having different levels of complexities. As an example, the proposed RTLCA formulation is used to analyze a reinforced concrete (RC) bridge accounting for the possible deterioration caused by earthquakes during its service life. The flexibility of the proposed RTLCA

formulation, allows the use of time-dependent stochastic models for earthquake occurrences accounting for both main shocks and aftershocks. Furthermore, the example accounts for the delays in repair after earthquakes and considers any damage accumulated during this delay due to aftershocks.

This section is organized into six subsections including this introduction. The second subsection describes the events typically observed in the life-cycle of an engineering system and introduces a few definitions used in the section. The third subsection describes the financial aspects of an engineering project and introduces the various costs associated to the operation of an engineering system. The fourth subsection proposes the RTLCA formulation and develops the equations for computing various LCA variables. The fifth subsection briefly describes an application of the SSA deterioration model proposed in Section 4 to compute the probabilities and probability distributions required to implement the RTLCA model. The sixth subsection uses the proposed RTLCA formulation to analyze the life-cycle of an example RC bridge. Finally, the seventh section presents the conclusions derived from this work.

5.2 Life-cycle of an engineering system

Figure 5-1 shows the various events in the life-cycle of an engineering system that is experiencing deterioration. The state of the system at a given time t is described in terms of the probability of ultimate failure $P_f(t)$ of the system given that a load acts on the system at time t. Changes in $P_f(t)$ occur in the form of discrete or continuous increments. Discrete increments are due to shocks that cause sudden changes in the system properties. Loads and deterioration mechanisms that are active for a short duration of

time (e.g., impact loads, seismic loads, and fires) are example of such shocks. Continuous increments in $P_f(t)$ are due to a gradual deterioration of the system properties due to phenomena like corrosion of steel, alkali-silica reactions (ASR), delayed ettringite formation (DEF), creep, etc.

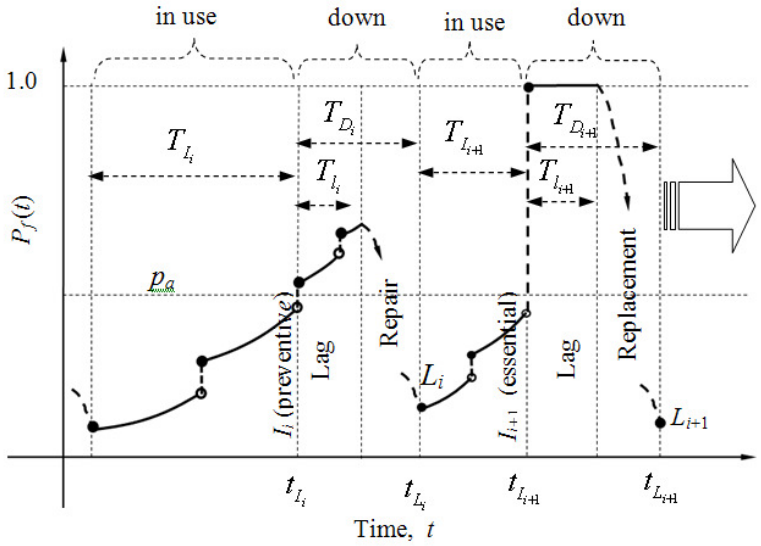

Figure 5-1. Life-cycle of an engineering system

Figure 5-1 shows that an engineering system experiences alternating phases of being in use and in down-time. A system is said to be in use at time t if the system is functioning at that time. On the other hand, a system is said to be down or experiencing down-time if the system is either abandoned or removed from the service for repairs or replacement. In this paper, we call the start of a down-time as an *intervention* (I). The down-time of a system ends when the repair or replacement is complete and the system starts functioning again. In this paper, we call this event *renewal* (L). Interventions can

be *preventive* if the system is removed from service in order to conduct repairs or maintenance work. On the other hand, an intervention is *essential* if it is initiated because of the occurrence of an ultimate failure. Preventive interventions are typically made when a pre-determined intervention criterion is met. Some examples of intervention criteria are: the exceedance of a threshold intensity of the applied load, a serviceability type failure such as exceedance of a threshold level for damage or $P_f(t)$, and reaching a pre-planned time interval between two interventions (like in the case of a scheduled maintenance). Figure 5-1 shows that the i^{th} intervention I_i that occurs at time t_{I_i} is preventive and is conducted because $P_f(t) \geq p_a$. The figure also shows that I_{i+1} is an essential intervention and occurs because the system experiences an ultimate failure at time $t_{I_{i+1}}$ because of which $P_f(t)$ jumps to 1.0. The corresponding renewal events L_i and L_{i+1} occur at time t_{L_i} and $t_{L_{i+1}}$, respectively. In the figure, T_{I_i} is the time interval between L_{i-1} and I_i and T_{D_i} is the down-time following I_i.

For some systems, deterioration does not progress during the down-time because the system is removed from service and it is immediately repaired. However, in some cases (as shown in the figure) the actual repair work may not begin immediately at t_{I_i} and a lag period (T_{l_i} following I_i and $T_{l_{i+1}}$ following I_{i+1}) may exist during which the deterioration process may continue. Generally, this is the time required for the mobilization of the required resources. For example, an infrastructure that has been closed due to damage from an earthquake is still exposed to aftershocks before the

repairs or replacement might take place. In such cases, the lag period may significantly affect the LCA and hence must be considered.

5.3 Financial considerations for a system

In addition to the initial cost of construction or manufacturing of a system C_C, we group the remaining costs incurred during the life-cycle of the system into cost of operation $C_{Op}(t)$ and failure losses $C_L(t)$. The cost $C_{Op}(t)$ is the total cost of repairs and replacement of the system following the serviceability and ultimate failures in order to operate the system up to time t. The cost of operation is written as $C_{Op}(t) = \sum_{i=1}^{\infty}[c_{Op_i} e^{-\gamma t_{I_i}} 1_{\{i \le N_L(t)\}}]$, where c_{Op_i} is the cost of repair or replacement corresponding to I_i, γ is the discount rate to compute the net present value (NPV) of the cost, $N_L(t)$ is the number of renewals in time t and 1_X is the indicator function which is equal to 1 if X is true and 0 otherwise. The failure loss $C_L(t)$ is the sum of losses arising from injuries, deaths or damage to user's property until time t. Such losses are observed only during ultimate failures. The loss $C_L(t)$ does not include the cost of replacing the system. Therefore, $C_L(t) = \sum_{i=1}^{\infty}[c_{L_i} e^{-\gamma t_{I_i}} 1_{\{i \le N_I(t)\}}]$, where c_{L_i} is the loss corresponding to I_i and $N_I(t)$ is the number of interventions in time t. The value of c_{L_i} is 0 if I_i is not due to an ultimate failure and it is positive otherwise. The costs $C_{Op}(t)$ and $C_L(t)$ are often called direct and indirect costs, respectively. The distinction between $C_{Op}(t)$ and $C_L(t)$ is important because the owner of the system may choose not to repair or replace the system at t_{I_i} to avoid c_{Op_i} but c_{L_i} is inevitable. Also, this

distinction is important because often the liability for $C_{Op}(t)$ and $C_L(t)$ belong to different agencies and their values affect the decisions. In addition to the described costs, another important financial factor is benefit $Q(t)$. The benefit $Q(t)$ is the direct or indirect benefit derived from operating a system for time t (e.g., price of automobile fuel saved by commuters using a bridge). The operation of a system for time t is considered financially justified if

$$Q_{net}(t) = Q(t) - C_{Op}(t) - C_L(t) - C_C > 0 \tag{5-1}$$

5.4 Proposed formulation for LCA

In this study, we propose the RTLCA formulation which is based on renewal theory (Grimmett and Stirzaker 2001). In renewal theory, a renewal process $N_E(t)$ is the number of occurrences in time t of an event E, called the renewal event. The time intervals between consecutive occurrences of E, also called the renewal times, are considered statistically independent and identically distributed (SIID). Therefore mathematically, $N_E(t) = \max\{n : t_{E_n} \le t\}$, where $\max\{\cdot\}$ is the maximum value function, E_n is the n^{th} occurrence of E and t_{E_n} is the time of occurrence of E_n. Now if T_{E_i} are the renewal times, then $t_{E_n} = \sum_{i=1}^{n} T_{E_i}$. As mentioned earlier, $\{T_{E_i}\}$ is assumed to be a SIID sequence in renewal theory and based on this property, the renewal theory offers analytical solutions in the form of integral equations to compute several quantities that describe the renewal processes.

In the RTLCA formulation, we propose to model the occurrences of L_i as a renewal process assuming, as required in renewal theory, that the renewal times $\{T_{L_i}\}$ given by $\{T_{I_i} + T_{D_i}\}$ is SIID. This assumption requires that the events in the time interval $(t_{L_i}, t_{L_{i+1}}]$ are independent of the events in all other such intervals. This implies that the decisions associated to L_i must be based only on the events occurring within the time interval $(t_{L_{i-1}}, t_{L_i}]$. It also implies that the loading and deterioration process in the interval $(t_{L_i}, t_{L_{i+1}}]$ should be independent of the loading and deterioration process in other such intervals. Furthermore, we need to assume that the system is completely renewed after L_i and its properties at t_{L_i} are identical to the original properties at $t = 0$. This simplification along with the above mentioned assumptions are required to ensure that $\{T_{L_i}\}$ is a SIID sequence.

Furthermore, in the RTLCA formulation, L_i can be of type L_R or L_F, hereafter written as events $L_i \equiv L_F$ and $L_i \equiv L_R$ respectively. For any L_i, the events $L_i \equiv L_F$ and $L_i \equiv L_R$ occur with probabilities $P(L_R) = P(L_i \equiv L_R)$ and $P(L_F) = P(L_i \equiv L_F)$, independently of i. The type of renewal does not depend on the events that have occurred after t_{I_i}. For example, $L_i \equiv L_R$, even if there is a failure of the system in the lag period following I_i. It follows that $P(L_R) + P(L_F) = 1$ and

$$f_{T_L}(\tau) = f_{T_L|L_F}(\tau | L_F) P(L_F) + f_{T_L|L_R}(\tau | L_R) P(L_R) \qquad (5\text{-}2)$$

where $f_{T_L}(\tau)$ is the probability density function (PDF) of T_{L_i}, $f_{T_L|L_R}(\tau \mid L_R)$ is the PDF of T_{L_i} given that $L_i \equiv L_R$ and $f_{T_L|L_F}(\tau \mid L_F)$ is the PDF of T_{L_i} given that $L_i \equiv L_F$. Similarly,

$$f_{T_I}(\tau) = f_{T_I|L_F}\left(\tau \middle| L_F\right) P(L_F) + f_{T_I|L_R}\left(\tau \middle| L_R\right) P(L_R) \tag{5-3}$$

where $f_{T_I}(\tau)$ is the PDF of T_{I_i}, $f_{T_I|L_R}(\tau \mid L_R)$ is the PDF of T_{I_i} given that $L_i \equiv L_R$ and $f_{T_I|L_F}(\tau \mid L_F)$ is the PDF of T_{I_i} given that $L_i \equiv L_F$. In the following, we propose novel integral equations using renewal theory to estimate some important LCA variables based on the proposed RTLCA formulation. In order to implement the model, certain probabilities and probability distributions have to be computed that may require simulation of the actual events of any one renewal (because all renewal are SIID). However, since only one renewal needs to be simulated, this method is computationally more efficient than conducting Monte Carlo simulations of the entire life-cycle.

5.4.1 Computing the availability

It is useful to estimate the time for which a system is available for use in its life-span. This is because down-times cause inconvenience to the users and loss of income to the owner. In literature, availability of a system has been defined as the fraction of the time for which the system is available in a particular time-span. Following the same idea, we define availability of a system for the time interval $[0,t]$ as $A(t) = [T_A(t)]/t$, where $T_A(t) = \int_0^t 1_{\{\text{in use at } \tau\}} d\tau$. In order to estimate $A(t)$, we first compute $P_S(t)$ which is the probability that the system is in use at time t. This implies that the expectation of $A(t)$, $E[A(t)] = \int_0^t P_S(t)dt$. In the following, we propose an integral equation to compute $P_S(t)$

for the RTLCA formulation. Based on first intervention and Total Probability Rule (Ang and Tang 2007) I_1, we have

$$P_S(t) = P\left(\text{in use at } t, T_{I_1} > t\right) + P\left(\text{in use at } t, T_{I_1} \le t\right) \tag{5-4}$$

Noting that the system is in use if $t < T_{I_1}$, we have

$$P(\text{in use at } t, T_{I_1} > t) = P(T_{I_1} > t) \tag{5-5}$$

It follows that

$$P\left(\text{in use at } t, T_{I_1} \le t\right) = \int_0^\infty P\left(\text{in use at } t, T_{I_1} \le t \middle| T_{L_1} = \tau\right) f_{T_L}(\tau)\, d\tau \tag{5-6}$$

Since, the system is not in use in the interval (t_{I_1}, t_{L_1}) and given the assumption that system is completely renewed at t_{L_i}, we have

$$\begin{aligned} P\left(\text{in use at } t, T_{I_1} \le t \middle| T_{L_1} = \tau\right) &= 0 && t < \tau \\ &= P\left(\text{in use at } t \middle| T_{L_1} = \tau\right) = P_S(t-\tau) && t \ge \tau \end{aligned} \tag{5-7}$$

As a result, we have

$$P_S(t) = \left[1 - F_{T_I}(t)\right] + \int_0^t P_S(t-\tau) f_{T_L}(\tau)\, d\tau \tag{5-8}$$

where $F_{T_I}(t)$ is the cumulative distribution function (CDF) of T_{I_i}. This integral equation can be solved numerically for all t, by first discretizing t as $0, \Delta t, 2\Delta t, \ldots$ and re-writing Eq. (5-8) using a summation in the place of the integral. Then, after some rearrange-

ment of terms, Eq. (5-8) yields an algebraic equation to solve for $P_S(k\Delta t)$ in terms of $P_S[(k-1)\Delta t], P_S[(k-2)\Delta t], \ldots, P_S(0)$. Using $P_S(0)=1$, $P_S(k\Delta t)$ for all k can be computed starting from $k=1$ and moving forward.

5.4.2 Computing the age

In order to determine the level of deterioration in a system at time t, it is important to determine the age of the system or the time for which the system has been operating without any repairs. In renewal theory, age is defined as the time elapsed since the last renewal event (Grimmett and Stirzaker 2001). In RTLCA, we define age at time t as the time elapsed since the last renewal given that the system is in use at t and the age is zero if the system is down at t. Mathematically, age $\Lambda(t) = (t - t_{L_i}) 1_{\{\text{in use at } t\}}$, where $i = N_L(t)$. In the following, we propose an integral equation for computing the expectation $E[\Lambda(t)]$. Conditioning on the first renewal, we have

$$E\left[\Lambda(t)\right] = \int_0^\infty \int_0^{\tau_L} E\left[\Lambda(t) \middle| T_{I_1} = \tau_I, T_{L_1} = \tau_L\right] f_{T_I T_L}(\tau_I, \tau_L)\, d\tau_I d\tau_L \qquad (5\text{-}9)$$

where $f_{T_I T_L}(\tau_I, \tau_L)$ is the joint PDF for T_{I_1} and T_{L_1}.

$$\begin{aligned} E\left[\Lambda(t) \middle| T_{I_1} = \tau_I, T_{L_1} = \tau_L\right] &= t & t < \tau_I \\ &= 0 & \tau_I \le t < \tau_L \\ &= E\left[\Lambda(t - \tau_L)\right] & t \ge \tau_L \end{aligned} \qquad (5\text{-}10)$$

Therefore, we have

$$E\left[\Lambda(t)\right] = t\left[1 - F_{T_I}(t)\right] + \int_0^t E\left[\Lambda(t-\tau_L)\right] f_{T_L}(\tau_L)\, d\tau_L \tag{5-11}$$

Equation (5-11) is an integral equation that can be solved as explained earlier with respect to Eq. (5-8). The function $E[\Lambda(t)]$ can be used to predict the state of deterioration in the system at time t. For example, it can shown for the RTLCA formulation that the instantaneous rate of ultimate failure $\nu_F(t)$ can be approximated as

$$\nu_F(t) \approx \frac{f_{T_I|L_F}\left\{E\left[\Lambda(t)\middle| L_F\right]\right\} P(L_F)}{1 - F_{T_I}\left\{E\left[\Lambda(t)\right]\right\}} \tag{5-12}$$

Furthermore, if $\mathbf{x}(t)$ represents the properties of the system at time t and $\bar{\mathbf{x}}(t) = E[\mathbf{x}(t) \mid T_{I_1} > t]$, then $E[\mathbf{x}(t)] \approx \bar{\mathbf{x}}\{E[\Lambda(t)]\}$. This is a useful because $E[\mathbf{x}(t)]$ for the entire life-span of a system can be estimated by simulating the events occurring up to only the first intervention.

5.4.3 Computing the cost of operation

The expected value of $C_{Op}(t)$ can be estimated as follows:

$$E\left[C_{Op}(t)\right] = \int_0^\infty E\left[C_{Op}(t)\middle| T_{L_1} = \tau\right] f_{T_L}(\tau)\, d\tau \tag{5-13}$$

Based on the definition of $C_{Op}(t)$ and assuming complete renewal of the system at t_{L_1}, we have

$$E\left[C_{Op}(t)\middle|T_{L_1}=\tau\right]=0 \qquad t<\tau$$
$$=E\left[c_{Op_1}e^{-\gamma T_{L_1}}\middle|T_{L_1}=\tau\right]+E\left[C_{Op}(t-\tau)\right]e^{-\gamma\tau} \qquad t\geq\tau \tag{5-14}$$

Now writing $\bar{c}_{Op}(\tau)=E[c_{Op_1}e^{-\gamma T_{L_1}}\mid T_{L_1}=\tau]$, we have

$$E\left[C_{Op}(t)\right]=\int_0^t\left\{\bar{c}_{Op}(\tau)+E\left[C_{Op}(t-\tau)\right]e^{-\gamma\tau}\right\}f_{T_L}(\tau)\,d\tau \tag{5-15}$$

The computation of the function $\bar{c}_{Op}(\tau)$ is essential to compute $E[C_{Op}(t)]$. In some special cases $\bar{c}_{Op}(\tau)$ can be easily obtained. For example if c_{Op_1} is independent of T_{L_1}, then $\bar{c}_{Op}(\tau)=E[c_{Op_1}]e^{-\gamma\tau}$. For other cases, simulation of the events in the first renewal may be required.

5.4.4 Computing the failure losses

In the following, we propose the integral equation to compute $E[C_L(t)]$ for the RTLCA formulation:

$$E\left[C_L(t)\right]=E\left[C_L(t)\middle|L_1\equiv L_R\right]P(L_R)+E\left[C_L(t)\middle|L_1\equiv L_F\right]P(L_F) \tag{5-16}$$

where

$$E\left[C_L(t)\middle|L_1\equiv L_R\right]=\int_0^\infty E\left[C_L(t)\middle|L_1\equiv L_R,T_{L_1}=\tau\right]f_{T_L|L_R}\left(\tau\middle|L_R\right)d\tau \tag{5-17}$$

and

$$E\left[C_L(t)\middle|L_1\equiv L_R,T_{L_1}=\tau\right]=0 \qquad t<\tau$$
$$=E\left[C_L(t-\tau)\right]e^{-\gamma\tau} \qquad t\geq\tau \tag{5-18}$$

Therefore,

$$E\left[C_L(t)\middle|L_1 \equiv L_R\right] = \int_0^t E\left[C_L(t-\tau)\right] e^{-\gamma\tau} f_{T_L|L_R}\left(\tau\middle|L_R\right) d\tau \tag{5-19}$$

Similarly,

$$E\left[C_L(t)\middle|L_1 \equiv L_F\right] = \int_0^\infty E\left[C_L(t)\middle|L_1 \equiv L_F, T_{L_1} = \tau\right] f_{T_L|L_F}\left(\tau\middle|L_F\right) d\tau \tag{5-20}$$

where writing T_{DF} as the down-time after an ultimate failure, we have

$$\begin{aligned} &E\left[C_L(t)\middle|L_1 \equiv L_F, T_{L_1} = \tau\right] \\ &\quad = 0 && t < \tau - T_{DF} \\ &\quad = c_L e^{-\gamma(\tau - T_{DF})} && \tau - T_{DF} \le t \le \tau \\ &\quad = c_L e^{-\gamma(\tau - T_{DF})} + E\left[C_L(t-\tau)\right] e^{-\gamma\tau} && \tau \le t \end{aligned} \tag{5-21}$$

It follows that

$$\begin{aligned} E\left[C_L(t)\middle|L_1 \equiv L_F\right] = c_L e^{\gamma T_{DF}} &\int_0^{t+T_{DF}} e^{-\gamma\tau} f_{T_L|L_F}\left(\tau\middle|L_F\right) d\tau \\ &+ \int_0^t E\left[C_F(t-\tau)\right] e^{-\gamma\tau} f_{T_L|L_F}\left(\tau\middle|L_F\right) d\tau \end{aligned} \tag{5-22}$$

Combining Eqs.(5-16), (5-19) and (5-22), and using $P(L_R) + P(L_F) = 1$, we have we have

$$E\left[C_L(t)\right] = P(L_F)c_L e^{\gamma T_{D_1}} \int_0^{t+T_{DF}} e^{-\gamma\tau} f_{T_L|L_F}\left(\tau \middle| L_F\right) d\tau + \int_0^t E\left[C_L(t-\tau)\right] e^{-\gamma\tau} f_{T_L|L_F}\left(\tau \middle| L_F\right) d\tau \tag{5-23}$$

5.4.5 Computing the benefit

The benefit $Q(t)$ accounting for the discount rate is as follows:

$$Q(t) = q\int_0^t P_S(\tau) e^{-\gamma\tau} d\tau \tag{5-24}$$

where q is the benefit derived from having the system in use for a unit time.

5.5 The deterioration process

In order to implement the proposed LCA model we need the conditional PDFs $f_{T_I|L_R}(\tau \mid L_R)$, $f_{T_I|L_F}(\tau \mid L_F)$, $f_{T_L|L_R}(t \mid L_R)$, $f_{T_L|L_F}(t \mid L_F)$ and the probability $P(L_F)$. These quantities depend on the process of deterioration, the process of loads (magnitude and time of occurrence) and the intervention criteria. In this subsection, we briefly describe the multiplicative form of Stochastic Semi-Analytical (SSA) model proposed in Section 4 for modeling deterioration processes. This formulation is used in the following sub-section to compute the mentioned distributions and probabilities based on a given intervention criteria.

The capacity of a deteriorating system at time t, $C_t = C[\mathbf{x}(t)]$ is a stochastic process, where $\mathbf{x}(t)$ represents the properties of system at t. Similarly, the demand $D_{t_n} = D[\mathbf{x}(t_n), S_{t_n}]$ is a stochastic process, where S_{t_n} is the n^{th} load since $t = 0$ and t_n is

the time of occurrence of the n^{th} load. The number of loads to failure n_F is given by $n_F = \min\{n : g_{t_n} \le 0\}$, where $g_{t_n} = C_{t_n^-} - D_{t_n}$ and t^- is the time instant immediately before t. Accounting for the deterioration process, we have

$$g_{t_n} = C_0 \Gamma_{C,t_n} + Y_{t_n} \Gamma_{D,t_n} \tag{5-25}$$

where t_n is the time of occurrence of the n^{th} load, $Y_{t_n} = D[\mathbf{x}(0), S_{t_n}]$ are SIID and $\Gamma_{C,t}$ and $\Gamma_{D,t}$ represent the total effect of deterioration on capacity and demand at time t considering the events in time-span $[0,t]$. By suitable rearrangement of terms, $n_F = \min\{n : \hat{Y}_{t_n} + W_{t_n} \ge 1\}$, where $\hat{Y}_{t_n} = D[\mathbf{x}(0), S_{t_n}] / C[\mathbf{x}(0)]$ is the normalized demand with respect to the capacity of the un-deteriorated system, and $W_t = [1 - \Gamma_{C,t} / \Gamma_{D,t}]$. As a result of these definitions, $\hat{Y}_{t_n}$ are SIID random variables and W_t is a stochastic process that captures the effect of deterioration on the system. The process W_t may consist of both shock and gradual deterioration process. Assuming that the process of gradual deterioration and shocks are mutually independent, W_t can be written as

$$W_t = \sum_{i=1}^{N(t^-)} Z_{t_n} + R(t) \tag{5-26}$$

where $N(t)$ is the number of loads or shocks in the time interval $[0,t]$, Z_{t_n} is the shock at t_n and $R(t)$ is the state of the gradual process at t.

In the proposed RTLCA formulation, the SSA model can be used for computing $P_f(t) = P[\hat{Y}_{t_n} > 1 - W_t] = 1 - F_{\hat{Y}}(1 - W_t)$, where $F_{\hat{Y}}(y)$ is the CDF of $\hat{Y}_{t_n}$ which as discussed

earlier is SIID independent of t_n. In addition to $F_{\hat{Y}}(y)$, to construct the stochastic process W_t as per Eq. (5-26), we need a model for stochastic process $\{t_n\}$ and the conditional distribution $F_{Z|\hat{Y}}(z|\hat{Y}_{t_n})$ which captures the dependence of the shock Z_{t_n} on $\hat{Y}_{t_n}$. The process $\{t_n\}$can be obtained by modeling the time of occurrence of loads and $F_{\hat{Y}}(y)$ and $F_{Z|\hat{Y}}(z|\hat{Y}_{t_n})$ can be obtained by modeling the distribution of the magnitude of loads and the response of the system to loads.

5.6 LCA of an example RC bridge located in a seismic region

In this subsection, we apply the proposed RTLCA model to the example highway RC bridge with one single-column bent shown in Table 3-4. The bridge is assumed to be located in Los Angeles, CA. We primarily focus on the deterioration and failure of the bridge due to earthquakes occurring during its service life. Furthermore, we consider the failure of the bridge caused by excessive lateral deformation of the bridge column. This is generally the most important failure mode for seismically designed bridges.

The application of the RTLCA for this example system required two steps. The first step consists of constructing the stochastic process $\{t_n\}$ (i.e., the time of occurrences of earthquakes) and developing the CDF $F_{\hat{Y}}(y)$ for $\hat{Y}_{t_n}$ specific to the seismicity of Los Angeles and the properties of the example bridge. Also in this step the model for seismic deterioration $Z_{t_n} = Z(\hat{Y}_{t_n})$ needs to be developed to completely characterize the process $\{\hat{Y}_{t_n} + W_{t_n}\}$. In the second step, we simulate the process $\{\hat{Y}_{t_n} + W_{t_n}\}$ to compute the distributions of T_{I_i} and T_{L_i}, and the values of the conditional probabilities $P(L_R)$ and

$P(L_F)$. For this purpose, we need to define an intervention criterion. Then, we numerically solve the previously derived integral equations.

5.6.1 Stochastic model for $\{t_n\}$ **and** $\{\hat{Y}_{t_n}\}$

A FE model of the bridge is developed in OpenSees (Mackenna and Fenves 2000) in order to assess it dynamic properties. The details regarding the FE model is described in Section 3. This FE model is used to compute $F_{\hat{Y}|S_a}(y \mid S_a)$, the CDF of $\hat{Y}_{t_n}$ conditioned that the value of PSA. This conditional CDF can be computed using the probabilistic deformation demand and capacity models developed by Gardoni et al. (2003) and Choe et al. (2007) respectively. Now in order to compute $f_{S_a}(s)$ the PDF for PSA, we obtain the regional seismic hazard curve for Los Angeles corresponding to the natural period of the bridge. The seismic hazard curve is obtained using OpenSHA (Field et al. 2003). The CDF $F_{\hat{Y}}(y)$ is now computed by performing the integration $\int F_{\hat{Y}|S_a}(y \mid S_a) f_{S_a}(s) ds$. It is found that $F_{\hat{Y}}(y)$ closely matches the CDF of Gamma distribution with parameters (0.678, 0.16). Using $F_{\hat{Y}}(y)$, we the probability of failure of the system in as-built state is given by $P_f(0) = 1 - F_{\hat{Y}}(1) = 7.6716E-04$. 0

Following Reasenberg and Jones (1989), the occurrence of main shocks can be modeled as a homogeneous Poisson process, where the rate $\lambda_m(M)$ of main shocks with magnitude M_m greater than or equal to M is given as follows:

$$\lambda_m(M) = 10^{B_1 - B_2 M} \tag{5-27}$$

where B_1 and B_2 are regional constants. It can be seen in eq. (5-27) that the rate of all main shocks (i.e., $M_m > 0$) is given by $\lambda_m(0) = 10^{B_1}$. It can be derived from Eq. (5-27) that $P(M_m > M) = 10^{-B_2 M}$. The instantaneous rate $\lambda_a(\tau, M)$ for aftershocks of magnitude $M_a \geq M$ following a main shock of magnitude M_m is given by the modified Omori's Law (Utsu 1961) as follows:

$$\lambda_a(\tau, M) = \frac{10^{B_1 + B_2(M_m - M)}}{(\tau + c)^p} \tag{5-28}$$

where τ is the time elapsed since the main shock, and c and p are regional constants. Rearranging the terms, the rate of all aftershocks given that $M_m = M$

$$\lambda_a(\tau, 0) = \frac{\lambda_m(0)}{\left[1 - F_{M_m}(M)\right]}\left[\frac{1}{(\tau + c)^p}\right] \tag{5-29}$$

where $F_{M_m}(M)$ is the CDF for M_m. It is also found in past research that the probability distribution of the magnitude of aftershocks is independent of the magnitude of main shocks and is indeed the same as that of main shocks. As a simplification, we assume that all earthquakes (main and aftershocks) at the bridge sites originate from a single point source. Now since the distribution of earthquake magnitudes is same for both main shocks and aftershocks, the distribution of $\hat{Y}_{t_n}$ remains the same for main shocks and aftershocks. Now based on Eq. (5-29), we assume that the time-dependent rate of aftershocks $\lambda_a'(\tau)$ following a main shock with $\hat{Y}_{t_n} = y$ is given as follows:

$$\lambda_a'(\tau) = \frac{\lambda_m(0)}{\left[1 - F_{\hat{Y}}(y)\right]}\left[\frac{1}{(\tau + c)^p}\right] \tag{5-30}$$

Equation (5-30) is exact if there exists an one-to-one mapping between earthquake magnitude and $\hat{Y}_{t_n}$ and only one earthquake source contributes to the seismic hazard at the bridge site.

5.6.2 Modeling the shock process $\{Z_{t_n}\}$ due to seismic degradation

The failure of the bridge here is considered as the event where the deformation demand on the bridge column during an earthquake exceeds the available deformation capacity of the column. Both the deformation demand and the capacity may be affected by structural deterioration caused by earthquakes to the columns. In this example, we consider two distinct seismic degradation phenomena in RC columns that affect the probability of failure of the columns. Firstly, we consider the degradation in deformation capacity of RC columns due to low-cycle fatigue of longitudinal reinforcement using the seismic degradation model developed in Section 2. Secondly, we consider the effect of seismic degradation on static pushover properties of an RC column as modeled in Section 3. Based on these degradation models we generate data to develop $F_{Z|\hat{Y}}(z \mid \hat{Y}_{t_n})$, the CDF of Z_{t_n} conditioned on the value of $\hat{Y}_{t_n}$. This conditional CDF will be used later to model the shock deterioration process caused by earthquakes. Since, we do not consider gradual deterioration in this analysis, we compute $Z_{t_n} = [1 - \Gamma_{C,t_n} / \Gamma_{D,t_n}]$. Following methodology is used generate the required data:

(i) Obtain the elastic response spectrums for S_a for the region of interest. These response spectrums can be obtained from PEER strong motion database.

(ii) Start with the as-built state of the bridge properties $\mathbf{x}$. Draw a response spectrum from the database and obtain the S_a for $T_n = 0.84$ s (natural period of the bridge)

(iii) Simulate $\hat{Y}_{t_n}$ for S_a using the deformation demand model and deformation capacity model for RC bridge columns by Gardoni et al. (2003) and Choe et al. (2007) respectively.

(iv) Now simulate the values of K', Δ_y' and DI using Eqs. (3-1), (3-2), and (3-4).

(v) Then simulate the degraded deformation capacity and compute Γ_{C,t_n}.

(vi) Now we need to estimate the effect of seismic degradation on future seismic deformation demand caused by the past earthquake having S_a simulated in step (i). For this purpose we use the response spectrum used in step (ii) for generating the S_a corresponding to the period of the degraded system. Then, we estimate the change in demand to compute Γ_{D,t_n}. This step completes the computations for one data point $(\hat{Y}_{t_n}, Z_{t_n})$. Several such data points need to computed to estimate $F_{Z|\hat{Y}}(z \mid \hat{Y}_{t_n})$.

Figure 5-2 shows the obtained data obtained using the described steps. The range of obtained Z_{t_n} is [0,1] because it is found that $\Gamma_{C,t_n} \le 1$ due to capacity degradation and $\Gamma_{D,t_n} \ge 1$ because demand is amplified caused by stiffness degradation.

Now, we propose $F_{Z|\hat{Y}}(z \mid \hat{Y}_{t_n}) \sim Beta(A_z, B_z)$, where the mean of the distribution given by $A_z / (A_z + B_z) = k_{z1} \exp(-k_{z2} / \hat{Y}_{t_n})$. This model satisfies the condition that $0 \le Z_{t_n} \le 1$ (because $Z_{t_n} \sim Beta(A_z, B_z)$) and the mean of the distribution follows the trend of the data points. The parameters k_{z1} and k_{z2} can be computed by maximizing the following likelihood function:

$$\hat{L}\left(k_{z1}, k_{z2} \middle| \{Z_{t_n,i}, \hat{Y}_{t_n,i}\}\right) = \prod_i f_{Z|\hat{Y}}\left(Z_{t_n,i} \middle| \hat{Y}_{t_n,i}\right) \tag{5-31}$$

where $\{Z_{t_n,i}, \hat{Y}_{t_n,i}\}$ are the data points and $f_{Z|\hat{Y}}(Z_{t_n} \mid \hat{Y}_{t_n})$ is the conditional PDF corresponding to $F_{Z|\hat{Y}}(z \mid \hat{Y}_{t_n})$. It is often more convenient to maximize the natural logarithm of liklihood function or log-liklihood instead of the liklihood function itself. By maximizing the log-liklihood function, it is found that $k_{z1} = 0.546$ and $k_{z2} = 0.5$. Figure 5-2 shows the fit obtained using the proposed Beta distribution. We also show the 0.95 probability interval centered on the mean.

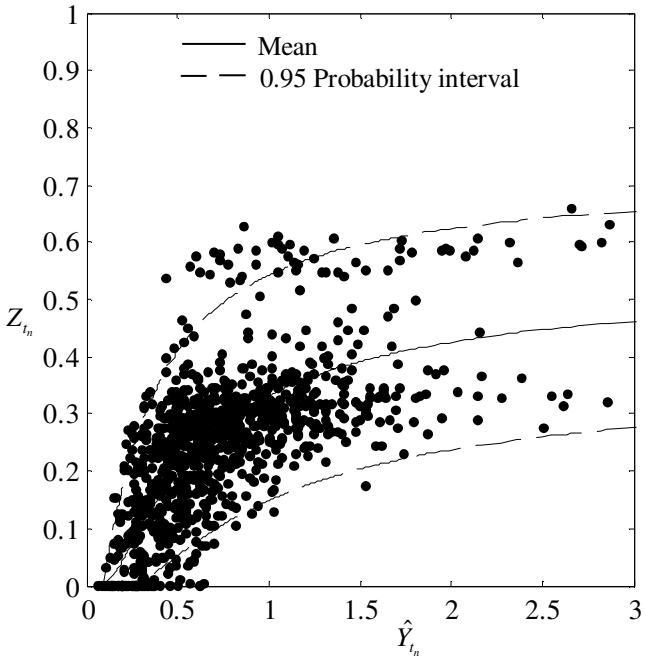

Figure 5-2. Modeling of shock deterioration process accounting seismic damage

5.6.3 Intervention criteria, renewal time and cost of renewals

As discussed earlier, there can be several criteria for interventions. In this example, we assume that a bridge is repaired after the i^{th} earthquake if the value of $P_f(t_i^+) \geq p_a$, where p_a is pre-determined acceptable probability of failure. As an example, we conduct the analysis for $p_a = 0.001, 0.005, 0.01, 0.05, 0.10$. Generally, in the case of civil infrastructure systems, there is a time lag before repairs can be initiated. It is important to consider this time lag because earthquakes are usually followed by aftershocks which may cause further damage before the repairs. We assume, for this example, that the time lag is 3 months (0.25 years) to initiate repairs. We assume that the time to replace a bridge is 2 years and the time to repair a damaged bridge is given by a fraction of the 2

years proportional to the probability of failure at the time at which the repairs begins, i.e., $P_f(t_{I_i}+0.25)\times 2$ years (where $(t_{I_i}+0.25)=$ the time at which repairs begin accounting for the time lag.) We also assume the same proportionality also for c_{Op_i}, i.e., $c_{Op_i}=P_f(t_{I_i}+0.25)\times C_C$. In addition, the following values are considered for c_{F_i}, γ and q: $c_{F_i}=2.0C_C$, $\gamma=0.04$ year^{-1} and $q=0.1C_C$ year^{-1}. Table 1 shows the functions $\overline{c}_{Op}(t)$ for all considered values of p_a. Since $\overline{c}_{Op}(\tau)=E[c_{Op_1}e^{-\gamma T_{L_1}}\,|\,T_{L_1}=\tau]$ is an expectation conditioned the value of T_{L_i}, it can be obtained by performing a statistical regression using the $c_{Op_1}e^{-\gamma T_{L_1}}$ versus T_{L_i} data . We obtain this data by simulating the events in the first renewal L_1 and perform the regression in the logarithmic space. It is found that $\overline{c}_{Op}(t)$ increases with the increase in p_a. The functions $\overline{c}_{Op}(t)$ for different values of p_a in Table 1 show that the expected cost of repairs and replacement increases by increasing p_a. This is because the value of $P(L_F)$ increases by increasing p_a which results in greater losses due to failures.

5.6.4 Results and discussions

Table 5-1 and Table 5-2 show the values of $P(L_R)$ and the parameters of Gamma distributions used to fit the distributions $f_{T_I}(\tau)$, $f_{T_L}(\tau)$, $f_{T_I|L_F}(\tau\,|\,L_F)$, $f_{T_L|L_F}(t\,|\,L_F)$ It is observed that $P(L_R)$ increases when p_a decreases. This implies that the system is more likely to have preventive interventions than essential interventions by decreasing the

value of p_a. We also observe that expectations of T_{I_i} and T_{L_i} decrease when p_a decreases. This implies that the frequency of intervention and renewal events increases by decreasing p_a. Table 5-2 shows that $E(T_{L_i} \mid L_F)$ and $E(T_{I_i} \mid L_F)$ increase when p_a increases.

Table 5-1. Probabilities and PDFs for the renewal model

p_a	$P(L_R)$	$f_{T_L}(t)$	$f_{T_I}(t)$	$\overline{c}_P(t)$
0.0010	0.998	(1.840, 15.613)	(1.817, 15.613)	$\exp(-0.0343\tau - 4.626)$
0.0050	0.991	(2.452, 16.185)	(2.386, 16.407)	$\exp(-0.0364\tau - 2.970)$
0.0100	0.983	(2.758, 16.014)	(2.674, 16.272)	$\exp(-0.0380\tau - 2.339)$
0.0500	0.921	(3.458, 15.780)	(3.304, 16.160)	$\exp(-0.0387\tau - 1.059)$
0.1000	0.840	(3.713, 15.866)	(3.524, 16.304)	$\exp(-0.0391\tau - 0.622)$

Table 5-2. Conditional PDFs for the renewal model

p_a	$f_{T_L \mid L_F}(t \mid L_F)$	$f_{T_I \mid L_F}(\tau \mid L_F)$
0.0010	(2.235, 12.350)	(1.867, 13.693)
0.0050	(2.683, 14.387)	(2.341, 15.607)
0.0100	(2.976, 15.033)	(2.679, 15.905)
0.0500	(3.400, 16.045)	(3.111, 16.836)
0.1000	(3.676, 16.011)	(3.390, 16.735)

Figure 5-3 shows that the values of $P_s(t)$ converge around $t = 100$ years. It is found that initially (i.e., for $t < 25$ years) $P_s(t)$ is higher for higher values of p_a but the converged values are higher for smaller values of p_a. This implies that for smaller values of p_a the bridge is more likely to be in use in the long run than for higher values of p_a. This trend is reversed in the early part of the service life. This is because smaller

values of p_a necessitate more frequent interventions initially than the higher values of p_a. However, in the long-run with smaller p_a, bridges are less likely to fail resulting in higher probability of being in use at a given time.

Figure 5-4 shows the plots for $A(t)$ for p_a values 0.001, 0.005, 0.010, 0.050, 0.100. In the figure, the vertical axis represents $A(t)$ and the horizontal axis represents t. The plots show the same trends as in Figure 3 except that no convergence is observed for $t \leq 150$ years. The plots imply that smaller values of p_a is beneficial in long-run because ultimate failures are avoided to a greater extent.

Figure 5-5 and Figure 5-6 show two measures that indicate the state of the bridge. Figure 5-5 shows $E[\Lambda(t)]$ versus t and Figure 5-6 shows $\nu_F(t)$ versus t for the values of p_a considered earlier. Figure 5-5 and Figure 5-6 show that the example bridge is expected to deteriorate for the initial 50 years and then both $E[\Lambda(t)]$ and $\nu_F(t)$ remain approximately constant. It is also observed that the higher values of p_a result in greater deterioration of the bridge. However, there is a significant difference in the condition of a bridge as captured by $E[\Lambda(t)]$ and $\nu_F(t)$. The values of $\nu_F(t)$ are more accurate indicator of the condition of the bridge because they indicate the amount of deterioration experienced since the last renewal while $E[\Lambda(t)]$ indicates only the time elapsed since last renewal.

Figure 5-7 shows the relation between the expectation of the cost $C_{Total}(t) = C_{Op}(t) + C_L(t)$ and p_a. It is found that $E[C_{Total}(t)]$ increases by increasing p_a.

The rate of increase of $E[C_{Total}(t)]$ decreases with time and $E[C_{Total}(t)]$ is expected to eventually become constant. This is because the NPV of costs incurred after a sufficiently long time is small. This implies that for a given intervention criteria, the costs incurred after a sufficiently long period of time ($t > 150$ years in this example) are irrelevant.

Figure 5-8 shows the value of $E[Q_{net}(t)]/C_C$ with respect to t. At $t = 0$, $E[Q_{net}(t)]/C_C = -1$ because the only cost incurred at $t = 0$ is the construction cost and there is no accumulated benefit. Gradually benefit accumulates and a breakeven (i.e., $Q_{net}(t) = 0$) is achieved around 12 years. Based on Figure 5-8, it is found that it is economically advisable to lower the values of p_a. However, the figure does not imply that the benefits can be increased indefinitely by increasing the rate of interventions. This conclusion is correct only if interventions are conducted after an earthquake and hence the maximum rate of interventions can only be equal to the rate of earthquakes (i.e., repair after every earthquake.)

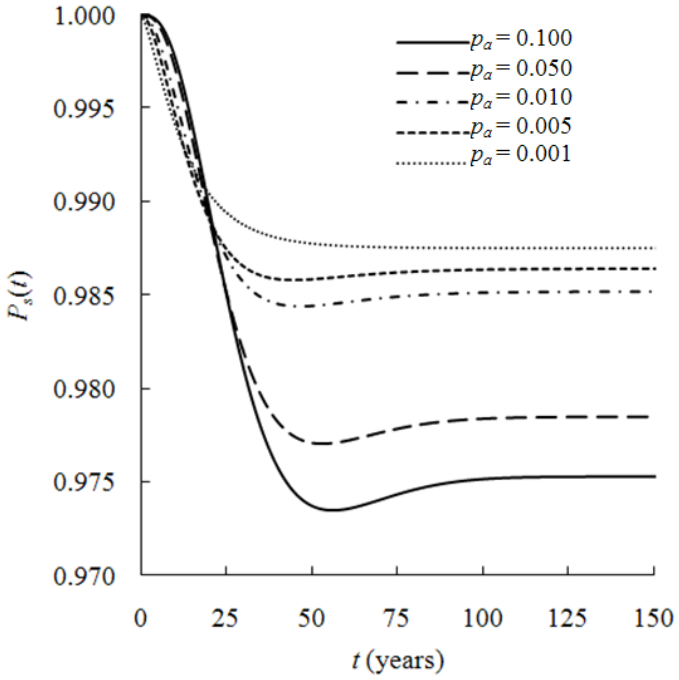

Figure 5-3. Effect of p_a on the values of $P_s(t)$

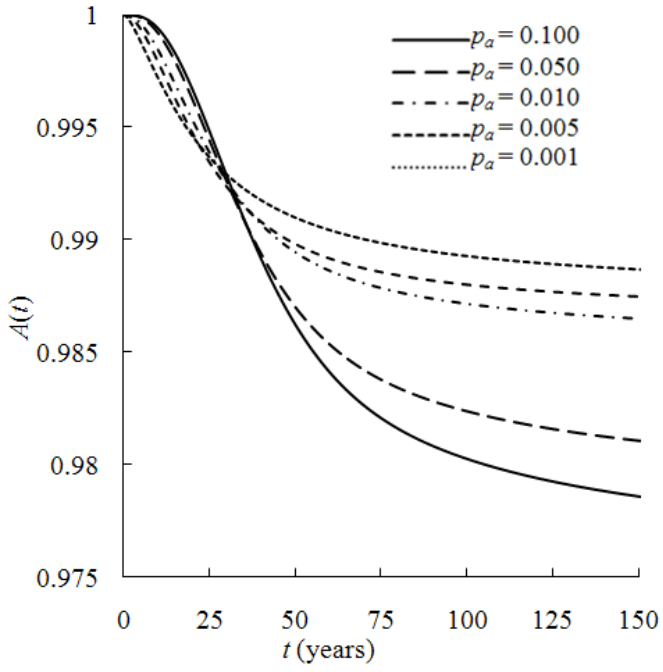

Figure 5-4. Effect of p_a on the availability of the system

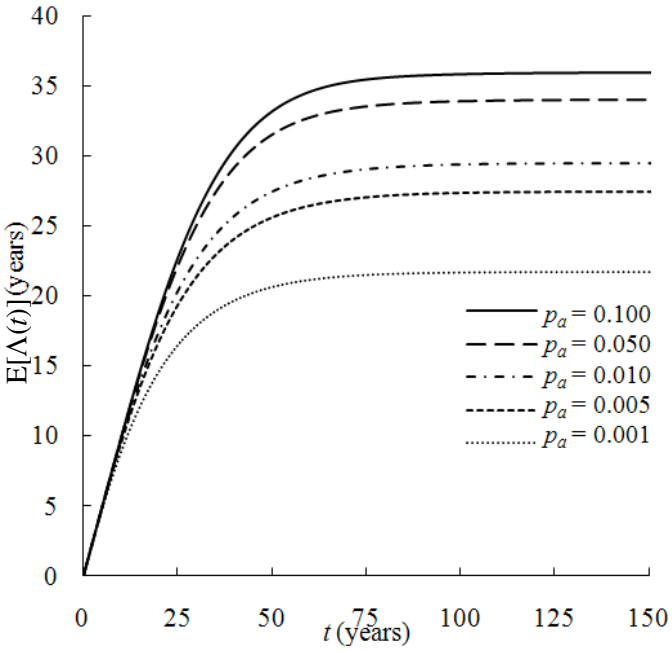

Figure 5-5 Effect of p_a on the age of the system

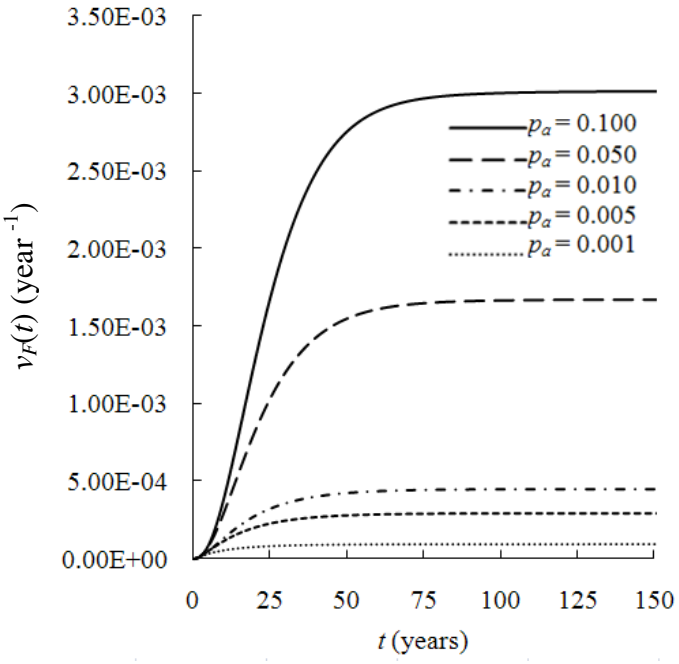

Figure 5-6. Effect of p_a on the failure rate of the system

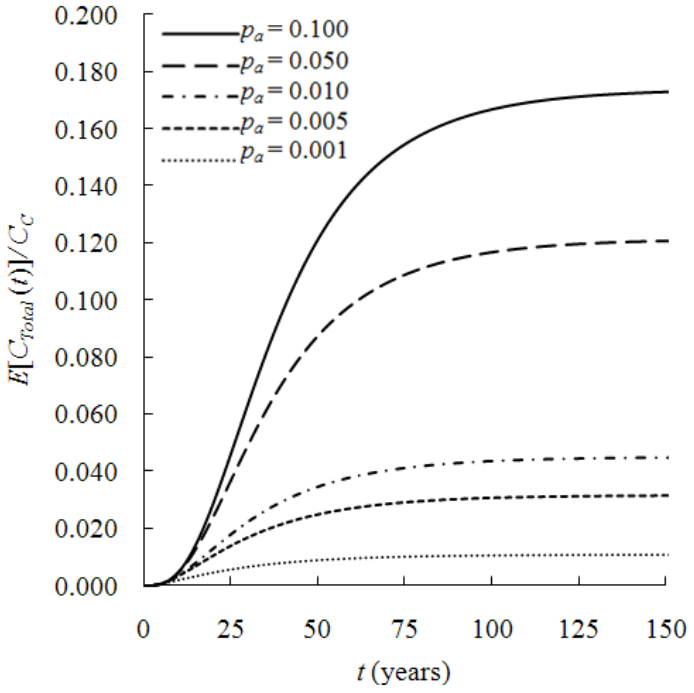

Figure 5-7. Effect of p_a on the total expected cost of operation and failures

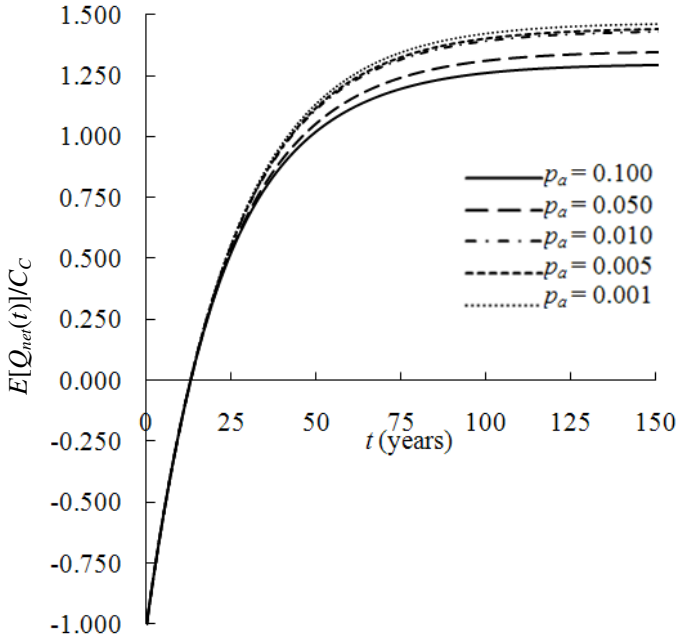

Figure 5-8. Effect of p_a on $Q_{net}(t)$

5.7 Conclusions

Life-cycle analysis (LCA) provides comprehensive information regarding the performance of an engineering system. In particular, LCA is extremely important for making decisions regarding systems that are susceptible to deterioration process.

In this research, we propose a LCA model based on renewal theory named RTLCA. The proposed model predicts the expected values of time-dependent performance indicators such as cost of operation and failures, failure rate and probability of being in use or being out of service. The merits of the proposed RTLCA model are that it is not dependent on a particular deterioration model or an operation strategy which are the shortcomings of the existing models. Furthermore, we apply the proposed RTLCA model to analyze the life-cycle of a typical reinforced concrete (RC) bridge in a seismic region accounting for seismic damage during its life-cycle. An example operation strategy is analyzed, where the bridge is repaired after an earthquake in case the instantaneous probability of failure conditioned on the occurrence of an earthquake exceeds an allowable limit. The results show that it is economically more beneficial to reduce the acceptable limit which implies frequent interventions. However, this does not imply that interventions can be increased indefinitely to maximize the benefits. The results only conclude that it may be most beneficial to repair after every significant earthquake. These results cannot be extended to other systems or for different loading scenarios.

6. SECOND ORDER LOGARITHMIC FORMULATION FOR HAZARD CURVES AND CLOSED-FORM APPROXIMATION TO ANNUAL FAILURE PROBABILITY

6.1 Introduction

Closed-form solutions to compute failure probabilities are helpful in engineering for laying out design options and for estimating initial design parameters. With the growing interest in performance-based engineering, wherein design is essentially based on failure probabilities and expected losses, closed-form solutions to compute annual failure probabilities can be crucial for making engineering decisions. Closed-form solutions are generally expected to yield approximate results but wherever possible, accuracy must be pursued in order to improve the design process.

Typically, annual failure probabilities are used as performance measures while making recommendations for new designs, repairs and maintenances (Stewart and Dimitri 2003; Kong and Frangopol 2003). In the context of performance-based seismic design, Cornell et al. (2002) developed a closed-form solution to estimate annual failure probabilities. This solution relies on a linear logarithmic approximation of hazard curves (linear in the logarithmic scale). A hazard curve is a plot of the annual probability of exceedance of a hazard intensity versus the hazard intensity. This approximation has been widely used in the existing literature because it leads to a convenient closed-form solution for the annual failure probability. However, it is well known that hazard curves significantly deviate from a linear logarithmic form (Bradley et al. 2007).

This section proposes a novel and more accurate formulation to model hazard curves named Second Order Logarithmic Form (SOLF), and derives a new closed-form solution for annual failure probabilities based on the proposed SOLF. For illustration, we apply the proposed formulation to an example reinforced concrete (RC) bridge subject to seismic hazard. The structural properties of the bridge are selected so as to represent RC bridges designed as per Caltrans' specifications (Caltrans 2006). We compare the results obtained using SOLF with those obtained following the linear logarithmic formulation and an independent numerical integration procedure that uses the actual hazard data.

This section is organized into seven subsections. The first subsection presents the general formulation for computing annual failure probability and discusses the shortcomings of the existing linear logarithmic formulation for hazard curves. The second subsection presents the proposed SOLF for hazard curves. The third subsection provides brief discussions on probabilistic formulations for demand, capacity, and fragility functions. The fourth subsection develops the closed-form solution for annual failure probability based on the proposed SOLF. Then, the fifth subsection presents an application of SOLF and the associated closed-form solution for the annual failure probability to an RC bridge subject to seismic hazard. Finally, the sixth subsection presents the conclusions from this section.

6.2 Annual failure probability

The annual failure probability, P_{fA}, of a system corresponding to a specified performance level due to a certain hazard is given as follows:

$$P_{fA} = P_A\left[C(\mathbf{x}) - D(\mathbf{x}, S) < 0\right] \tag{6-1}$$

where, $P_A[\cdot]$ is the annual probability, $C(\mathbf{x})$ is the capacity of the system corresponding to the specified performance level, $D(\mathbf{x}, S)$ is the demand on the system, $\mathbf{x}$ is the vector of system properties and S is the intensity of the hazard. The Total Probability Rule (Ang and Tang 2007) can be used to compute P_{fA} as follows:

$$P_{fA} = \int_S F(s)\, \tilde{f}_S(s)\, ds \tag{6-2}$$

where $F(s)$ is the fragility function defined as the probability of failure conditioned on the value of S, and $\tilde{f}_S(s)$ is the annual probability density function (PDF) of the mixed random variable S.

Typically, there is a positive probability of no occurrence of a hazardous event within a time-span of one year i.e., $P_A[S=0] > 0$. Therefore, there is a probability mass $P_A[S=0]$ in $\tilde{f}_S(s)$ at $S=0$. In addition to the probability mass, $P_A[S=0]$, $\tilde{f}_S(s)$ consists of a continuous part, $f_S(s)$, as shown in the following equation:

$$\tilde{f}_S(s) = f_S(s) + P_A[S=0]\,\delta(s) \tag{6-3}$$

where $\delta(s)$ is the Dirac delta function defined as

$$\begin{aligned} \delta(s) &= \infty, \qquad s = 0 \\ &= 0, \qquad s \neq 0 \end{aligned} \tag{6-4}$$

$$\int_{-\tau}^{\tau} \delta(s)\, ds = 1 \tag{6-5}$$

where $\tau > 0$ is an arbitrarily small value. Figure 6-1 shows the plot of $\tilde{f}_S(s)$.

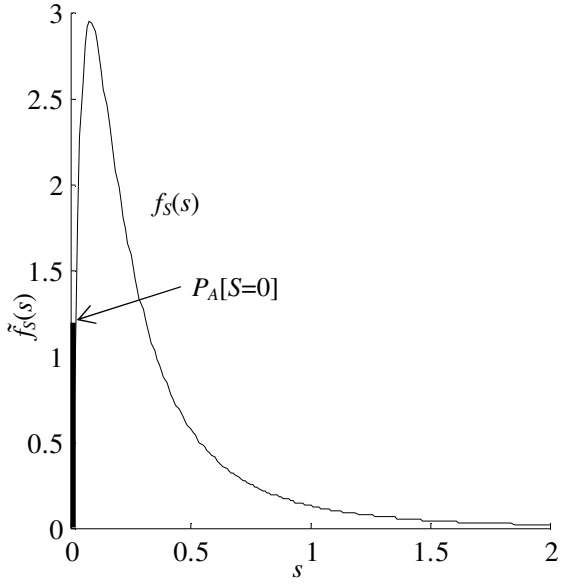

Figure 6-1. Annual PDF for S

The function $f_S(s)$ can be obtained as the derivative of the function $-[P_A(S > s)]$ with respect to s where $P_A(S > s)$ is the hazard curve. In engineering, the hazard curve for S is commonly approximated as follows (Cornell et al. 2002; Kennedy 1999):

$$P_A\left(S > s\right) = k_0 s^{-k_1} \tag{6-6}$$

where $k_0 > 0$ and $k_1 > 0$ are regional empirical constants. However, Eq. (6-6) has a linear form in logarithmic scale and does not provide an accurate fit to hazard curves that do not follow a linear logarithmic form (Bradley et al. 2007).

6.3 Second order logarithmic form

This study proposes a Second Order Logarithmic Form (SOLF) to model the hazard curves. This formulation provides a significantly improved fit to hazard curves with respect to the

existing linear logarithmic form and still enables a closed-form expression for P_{fA}. The SOLF is written as

$$\ln\left\{P_A\left[S > s\right]\right\} = a_1 + a_2\left[\ln\left(\frac{s}{S_{\min}}\right)\right]^2 \qquad s \geq S_{\min} \tag{6-7}$$

where $\ln(\cdot)$ is the natural logarithm. The expression in Eq. (6-7) is a concave parabola in the log-log plot with the vertex at $[\ln(S_{\min}), a_1]$ for $a_2 < 0$. As seen in Eq. (6-7), we use only the part of parabola where $s \geq S_{\min}$ (i.e., the right portion) to satisfy the condition that a hazard curve is a monotonically decreasing function.

Figure 6-2 shows the seismic hazard curve for San Francisco, CA given in Leyendecker et al. (2000) and shows the fit obtained by SOLF and the linear logarithmic form. The values of a_1, a_2 and $S_{\min}$ are found to be –2.85, –0.76 and 0.17, respectively, and k_1 and k_2 are found to be –2.14 and 0.0019. It is seen that the linear logarithmic form significantly overestimates $P_A(S > s)$ at small and high values of s and underestimates the same at intermediate values of s, which can lead to inaccurate estimates of P_{fA}. SOLF provides a significant improvement in the fit with respect to the linear logarithmic form over a wider range of s. It is also noted that, while SOLF does not provide values of the hazard curve for $s < S_{\min}$, this is not expected to affect the estimation of P_{fA} because, with reference to Eq. (6-2), $F(s) \approx 0$ for $s < S_{\min}$. Therefore, P_{fA} based on the SOLF formulation can be computed as follows:

$$P_{fA} = \int_{S_{\min}}^{\infty} F(s) f_S(s) ds \tag{6-8}$$

where $f_S(s)$ is the derivative of the function $-[P_A(S > s)]$ with respect to s. The following section briefly discusses the probabilistic formulation for demand, capacity, and fragility function.

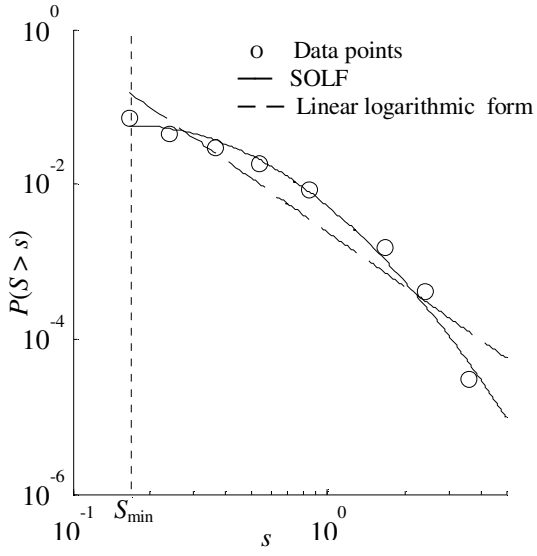

Figure 6-2. Comparison of SOLF and linear logarithmic form for hazard curves

6.4 Probabilistic demand, capacity, and fragility function

Probabilistic models for demand and capacity are generally written in a transformed space (e.g., taking the natural logarithm of the quantities of interest). This is done so that the standard deviation of the modeling error in the transformed space is approximately constant (homoskedasticity assumption) and the error follows a normal distribution (normality as-

sumption) (Gardoni et al.2002, 2003; Ramamoorthy et al.2006; Choe et al. 2007; Huang et al. 2010; Zhong et al. 2009). The general probabilistic demand model can be written as

$$D(\mathbf{x},\boldsymbol{\Theta}_d,S)=\hat{d}(\mathbf{x},S)+\gamma_d(\mathbf{x},\boldsymbol{\theta}_d,S)+\sigma_d\varepsilon_d \tag{6-9}$$

where $\boldsymbol{\Theta}_d=(\boldsymbol{\theta}_d,\sigma_d)$ is a vector of unknown model parameters modeled as random variables, $\hat{d}(\mathbf{x},S)$ is a deterministic capacity model, $\gamma_d(\mathbf{x},\boldsymbol{\theta}_d,S)$ is a collection of bias correction terms, ε_d is a standard normal random variable, and $\sigma_d\varepsilon_d$ is the model error. Similarly, a probabilistic capacity model can be written as

$$C(\mathbf{x},\boldsymbol{\Theta}_c)=\hat{c}(\mathbf{x})+\gamma_c(\mathbf{x},\boldsymbol{\theta}_c)+\sigma_c\varepsilon_c \tag{6-10}$$

where $\boldsymbol{\Theta}_c=(\boldsymbol{\theta}_c,\sigma_c)$ is a vector of unknown model parameters modeled as random variables, $\hat{c}(\mathbf{x})$ is a deterministic model, $\gamma_c(\mathbf{x},\boldsymbol{\theta}_c)$ is a collection of bias correction terms, ε_c is a standard normal random variable, and $\sigma_c\varepsilon_c$ is the model error.

Choe et al. (2007) and Huang et al. (2010) reported that ε_c and ε_d are typically the most important random variables in the probabilistic capacity and demand models. Therefore, in order to write the fragility function we can ignore the randomness in $\boldsymbol{\Theta}_d$, $\boldsymbol{\Theta}_c$ and $\mathbf{x}$ and consider them as deterministic values. This implies that the distribution for D conditioned on the value of S can be assumed to be normal with expected value $E[D\mid S]=\hat{d}(\mathbf{x},S)+\gamma_d(\mathbf{x},\boldsymbol{\theta}_d,S)$ and variance $\sigma_d^{\,2}$. Similarly, C can be assumed to be normally distributed with expected value $E[C]=\hat{c}(\mathbf{x})+\gamma_c(\mathbf{x},\boldsymbol{\theta}_c)$ and variance $\sigma_c^{\,2}$. Based on this observation, the fragility function can be written as:

$$F(\mathbf{x},S)=\Phi\left\{\frac{E\left[D\middle|S\right]-E[C]}{\sqrt{\sigma_d{}^2+\sigma_c{}^2}}\right\} \tag{6-11}$$

where, $\Phi\{\cdot\}$ is the standard normal cumulative distribution function (CDF). The following section develops the proposed closed-form expression for P_{fA} using Eqs. (6-8) and (6-11).

6.5 Proposed solution for annual failure probability

In order to obtain a closed-form solution of the integral in Eq. (6-8), we assume $E[D\,|\,S]$ can be written as follows:

$$E\left[D\middle|S\right]=b_1(\mathbf{x})\ln(S)+b_2(\mathbf{x}) \tag{6-12}$$

where, $b_1(\mathbf{x})$ and $b_2(\mathbf{x})$ are in general functions of $\mathbf{x}$. This assumption results in some loss of generality. However, this form was found to be fairly accurate in some structural and geotechnical applications for approximating the relationship between an intensity measure and the demand variable (Cornell et al. 2002; Ramamoorthy et al. 2006; Bazzurro and Cornell 2004). Based on this assumption, a closed-form solution to the integral in Eq. (6-8) can be obtained through a change of variables. The integral in Eq. (6-8) is now written as follows:

$$P_{fA}=\int_{S_{\min}}^{\infty}\Phi\left\{\frac{b_1\ln(s)+b_2-E[C]}{\sqrt{\sigma_d{}^2+\sigma_c{}^2}}\right\}f_S(s)ds \tag{6-13}$$

Now writing $R=\ln(S/S_{\min})$, we obtain the annual CDF $F_R(r)$ for R as follows:

$$F_R(r)=1-P_A[R>r] \tag{6-14}$$

$$1-P_A[R>r]=1-P_A\left[S>S_{\min}\exp(r)\right]=1-\exp\left(a_1+a_2r^2\right)\quad r>0 \tag{6-15}$$

Therefore,

$$P_{fA} = \int_0^{\infty} \Phi\left\{\frac{b_1 r - \tilde{C}}{\sigma}\right\} f_R(r)\, dr \tag{6-16}$$

where, $\tilde{C} = E[C] - b_2 - b_1 \ln(S_{\min})$, $\sigma = \sqrt{\sigma_d{}^2 + \sigma_c{}^2}$ and $f_R(r)$ is the annual PDF for R. Integrating by parts we obtain

$$P_{fA} = -\exp\left(a_1 + a_2 r^2\right)\Phi\left\{\frac{b_1 r - \tilde{C}}{\sigma}\right\}\Big|_0^{\infty} + \frac{b_1}{\sigma}\int_0^{\infty} \phi\left\{\frac{b_1 r - \tilde{C}}{\sigma}\right\}\exp\left(a_1 + a_2 r^2\right) dr \tag{6-17}$$

where $\phi\{\cdot\}$ is the standard normal PDF. By rearranging the terms in $\phi\{\cdot\}$ and $\exp(\cdot)$, and by carrying out the integral we obtain the following result:

$$P_f = \exp\left(a_1\right)\Phi\left[-\frac{\tilde{C}}{\sigma}\right] + \frac{b_1 \exp\left(a_1\right)}{\sqrt{b_1{}^2 - 2a_2\sigma^2}}\exp\left[\frac{a_2\tilde{C}^2}{b_1{}^2 - 2a_2\sigma^2}\right]\Phi\left[\frac{b_1\tilde{C}}{\sigma\sqrt{b_1{}^2 - 2a_2\sigma^2}}\right] \tag{6-18}$$

Eq. (6-18) is a general expression for P_{fA} based on the proposed SOLF of the hazard curve. In case the probabilistic model for C is developed using a logarithmic transformation, Eq. (6-18) can be further simplified. In this case, the term $\tilde{C}$ is the natural logarithm of the ratio $\exp\{E[C]\} / \exp\{b_1 \ln(S_{\min}) + b_2\}$, where $\exp\{E[C]\}$ is the median of the capacity in the original space and $\exp\{b_1 \ln(S_{\min}) + b_2\}$ is the median of the demand conditioned on $S = S_{\min}$. Now writing $\psi = \exp\{E[C]\} / \exp\{b_1 \ln(S_{\min}) + b_2\}$, we obtain

$$P_f = \exp\left(a_1\right)\Phi\left[-\frac{\ln\left(\psi\right)}{\sigma}\right] + \frac{b_1 \exp\left(a_1\right)}{\sqrt{b_1{}^2 - 2a_2\sigma^2}}\exp\left\{\frac{a_2\left[\ln\left(\psi\right)\right]^2}{b_1{}^2 - 2a_2\sigma^2}\right\}\Phi\left[\frac{b_1 \ln\left(\psi\right)}{\sigma\sqrt{b_1{}^2 - 2a_2\sigma^2}}\right] \tag{6-19}$$

It is found that the expression in Eq. (6-19) can be further simplified for most conditions of practical significance. The term $\Phi[-\ln(\psi)/\sigma] < 10^{-3}$ for $\ln(\psi)/\sigma > 3.0$.

Generally it is observed $\psi > 5.0$ and $\sigma < 0.5$ (which implies that $\ln(\psi)/\sigma > 3.0$) in the cases of practical significance. This is because $\psi \le 5.0$ corresponds to a value of the median capacity that is less than five times the median demand corresponding to $S_{\min}$. Also, $\sigma \ge 0.5$ indicates a large model error in the demand and capacity models, which is typically not observed for engineering systems in particular due to the use of appropriate variance stabilizing transformations. Now, noting that $\Phi[-\ln(\psi)/\sigma]$ decreases with increase in ψ and $\exp(a_1) = P[S > S_{\min}] < 1$, we can ignore the term $\Phi[-\ln(\psi)/\sigma]$. Also, noting that $\Phi[\ln(\psi)/\sigma] = 1 - \Phi[-\ln(\psi)/\sigma]$ and $b_1 / \sqrt{b_1^2 - 2a_2\sigma^2} > 1$ we can assume that $\Phi[b_1 \ln(\psi)/\sigma\sqrt{b_1^2 - 2a_2\sigma^2}] \approx 1.0$. Therefore, using Eq. (6-19), we can write

$$P_{fA} \approx \frac{b_1 \exp(a_1)}{\sqrt{b_1^2 - 2a_2\sigma^2}} \exp\left[\frac{a_2\left[\ln(\psi)\right]^2}{b_1^2 - 2a_2\sigma^2}\right] \tag{6-20}$$

Now by introducing the term $P_0 = P_A(S > s_0)$, where s_0 is the intensity of the design event, we can rearrange Eq. (6-20) into the following useful form:

$$P_{fA} \approx \sqrt{\xi} e^{a_1} \left(P_0 e^{-a_1}\right)^{\xi} \tag{6-21}$$

where, $\xi = b_1^2 / (b_1^2 - 2a_2\sigma^2)$. The expression in Eq. (6-21) enables the computation of the probability P_0 at the intensity level s_0 of the design event from a target value for P_{fA}. Therefore, Eq. (6-21) can be useful in design.

6.6 Application to an RC bridge subject to seismic hazard

Here, we apply the proposed SOLF to compute P_{fA} for an example RC bridge with respect to seismic hazards of San Francisco, CA and Memphis, TN. These locations are

chosen to demonstrate the application for two different hazard levels. The structural properties of the bridge are chosen so as to represent the behavior of a typical single-column RC over-pass bridge designed as per Caltrans specifications. In this application, we choose to compute P_{fA} for lateral deformation failure of the bridge column. This is because under seismic loading, the lateral deformation failure of columns is the most critical mode of failure for RC bridges designed as per Caltrans specifications. We compute the P_{fA} values conditioning on the median ductility capacity μ of the RC column, which is defined as the ratio between the deformation capacity and the deformation at yield. We compare the values of P_{fA} obtained using SOLF and those obtained following the linear logarithmic form and by numerically integrating Eq. (6-2).

6.6.1 Seismic deformation demand and deformation capacity

Various probabilistic seismic deformation demand models for RC bridges are available (Gardoni et al. 2003; Zhong et al. (2009) and Huang et al. 2010.) These models are developed using a logarithmic transformation and include $\hat{d}(\mathbf{x},S)$, $\gamma_d(\mathbf{x},S,\boldsymbol{\theta}_d)$ and $\sigma_d\varepsilon_d$. In this application, we use the demand model by Gardoni et al. (2003). The probabilistic deformation demand model used is as follows:

$$D_\delta = 0.61 + 3.90\theta_{2d} + (1+\theta_{2d})\hat{d}(\mathbf{x},S_a) + \sigma_d\varepsilon_d \tag{6-22}$$

$$\begin{aligned} \hat{d}(\mathbf{x},S_a) &= \ln\left(\frac{S_a\Delta_y}{A_y H}\right) && S_a \le A_y \\ &= \ln\left\{\left[\left(1-\frac{1}{c}\right)+\frac{1}{c}\left(\frac{S_a}{A_y}\right)^c\right]\frac{\Delta_y}{H}\right\} && S_a > A_y \end{aligned} \tag{6-23}$$

where D is the natural logarithm of the deformation demand, S_a is the PSA (normalized with $g = 9.812$ m/sec^2) computed from elastic response spectrum for given natural period T_n, θ_{2d} is a normal random variable with mean –0.153 and standard deviation 0.028, σ_d is a lognormal random variable with mean 0.216 and standard deviation 0.022, Δ_y is the displacement at yield, H is the height of the structure, $A_y = V_y / w$, V_y is the shear force at yield, w is the weight of the structure, and $c = T_n / (1 + T_n) + 0.42 / T_n$ computed assuming an elasto-plastic behavior. In this work, we compute P_{fA} as a function of $E[C]$. As per Choe et al. (2007), C corresponding to collapse has $\sigma_c = 0.383$. In the following example we assume that $\sigma_c = 0.383$ for all performance levels.

6.6.2 Numerical example

Table 6-1 shows the structural properties of the example RC bridge. The hazard curves for S_a corresponding to T_n of the structure for San Francisco and Memphis are illustrated in Figure 6-3. The figure shows the data points for hazard curve for S_a corresponding to $T_n = 0.2s$ obtained from Leyendecker et al.(2000). The figure also shows the fit obtained using the available linear logarithmic form and the proposed SOLF. The values obtained for k_0 and k_1 in Eq. (6-6) are (–2.14, 0.0019) and (–1.04, 3.882E–04) for San Francisco and Memphis respectively. It is seen that the SOLF provides a significant improvement in the fit for both the locations. The values obtained for a_1, a_2 and $S_{\min}$ in Eq. (7) are (–2.85, –0.76, 0.17) and (–3.31, –0.14, 0.0035) for San

Francisco and Memphis, respectively. To compute the values of b_1 and b_2 in Eq. (6-12), a linear fit is obtained to the relation shown in Eq. (6-23). This fit is obtained (see Figure 6-4) for $0 < S_a < 10.0$, where S_a has a significant probability. The values of b_1 and b_2 are found to be 0.89 and −5.26, respectively.

Table 6-1. Structural properties of example RC bridge

Parameters	Symbols	Value	Units
Natural period	T_n	0.20	s
Mass	m	3.0E05	kg
Drift at yield	$\hat{\Delta}_y / H$	0.01	
Height	H	5.0	m

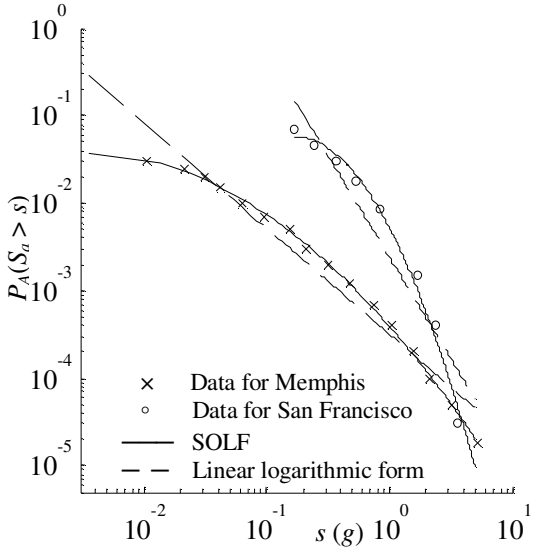

Figure 6-3. Hazard data for San Francisco and Memphis and the fits obtained using SOLF and linear logarithmic form

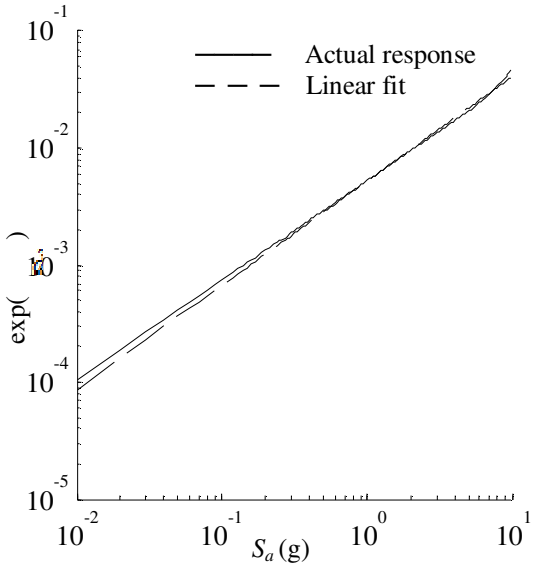

Figure 6-4. Fit to obtain the values $b_1 = 0.89$ and $b_2 = -5.26$

We compare the solution of the SOLF formulation with the solution proposed by Cornell et al. (2002) and by numerically integrating $F(\mathbf{x}, s)$ with $f_S(s)$. In order to perform the numerical integration, we first obtain the best possible fit for the hazard data in logarithmic using higher order polynomial. We choose polynomials to obtain the fit because it is convenient to differentiate polynomials so as it to obtain $f_S(s)$. It is found that third order polynomial is sufficient for an accurate fit (see Figure 6-5). We perform the numerical integration beyond the maximum value of s for which hazard data is available. This is done to achieve convergence for the integral because higher values of s significantly contribute to P_{fA}.

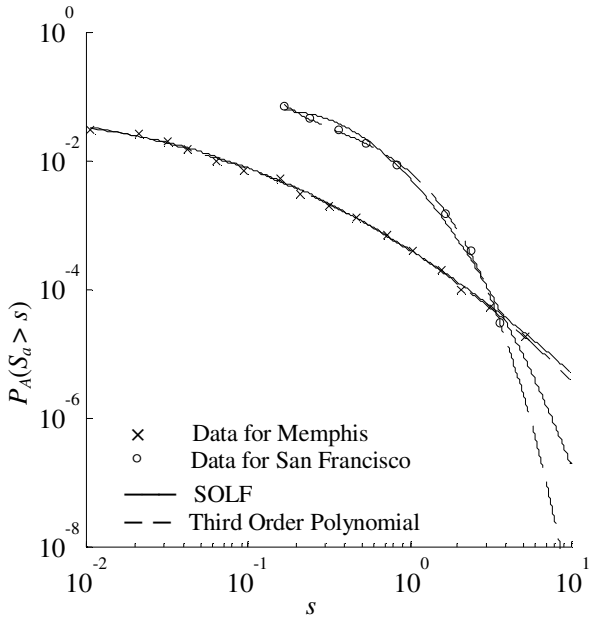

Figure 6-5. Third order polynomial fit for hazard curves used in numerical integration

We compute the values of P_{fA} conditioning on the value of median ductility capacity given by $\mu_c = \exp\{E[C]\}/\Delta_y$. Figure 6-6 and Figure 6-7 show the estimates of P_{fA} based on the three methods. It is seen that the estimates of P_{fA} obtained using the SOLF formulation closely match those obtained by numerical integration. On the contrary, the available solution proposed by Cornell et al. (2002) for the linear logarithmic form, significantly deviates from the numerical integration for both the locations. In particular, the linear logarithmic form overestimates P_{fA} for $0.2 > \mu_c > 2.7$ and underestimates P_{fA} for $0.2 < \mu_c < 2.7$ for San Francisco.

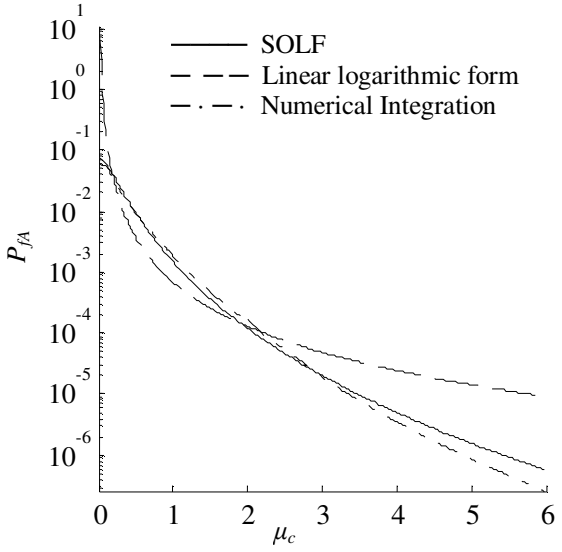

Figure 6-6. P_{fA} values for San Francisco conditioning on the value of μ_c

Similarly, linear logarithmic form overestimates P_{fA} for $0.02 > \mu > 0.6$ and underestimates P_{fA} for $0.02 < \mu_c < 0.6$ for San Francisco. These deviations reflect the deviation of the linear logarithmic form the actual hazard data. Moreover, the solution provided by Cornell et al. (2002) form the linear logarithmic form has a mathematical discrepancy, i.e., the value of $P_{fA} \to \infty$ as $\mu_c \to 0$ whereas in theory $P_{fA} \to P_A[S_a > 0]$ as seen in SOLF and numerical integration. It is also found that the upper limit of s used in numerical integration should not be limited to the maximum value of available data because the tail of the density function of S_a makes a significant contribution to the estimates of P_{fA}. Therefore, a reasonable extrapolation is necessary to correctly estimate the integral.

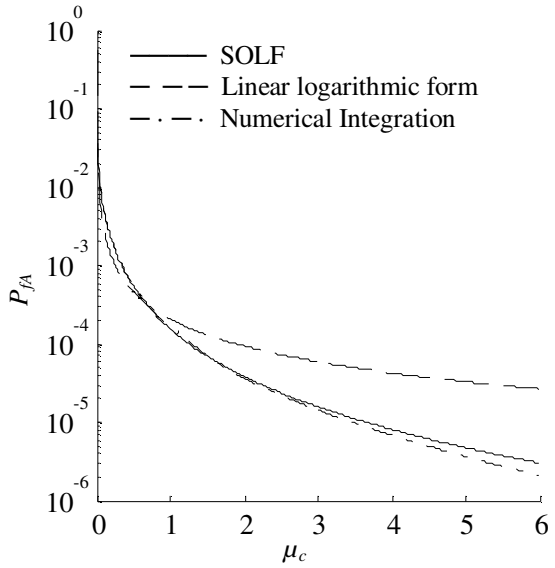

Figure 6-7. P_{fA} values for Memphis conditioning on the value of μ_c

Figure 6-8 compares the P_{fA} versus P_0 plots for San Francisco and Memphis. It is observed that P_{fA} increases with increase in P_0. This is because higher P_o means that the structure is designed for a smaller seismic event and therefore the structure has a smaller capacity. It is also seen that by designing for seismic events with same hazard values, different values of P_{fA} are obtained. This is expected due to the difference in the levels of seismicity. Such estimates are helpful for developing design and retrofit guidelines to achieve uniform performance of structures built across regions of varying seismic hazards. A detailed analysis of performance of structures under varying hazard levels and the importance of such analysis in the design process is discussed in Williams et al. (2009).

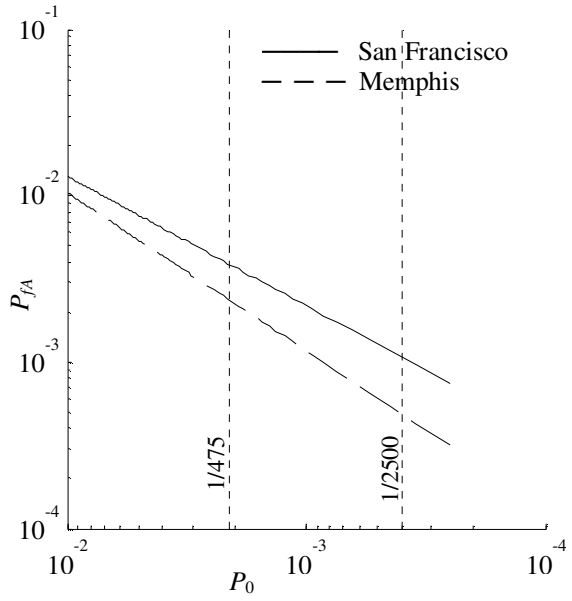

Figure 6-8. Plot of P_{fA} versus P_0 for San Francisco and Memphis

6.7 Conclusions

Closed-form solutions play an important role in engineering design and decision making. In particular, with the advent of performance-based engineering, closed-form solutions to compute the annual failure probability P_{fA} are needed. However, the existing closed-form solution relies on a convenient linear logarithmic form to model the hazard curve, which is an inadequate approximation.

In this section, we propose a novel second order logarithmic form (SOLF) to accurately represent hazard curves. Furthermore we derive a closed-form solution to compute P_{fA} using SOLF. We apply the proposed formulation to an example RC bridge

subject to the seismic hazard of two locations San Francisco, CA and Memphis, TN and compare the estimates with those of the existing linear logarithmic form and an independent numerical integration procedure. It is found that estimates based on the proposed SOLF match closely those obtained from numerical integration. It is found that the approach based on linear logarithmic formulation significantly overestimates P_{fA} for small and large values of capacity and underestimates the same for intermediate capacity values. This is because the linear logarithmic form for hazard curve intersects the actual hazard curve at two points. This linear form underestimates the hazard values between the two points of intersection and overestimates the same outside the two points. Using the SOLF formulation we derive a relationship between P_{fA} and the probability of exceedance P_0 corresponding to a selected design intensity. It is found that for a same value of P_0, San Francisco has higher P_{fA} than Memphis. This is expected due to the higher seismicity of San Francisco. Such analysis can be used to develop design guidelines to achieve uniform seismic performance of structures built across regions of varying seismicity. The developed SOLF formulation is general and can be applied to various other hazards (e.g., hurricanes and floods).

7. CONCLUSIONS

7.1 Summary

Infrastructure systems are critical to the socio-economic prosperity of any country. While building new infrastructure is essential, it is equally important to efficiently operation the built infrastructure to maximize the benefits. Any lack of planning or short-sighted objectives in handling infrastructure systems may lead to massive wastage of resources and social distress as witnessed in the past.

Today, the deterioration of public infrastructure systems such as roads, bridges and tunnels is one of the major issues in civil engineering. Deterioration reduces the reliability of systems and often results in the collapse and breakdown of the systems. In this research, we propose novel stochastic models to perform life-cycle analysis (LCA) of deteriorating engineering systems. The models are helpful in optimizing the reliability of systems and the costs associated with operating a system. Furthermore, we specifically study the process of seismic degradation of reinforced concrete (RC) bridge columns and perform LCA of RC bridges in a seismically active region accounting for the seismic degradation.

7.2 Significant contributions

The primary contributions of this research are as follows:

1. *Evaluation of the seismic vulnerability of RC bridges degraded due to past earthquakes*: Sections 2 and 3 are dedicated to model seismic degradation of RC bridge columns. In these sections, the effect of earthquakes on the capacity and future seismic demands are evaluated and future seismic vulnerability of degraded

RC bridges are assessed. It is shown that there is considerable probability of observing multiple damaging earthquakes in a bridge's life-span and that seismic degradation significantly effects the vulnerability of RC bridges with respect to future earthquakes. This contribution is important given that currently seismic design practices typically focus only on one-time seismic performance of a structure.

2. *Modeling of deterioration processes*: Section 4 proposes a novel stochastic model, SSA, to model a general process of deterioration in engineering systems. This model accounts for the effect of deterioration on both capacity and future demands on the system. The SSA model proposes a computationally efficient semi-analytical solution to compute the time to failure and level of deterioration in a system. The SSA model is an important contribution because it addresses some of the important issues in the available models in literature and hence is expected to improve the reliability analysis of deteriorating systems.
3. *Life-cycle Analysis (LCA) of deteriorating engineering systems*: Section 5 proposes a novel LCA model named RTLCA. The RTLCA model is applicable to a wide variety of engineering systems, deterioration processes and operation strategies. The proposed model will be helpful in efficient management of infrastructure systems and hence will help in maximizing the benefits from infrastructure systems.
4. *Improved Hazard Analysis and Closed-form solutions*: Section 6 proposes a novel mathematical model for hazard curves named SOLF. The SOLF formulation reduces the error in the estimation of annual failure probability of structures subject to

natural hazards compared to an existing closed-form method that is often used in hazard analysis.

7.3 Future work

Future research is required in developing frameworks to update the LCA estimates from theoretical predictive models such as RTLCA using the data obtained from the field tests (such as NDT) conducted on infrastructure systems. This is important because the data from field tests conducted from time to time can help in eliminating some uncertainties in the model predictions that are based on initial state of the system. Furthermore, the proposed stochastic LCA and deterioration models should be generalized to account for multiple modes of failure in a infrastructure. This is important because often large infrastructure systems possess several important modes of failure which govern their reliability.

REFERENCES

ASCE (2011). "Report card for America's infrastructure", <http://www.infrastructure reportcard.org/> (20 May 2012).

Ahmad, S. (2003). "Reinforcement corrosion in concrete structures, its monitoring and service life prediction ─ a review." *Cement and Concrete Composites*, 25(4-5), 459-471.

Ang, A. A-H., and Tang, W. H. (2007). *Probability concepts in engineering: emphasis on applications in civil & environmental engineering*, (2nd ed.), John Wiley and Sons, New York.

Atkinson, A. C., and Donev, A. N. (1992). *Optimum Experimental Designs*, Oxford University Press.

Baker, J. W. (2011). "The conditional mean spectrum: A tool for ground motion selection." *Journal of Structural Engineering*, 137, 322–331.

Balakrishnan, S., and Murray, D. W. (1988). "Concrete Constitutive Model for NLFE Analysis of Structures." *Journal of Structural Engineering*, ASCE, 114(7), 1449-1466.

Basöz, N., and Kiremidjian, A. S. (1996). ''Risk Assessment for Highway Transportation Systems.", *Technical Report No. 118*, John A. Blume Earthquake Engineering Center, Civil Engineering Department, Stanford University, Stanford, California.

Basöz, N., and Mander, J. (1999). "Enhancement of the Highway Transportation Lifeline Module in HAZUS." *Final Pre-publication Draft (#7) prepared for the National Institute of Building Science*, Mar. http://www.nibs.org/hazusweb/overview/pubs.php.

Bazzuro, P. and Cornell, C. A. (2004). "Nonlinear Soil-Site effects in probabilistic seismic hazard analysis." *Bulletin of the seismological society of America*, 94(6), 2110-2123.

Box, G. E. P., and Tiao, G. C. (1992). *Bayesian inference in Statistical Analysis*, Addison-Wesley, Reading, Mass.

Bradley, B. A., Dhakal, R. P., Cubrinovski, M., Mander J. B., and MacRae, G. A. (2007). "Improved seismic hazard model with application to probabilistic seismic demand analysis" *Earthquake Engineering and Structural Dynamics*, 36, 2211-2225.

Brown, J., and Kunnath, S. K. (2004). "Low-Cycle Fatigue Failure of Reinforcing Steel Bars." *ACI materials Journal*, 101(6), 457-466.

Caltrans. (2006). *Seismic design criteria*, *Version 1.4*, California Department of Transportation (Caltrans), Sacramento, CA.

Choe, D., Gardoni, P., and Rosowsky, D. (2007). "Closed-form fragility estimates, parameter sensitivity and Bayesian updating for RC columns." *Journal of Engineering Mechanics*, 133(7), 833–843.

Choe, D., Gardoni, P., Rosowsky, D., and Haukaas, T., (2008). "Probabilistic Capacity Models and Fragility Estimates for Corroding Reinforced Concrete Columns." *Reliability Engineering and System Safety*, 93, 383-393.

Choe, D., Gardoni, P., Rosowsky, D., and Haukaas, T. (2009). "Seismic Fragility Estimates for Reinforced Concrete Bridges subject to Corrosion." *Structural Safety*, 31(4), 275-283.

Coffin, L. F. Jr. (1954). "A Study of the Effects of Cyclic Thermal Stresses on a Ductile Metal." *Transactions of the ASME*, 76, 931–950.

Cornell, C. A., Jalayer, F., Hamburger, R. O., and Foutch, D. A. (2002). "Probabilistic basis for 2000 SAC federal emergency management agency steel moment frame guidelines." *Journal of Structural Engineering*, 128(4), 526-533.

Ditlevsen, O., and Madsen, H. O. (1996). *Structural reliability methods*, Wiley, New York.

Downing, S. A., and Socie, D. F. (1982). "Simple rainflow counting algorithms." *International Journal of Fatigue*, 4(1), 31–40.

El-Bahy, A., Kunnath, S. K., Stone, W. C., and Taylor, A. W. (1999a). "Cumulative Seismic Damage of Circular Bridge Columns: Benchmark and Low-Cycle Fatigue Tests." *ACI Structural Journal*, 96(4), 633-641.

El-Bahy, A., Kunnath, S. K., Stone, W. C., and Taylor, A. W. (1999b). "Cumulative Seismic Damage of Circular Bridge Columns: Variable Amplitude Tests." *ACI Structural Journal*, 96(5), 711-719.

Ellingwood, B. R., and Mori, Y. (1993). "Probabilistic methods for condition assessment and life prediction of concrete structures in nuclear power plants." *Nuclear Engineering and Design*, 142(2-3), 155–166.

Esary, J. D., Marshall, A. W., Proschan, F. (1973). "Shock models and wear processes." *The Annals of Probability*, 1(4), 627-649.

Field, E. H., Jordan, T. H., and Cornell, C. A. (2003). "OpenSHA: A Developing Community-Modeling Environment for Seismic Hazard Analysis." *Seismological Research Letters*, 74(3), 406-419.

Gardoni, P., and Rosowsky, D. (2011). "Seismic fragility increment functions for deteriorating reinforced concrete bridges." *Structure and Infrastructure Engineering*, 7(11), 869-879.

Gardoni, P., Der Kiureghian, A., and Mosalam, K. M. (2002). "Probabilistic Capacity Models and Fragility Estimates for RC Columns Based on Experimental Observations." *Journal of Engineering Mechanics*, ASCE, 128(10), 1024-1038.

Gardoni, P., Mosalam, K., Der Kiureghian, A. (2003). "Probabilistic Seismic Demand Models and Fragility Estimates for RC Bridges." *Journal of Earthquake Engineering*, 7(1), 79-106.

Ghosh, J., and Padgett, J. E. (2010). "Aging Considerations in the Development of Time-Dependent Seismic Fragility Curves." *ASCE Journal of Structural Engineering,* DOI: 10.1061/(ASCE)ST.1943-541X.0000260.

Grimmett, G. R., and Stirzaker, D. R. (2001). *Probability and Random Processes.* 3rd ed. Oxford University Press: New York.

Haldar, A., and Mahadevan, S. (2000). *Probability, Reliability and Statistical Methods in Engineering Design*, John Wiley, New York.

Haukaas, T., Hahnel, A., Sudret, B., Song, J., and Franchin, P. (2003). FERUM: Finite Element Reliability Using Matlab. http://www.ce.berkeley.edu/haukaas/ferum /ferum.html.

Hoshikuma, J., Kawashima, K., Nagaya, K., and Taylor, A. W. (1997). "Stress-Strain Model for Confined Reinforced Concrete in Bridge Piers." *Journal of Structural Engineering*, ASCE, 123(5), 624-633.

Huang, Q., Gardoni, P., and Hurlebaus, S. (2009). "Probabilistic Capacity Models and Fragility Estimates for Reinforced Concrete Columns Incorporating NDT Data." *Journal of Engineering Mechanics*, ASCE, 135(12), 1384-1392.

Huang, Q., Gardoni, P., and Hurlebaus, S. (2010). "Probabilistic Seismic Demand Models and Fragility Estimates for Reinforced Concrete Highway Bridges with One Single-column Bent." *ASCE Journal of Engineering Mechanics*, DOI: 10.1061/(ASCE)EM.1943-7889.0000186.

Kennedy, R. P. (1999). "Risk based seismic design criteria." *Nuclear Engineering and Design*, 192(2-3), 117-135.

Kim, S., Frangopol D. M., and Zhu, B. (2011). "Probabilistic optimum inspection/repair planning to extend lifetime of deteriorating structures." *ASCE Journal of Performance of Constructed Facilities*, 25(6), 534-544.

Klutke, G. A., and Yang, Y. J. (2002). "The availability of inspected systems subjected to shocks and graceful degradation." *IEEE Transaction on Reliability*, 51, 371–374.

Koh, S. K., and Stephens, R. I. (1991). "Mean Stress Effects on Low Cycle Fatigue for a High Strength Steel." *Fatigue & Fracture of Engineering Materials & Structures* 14(4), 413-428.

Kong, J. S., and Frangopol, D. M. (2003). "Life-cycle reliability-based maintenance cost optimization of deteriorating structures with emphasis on bridges." *Journal of Structural Engineering* 129(6), 818-828.

Kumar, R., Gardoni, P., and Sanchez-Silva, M. (2009). "Effect of cumulative seismic damage and corrosion on the life-cycle cost of reinforced concrete bridges." *Earthquake Engineering and Structural Dynamics*, 38(7), 887-905.

Leyendecker, E. V., Hunt, R. J., Frankel, A. D., and Rukstakes, K. S. (2000). "Development of maximum considered earthquake ground motion maps." *Earthquake Spectra* 16(1) (2000), 21-40.

Li, Y-F., and Sung, Y-Y. (2003). "Seismic repair and rehabilitation of a shear-failure damaged circular bridge column using carbon fiber reinforced plastic jacketing." *Canadian Journal of Civil Engineering*, 30, 819-829.

Mackie, K. R., and Stojadinović, B. (2005). "Fragility Basis for California Highway Overpass Bridge Seismic Decision Making.". *Report No. 2003/16*, University of California, Pacific Earthquake Engineering Research Center.

Mander, J. B., and Basöz, N. (1999). "Seismic Fragility Curve Theory for Highway Bridges." *5th US Conference on Lifeline Earthquake Engineering*, ASCE, Seattle, WA, USA.

Mander, J. B., and Cheng, C.-T. (1995). ‘‘Renewable hinge detailing for bridge columns.’’ *Proc.*, *Pacific Conf. on Earthquake Engineering*, Melbourne, Australia, 197–206.

Mander, J. B., Panthaki, F. D. and Kasalanati A. (1994). “Low-cycle Fatigue Behavior of Reinforcing Steel.” *Journal of Materials in Civil Engineering*, 6(4), 453-468.

Manson, S. S. (1953). “Behavior of Materials under Conditions of Thermal Stress.” *Heat Transfer Symposium*, University of Michigan Engineering Research Institute 9-75.

Maroney, B., Kutter, B., Romstad, K., Chai, Y. H., and Vanderbilt, E. (1994). “Interpretation of large scale bridge abutment test results.” *Proc., 3rd Annual Seismic Research Workshop*, California Dept. of Transportation, Sacramento, CA

McKenna, F., Fenves, G. L., Filippou, F.C., and Mazzoni, S. (2008). OpenSees: Open System for Earthquake Engineering Simulations. http://opensees.berkeley.edu/.

Mehta, P. K. (1994). “Mineral admixtures for concrete – an overview of recent developments. Advances in cement and concrete.” *Proc of an Engineering Foundation Conference*, *ASCE*, University of Newhampshire, Durham, 243-256.

Melchers, R. (2005). “The effect of corrosion on structural reliability of steel offshore structures.” *Corrosion Science*, 47(10), 2391-2410.

Miner, M. A. (1945). “Cumulative damage in fatigue.” *Journal of Applied Mechanics*, ASME, 12, A159-A164.

Mori, Y., and Ellingwood, B. R. (1994). “Maintaining: reliability of concrete structures, I: role of inspection/repair.” *Journal of Structural Engineering*, 120(3), 824–845.

Neves, L. C, and Frangopol, D. M. (2005). "Condition, safety and cost profiles for deteriorating structures with emphasis on bridges." *Reliability Engineering and System Safety*, 89(2), 189-198.

Noortwijk, J. M., Kallen, M. J., and Pandey, M. D. (2005). "Gamma processes for time-dependent reliability of structures." *Advances in Safety and Reliability*, 1457-1464

NTSB (2008). "Collpase of I-35W Highway Bridge, Minneapolis, Minnesota, August 1, 2007.", *Highway Accident Report*, National Transportation Safety Board (NTSB), https://www.ntsb.gov/doclib/reports/2008/HAR0803.pdf

Oswald, G. F., and Shuëller, G. I. (1984). "Reliability of deteriorating structures. Engineering Fracture Mechanics.", 20(3), 479-488.

Park, Y. J., and Ang, A. H.-S. (1985). "Mechanistic Seismic Damage Model for Reinforced Concrete." *Journal of Structural Engineering*, 111(4), 722-739.

Patxi, U. (2005). "Towards Earthquake Resistant Design of Concentrically Braced Steel Structures." PhD Thesis, University of California, Berkeley.

PEER "PEER Ground motion database", http://peer.berkeley.edu/peer_ground_motion_database/site (20 May 2012)

Pillai, R. G., Hueste, M. D., Gardoni, P., Trejo, D., and Reinschmidt, K. F. (2010). "Time-variant service reliability of post-tensioned, segmental, concrete bridges exposed to corrosive environments." *Engineering Structures*, 32(9), 2596-2605.

Pines, D., and Aktan, A. E. (2002). "Status of structural health monitoring of long-span bridges in the united states." *Progress in Structural Engineering and Materials*, 4(4), 372-380.

Rackwitz, R. (2000). "Optimization – the basis for code making and reliability verification." *Structural Safety*, 22(1), 27-60.

Ramamoorthy, S. K., Gardoni, P. and Bracci, J. M. (2006). "Probabilistic demand models and fragility curves for reinforced concrete frames." *Journal of Structural Engineering*, 132(10), 1563–1572.

Rao, C. R., and Toutenburg, H. (1997). *Linear Models, Least Squares and Alternatives*, Springer, New York, NY.

Reasenberg, P. A., and Jones, L. M. (1989). "Earthquake Hazard after and Mainshock in California." *Science*, 243(4895), 1173-1176.

Saadatmanesh, H., Ehsani, M. R., and Jin, L. (1997). "Repair of earthquake-damaged RC columns with FRP wraps." *ACI Structural Journal*, 94(2), 206-214.

Sanchez-Silva, M., Klutke, G. A., and Rosowsky, D. V. (2011). "Life-cycle performance of structures subject to multiple deterioration mechanisms." *Structural Safety*, 33(3), 206-217.

Schoettler, M. J., Restrepo, J. I., Seible, F., and Matsuda, E. (2005). "Seismic performance of retrofitted reinforced concrete bridge pier." *ACI Structural Journal*, 102(6), 849-859.

Shinozuka, M., Feng, M. Q., Kim, H-K., and Kim, S-H. (2000). "Nonlinear Static Procedure for Fragility Curve Development." *Journal of Engineering Mechanics*, 126(12), 1287-1295.

Smith, A. F. M., and Roberts, G. O. (1993). "Bayesian Computation Via the Gibbs Sampler and Related Markov Chain Monte Carlo Methods." *J. R. Statist. Soc. B*, 55(1), 3-23.

Sunasaka, Y., and Kiremidjian, A. S. (1993). "A method for structural safety evaluation under mainshock-aftershock earthquake sequences," *Report No. 105*, The John A. Blume Earthquake Engineering Center, Stanford University, Stanford, CA.

Stewart M. G., and Dimitri, V. V. (2003). "Multiple limit states and expected failure costs for deteriorating reinforced concrete bridges." *Journal of Bridge Engineering*, 8(6), 405-415.

Stewart, M. G. (2001). "Reliability based assessment of ageing bridges using risk ranking and life-cycle cost decision analyses." *Reliability Engineering and System Safety*, 74(3), 263-273.

Taylor, A., Stone, W., Berry, M., Camarillo, H., Mookerjee, A., and Parrish, M. (2003). "Test Results: Spiral Reinforced Columns." Structural Performance Database, <http://www.ce.washington.edu/~peera1/> (Aug 8. 2008).

Tsuno, K., and Park, R. (2004). "Prediction method for seismic damage reinforced concrete bridge columns." *Structural Eng. Earthquake Eng.*, JSCE, 21(2), 97-111.

USGS. "2008 Interactive Deaggregation",<https://geohazards.usgs.gov/deaggint/2008/index.php> (17 May, 2012)

Utsu, T., (1961). "A Statistical Study on the Occurrence of Aftershocks." *Geophysical Magazine*, 30, 521-605.

Utsu, T., Ogata, Y., and Matsu'ura, R. S. (1995). "The centenary of the Omori Formula for a decay law of aftershock activity." *Journal of the Physics of the Earth*, 43, 1-33.

Val, D. V. (2005). "Effect of different limit states on life-cycle cost of RC structures in corrosive environment." *Journal of Infrastructure. Systems*, 11(4), 231-240.

Val, D. V., and Stewart, M. G. (2005), "Decision analysis of deteriorating structures." *Reliability Engineering and System Safety*, 87(3), 377-385.

Val, D. V., Stewart, M. G., and Melchers, R. E. (2000). "Life-cycle performance of RC bridges: Probabilistic Approach." *Computer Aided Civil and Infrastructure Engineering*, 15(1), 14-25.

Van Noortwijk, J. M., and Frangopol, D. M. (2004). "Two probabilistic life-cycle maintenance models for deteriorating civil infrastructures." *Probabilistic Engineering Mechanics*, 19(4), 345-359.

Wen, Y. K., and Kang, Y. J. (2001). "Minimum building lifecycle cost design criteria. I: methodology." *Journal of Structural Engineering*, 127(3), 330-337.

Williams, R. J., Gardoni, P., and Bracci, J. M. (2009). "Decision analysis for seismic retrofit of structures." *Structural Safety*, 31(2), 188-196.

Wilson, J. C., and Tan, B. S. (1990). "Bridge abutments: Formulation of simple model for earthquake response analysis." *Journal of Engineering Mechanics*, 116(8), 1828-1837.

Wortman, M. A., Klutke, G. A., and Ahyan, H. (2006). "A maintenance strategy for systems subjected to deterioration governed by random shocks." *IEEE Transactions on Reliability*, 55 (3), 542-550.

Xiao, Y., and Ma, R. (1997). "Seismic retrofit of RC circular columns using prefabricated composite jacketing." *ACI Structural Journal*, 123(10), 1357-1364.

Yang, J. N. (1976). "Statistical Estimation of Service Cracks and Maintenance Cost For Aircraft Structures." *J. Aircraft AIAA*, 13(12), 929-937.

Zhang, J., and Makris, N. (2001). "Seismic response analysis of highway overcrossings including soil-structure interaction." *PEER Rep. No. 2001/02*, Pacific Engineering Earthquake Research Center, Univ. of California, Berkeley, CA.

Zhong, J., Gardoni, P., and Rosowsky, D. (2008). "Bayesian Updating of Seismic Demand Models and Fragility Estimates for Reinforced Concrete Bridges with Two-Column Bents." *Journal of Earthquake Engineering*, 13(5), 716-735.

Zhong, J., Gardoni, P., and Rosowsky, D. (2009). "Seismic fragility estimates for corroding reinforced concrete bridges." *Structure and Infrastructure Engineering*, DOI: 10.1080/15732470903241881.